ROLE OF THE VENTROMEDIAL HYPOTHALAMUS IN CONTROL OF INNATE DEFENSIVE BEHAVIOURS

NATALIA HANNA WRÓBLEWSKA

Trinity College

January 2018

This dissertation is submitted for the degree of Doctor of Philosophy

DECLARATION

The research in this dissertation was carried out under the supervision of Dr Tiago Branco at the MRC Laboratory of Molecular Biology, University of Cambridge and at the Sainsbury Wellcome Centre, University College London.

This dissertation is the result of my own work and includes nothing which is the outcome of work done in collaboration except as declared in the Preface and specified in the text.

It is not substantially the same as any that I have submitted, or, is being concurrently submitted for a degree or diploma or other qualification at the University of Cambridge or any other University or similar institution except as declared in the Preface and specified in the text. I further state that no substantial part of my dissertation has already been submitted, or, is being concurrently submitted for any such degree, diploma or other qualification at the University of Cambridge or any other University or similar institution except as declared in the Preface and specified in the text.

It does not exceed the prescribed word limit of 60,000 words set by the Degree Committee of the School of the Biological Sciences.

Natalia Hanna Wróblewska

In loving memory of Piotr Wróblewski

1930 – 2016

ABSTRACT

Our senses are constantly bombarded with information. How does the brain integrate such a variety of inputs to generate appropriate behaviours? Innate defensive behaviours are a good model to address this question. They are essential for animal survival and the brain circuits that control them are highly conserved across species. Moreover, the sensory inputs and behavioural outputs can be well defined and reliably reproduced in the lab. This allows us to study function of the individual components of the circuit controlling these behaviours.

Ventromedial hypothalamus (VMH) is a key brain region for controlling responses to predators; it has been shown that inactivating the VMH can reduce defensive behaviours. Interestingly, activating the VMH output neurons (SF1+ cells) can produce a variety of different behaviours, from immobility to escape, depending on the intensity of activation.

During my PhD I used a variety of approaches to address the question of the function of the VMH in control of defensive behaviours. At first I hypothesised that the VMH might act as a centre responsible for choosing an appropriate behavioural response according to the stimulus. I set to investigate how different activation levels of SF1+ neurons can produce such different behavioural outputs, and how this activity is modulated in vivo in response to predator stimuli.

I began the project by quantifying mouse defensive behaviours in response to olfactory and auditory predator cues, as well as to the optogenetic activation of SF1+ neurons. I then questioned whether there was heterogeneity within the population of SF1+ neurons, which could explain their ability to trigger different behaviours. I performed patch clamp recordings from acute brain slices and conducted a study of the electrophysiological properties of SF1+ neurons.

I next investigated how SF1+ neurons integrate excitatory inputs from the medial amygdala, a region which receives olfactory inputs from the accessory olfactory bulb. By combining optogenetics with slice electrophysiology and behavioural assessment, I described the physiology and relevance of this connection.

Finally, I investigated in vivo activity in the VMH in response to predator cues by performing calcium imaging of the VMH neurons in freely moving mice. By presenting different sensory stimuli, I addressed the question of heterogeneity of the input pattern to the VMH neurons and the relationship between the VMH activity and the behavioural output.

Taken all together, the results of this project have led to a hypothesis whereby the function of the VMH is to facilitate rather than directly control the choice of an appropriate behavioural response.

ACKNOWLEDGMENTS

A PhD thesis is always more than the sum of the printed n numbers. Upon reaching the destination it becomes clear how many shortcuts were missed on the way, but the truth is – the journey would not have been as picturesque and rewarding had we taken the shortest path. I am most grateful to everyone who walked parts of it with me and made this journey not only enjoyable, but also truly enriching.

First and foremost, I would like to thank Tiago. Thank you for your understanding, guidance and continuous scientific inspiration. Speaking to you has always reignited my scientific curiosity. I wish I had made use of this more often.

Thank you to all of the Branco lab members, past and present. You guys are not only incredibly helpful, but also so much fun to be around! It is hard to imagine a nicer group of people to work with. I am truly fond of all of you. While I cannot mention every single one of you (the lab has grown so much!), special thanks must go to Dom, who always went an extra mile to help myself and others.

Thank you to all those who enabled this project: the support staff from the LMB, SWC and the School of Clinical Medicine, as well as the Boehringer Ingelheim Fonds, Frank Edward Elmore Fund and James Baird Fund for the financial support.

It would be futile to try to mention all the people whose paths I crossed or joined, conversations and experiences which left a mark. I must however thank two people who had a pivotal influence during this long hiking trip. Thi – thank you for encouraging me to study my own brain. It is thanks to you I ascended a peak much higher than I ever imagined. And Sara – thank you for helping me understand the brains of others. You made me appreciate the value of companionship on every journey that we take.

CONTENTS

LIST OF FIGURES

LIST OF TABLES

Part I

INTRODUCTION

1

INTRODUCTION

The basic goal of all species is survival. Evolutionary drive has promoted self-preservation mechanisms, enabling animals to protect themselves from commonly encountered threats. Innate response to a life-threatening stimulus is therefore fear and defence, and it is the interaction between external stimuli and internal motivation that determines the behavioural output.

Our brains are constantly bombarded with stimuli and it is poorly understood how neural circuits integrate and interpret such a variety of inputs to generate appropriate behaviours. Defensive behaviours are a good model to address this problem, as the brain circuits that control them have evolved over millions of years and are highly conserved across species. The ventromedial hypothalamus (VMH), specifically its dorsomedial part (VMHdm) is a key brain region that controls responses to predators, but it is unknown how neurons in the VMHdm process information and produce the neuronal outputs that lead to defensive responses.

In this project I used a combination of electrophysiology, calcium imaging, optogenetics and behavioural techniques to investigate the role of the VMHdm in control of innate defensive behaviours in mice. In particular, I focused on VMHdm integration of inputs from the medial amygdala (MEA), which receives olfactory information about predators.

In this chapter I provide an overview of the circuits controlling innate defensive behaviours, with a specific focus on the VMHdm. I begin by describing behaviours which animals commonly display in the presence of predators. Next I give an overview of the neural circuits controlling these behaviours, with a focus on the roles of the medial

hypothalamic nuclei and more specifically the VMHdm. Then I discuss the stimuli used in the laboratory to elicit defensive behaviours, in particular olfactory stimuli, and an overview of the olfactory pathway involved in the control of these behaviours. Finally, I describe the aims of the project and the experimental approach I used to address them.

1.1 INNATE DEFENSIVE BEHAVIOURS

Innate defensive behaviours can be triggered by a range of threatening stimuli, such as predators, aggressive conspecifics, pain and features of the environment (Silva et al., 2016). They are necessary for survival of the animal and therefore have been observed across all species. Interestingly, different types of threat are processed by parallel circuits, with responses to predators and aggressive conspecifics being controlled by different brain regions (Silva et al., 2013, Silva et al., 2016). Defensive behaviours in response to conditioned stimuli are controlled through a yet separate pathway (review by Silva et al., 2016).

Innate defensive behaviours in response to predators have been studied extensively across a range of species, such as rabbit, rat, mouse, vole, deer and hamster (review by Apfelbach et al., 2005). They have been studied in the wild, as well as in the lab, and have been induced with a variety of aversive stimuli, from actual predators to unimodal sensory stimuli (see section 1.6). Seminal work has been performed by Blanchard and Blanchard, 1989, who comprehensively described defensive behaviours in rats in response to a cat. They used a so-called "visible burrow system", thereby shifting the field of study from the wild into the laboratory environment.

While threat is often said to induce "fear", that term is usually used to describe the conscious feeling experienced by an individual. It is not known whether emotions exist in species other than human,

however it has been argued that this internal emotional state consists of adaptive properties, which can be observed to different extends across species (Anderson and Adolphs 2014). While in this project I have focused primarily on defensive behaviours, rather than the internal emotional state of the animal, this perspective becomes important when interpreting the results.

Relation to other innate behaviours

Defensive behaviour is not the only behaviour essential for species survival and therefore it should not be considered in isolation. Other innate behaviours include feeding, aggression, sexual reproduction and caring for the offspring. All these behaviours must be orchestrated to optimise survival and reproduction.

Evidence suggests that these behaviours are not independent of each other. For instance, risk of predation affects the decision whether to engage in other behaviours, such as feeding (Lima and Dill, 1990). Since animals need to meet their energy requirements while minimising the risk of being captured by the predators, it has been hypothesised that they feed preferentially at times of low predation risk than when the risk is high (Lima and Bednekoff, 1999). For instance, field voles reduce their feeding in conditions of increased risk of predation (Koivisto and Pusenius, 2003), while impregnating food with fox faecal odour reduces food intake in mice (Coulston et al., 1993).

Similarly, female reproductive success is affected by predator odours (review by Apfelbach et al., 2015). It has been hypothesised that delaying breeding under high risk of predation maximises chances of survival (Ruxton and Lima, 1997). This has been first shown in voles, in which reproduction is suppressed in the presence of the scent of weasels (Ylonen, 1994). These changes in breeding have been suggested to be due to changes in mating (Ylonen, 1994), feeding (Heikkila al. 1993) or oestrous cycle (Jochym and Halle, 2013). While majority of evidence comes from studies in voles and hamsters, these findings have also been reproduced in mice and rats. Blanchard et al., 1995

have shown that exposure of mice to a cat reduces sexual behaviours, as well as eating and drinking, for up to 24h following exposure to the predator. More recently, exposure to a cat has been shown to slow down the rate of blastocyst formation in mice (Liu et al., 2012).

Other influences on expression of behaviour

Expression of innate behaviours can also vary depending on factors such as animal's age, sex, internal state, disease or circadian rhythm (review by Stowers et al., 2013). Innate defensive behaviours have been shown to change throughout development (review by Wiedenmayer, 2009), with older animals showing increased defensive behaviours (Hubbard et al., 2004). Hormonal levels can also affect expression of innate defensive behaviour. These can be sex dependent or change over time, such as during pregnancy. For instance, deficiency in testosterone in male rats increases freezing in response to synthetic fox odour exposure (King et al, 2005). Similarly, increased oxytocin levels in lactating females reduces anxiety (Bosch, 2013) and decreases freezing to a conditioned fearful stimulus (Rickenbacher et al., 2017).

Defensive behaviour also depends on the nature of the threat, environment and any previous experiences. In the laboratory setting differences in behaviour can also be due to the experimental set up, such as dimensions of the arena, amount of light and background noise, breeding conditions, animal handling and many more. Because of the multitude of factors which can affect defensive behaviours, many of which are difficult to control for, there is a lot of variability in published studies, some of which report opposite findings (review by Apfelbach et al., 2005).

1.2 COMPONENTS OF INNATE DEFENSIVE BEHAVIOURS

The most commonly expressed defensive behaviours include escape, freezing and avoidance, as well as changes in the activity pattern,

reduction in non-defensive behaviours and autonomic and endocrine changes (Apfelbach et al., 2015).

Freezing and fleeing

When rodents encounter a live predator, such as a cat, the initial defensive response is commonly flight back to the shelter, often followed by freezing lasting for variable lengths of time (Blanchard and Blanchard, 1989, Blanchard et al., 1991). Flight is the most common response when the threat is proximal and there are escape routes available, while freezing is more commonly seen when the threat is more distal or not escapable. It has been suggested that higher anxiety, for example due to anticipation of threat, is correlated with a higher likelihood of displaying freezing rather than fleeing in response to a threat (Mongeau et al., 2003).

Avoidance

Predator threat also induces avoidance, which can be described as a "habitat shift". Animals choose to spend less time in the area of higher predation risk, thereby decreasing chances of being predated on. Avoidance has been reported in multiple studies (review by Apfelbach et al., 2015). For instance, in a study by Dickman, 1992, mice avoided the traps containing cat or fox faeces, but not those containing conspecific odour.

Risk assessment

Another form of defensive behaviour is risk assessment, characterised by so called 'stretch-attends' and 'flat back' approaches, as well as 'head out' behaviour, where the animal is investigating the environment from within the safety of the shelter, only protruding the head out through the exit of the shelter (Blanchard and Blanchard, 1989). Cloth impregnated with cat fur odour has been shown to induce such risk assessment in rats (Blanchard and Blanchard, 1989) as well as mice (Blanchard et al., 1994). Risk assessment can also be

quantified by measuring the number of contact between the animal and the source of predator odour (File at al., 1993).

Changes in activity pattern

Changes in the activity pattern can be either short term, on a timescale of seconds to minutes, or long term, last ingfor days after threat encounter.

Short term changes include reduced mobility, which might be a mechanism to reduce the probability of encountering a predator (Borowski and Owadowska, 2001)(Apfelbach et al., 2015). It has been shown that less mobile voles have a smaller risk of being caught by predators (Norrdahl and Korpimäki, 1998). Rats also show reduced locomotor activity following exposure to cat odour, which lasts for hours after the exposure (McGregor et al., 2002). In the laboratory environment these temporary changes in the activity pattern can also be assessed by measuring the time mice spend outside the shelter and the latency to leave the shelter (Blanchard et al., 1994).

Long term changes have been largely studied in the natural habitat. Wild rats are normally nocturnal animals, but when exposed to the risk of predation by foxes, they change their foraging pattern and switch to hunting for food during day time instead of at night (Fenn and Macdonald, 1995). Similarly, wild voles exposed to a live weasel placed inside a cage within their territory showed a reduction in locomotion (Borowski, 1998b) and in the mean distance travelled (Borowski and Owadowska, 2001).

Reduction in non-defensive behaviours

As mentioned in section 1.1, animals regulate other behaviours, such as feeding and breeding, depending on the risk of predation. As the risk increases, animals reduce expression of these other competing behaviours in order to preserve the energy and reduce the risk of exposure to predators. As a result, measuring changes in expression of

non-defensive behaviours can be another way of assessing the effect of predators on prey.

Autonomic and endocrine changes

Exposure to cat odour not only produces a visible behavioural effect, but also raises levels of circulating corticosterone in rats (File et al. 1993, Muñoz-Abellán et al., 2011). Similar observations have been made during exposure of rats to ferret odour (Masini et al., 2005). In mice, elevation of adrenocorticotropic hormone (ACTH) has been observed following exposure to cat odour, snake skin and rat urine (Papes et al., 2010).

Predator exposure also induces short and long term cardiovascular changes. In rats exposure to cat odour has been shown to transiently elevate the heart rate as well as increase blood pressure for a more prolonged period of time (Dielenberg et al. 2001).

Interestingly, it has been reported that exposing rats to weasel anal secretion can increase corticosterone and adrenocorticotrophic hormone levels without markedly affecting the behaviour (Perrot-Sinal et al., 1999). This suggests that measuring endocrine and autonomic changes might allow detection of defensive responses otherwise undetectable.

1.3 OVERVIEW OF CIRCUITS CONTROLLING DEFENSIVE BEHAVIOURS

There are multiple brain areas implicated in control of innate defensive behaviours, based on the pattern of c-Fos expression, anatomical tracing, lesion studies, in vivo electrical stimulation, and more recently optogenetics. The studies summarised here have been conducted in rats and mice.

Broadly speaking, the circuit can be divided into three main units: detection, integration and output (Silva et al., 2016). The detection unit collects sensory information, which can be olfactory, auditory,

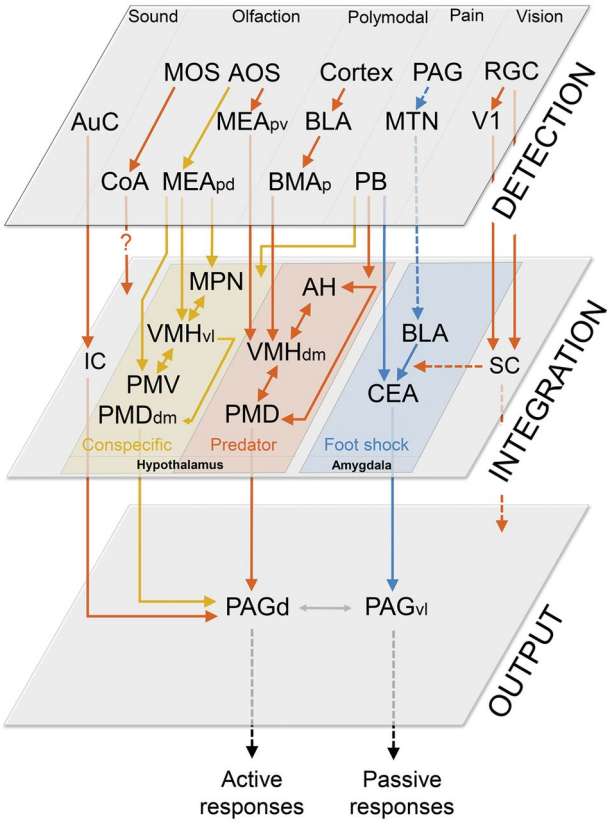

Figure 1.1: Overview of neural circuits controlling defensive behaviours. Abbreviations: AH—anterior hypothalamic nucleus; AOS—accessory olfactory system; AuC—auditory cortex; BLA—basolateral amygdala; BMA—basomedial amygdala; CEA—central nucleus of the amygdala; CoA—cortical amygdala; IC—inferior colliculus, MOS—main olfactory system; MEApd—posterior dorsal part of medial amygdala; MEApv—posterior ventral part of medial amygdala; MPN—medial preoptic nucleus; MTN—midline thalamic nuclei.PAGd—dorsal periaqueductal gray; PAGvl—ventrolateral periaqueductal gray; PB—parabrachial nucleus; PMDdm—dorsomedial part of the dorsal premammillary nucleus; PMV—ventral premammillary nucleus; RGN—retinal ganglion cells; SC—superior colliculus; VMHdm—dorsomedial part of the ventromedial hypothalamic nucleus; VMHvl—ventrolateral part of the ventromedial hypothalamic nucleus; V1—primary visual cortex. Figure from Silva et al., 2016.

visual or nociceptive. It includes primary sensory areas where the sensory inputs are processed, such as the olfactory bulb and the choclear nuclei.

Information from the sensory unit is then passed on to the integration unit of the circuit. Here information about the threat, environment and the internal state of the animal is integrated, enabling choice of the most appropriate behavioural response. Interestingly, different types of threat are processed separately at this stage, with different brain regions being activated when threat is coming from predators and conspecifics. In rodents, predator and conspecific threats are integrated by parallel circuits within the medial hypothalamus (Canteras et al., 1997, Silva et al., 2013), described collectively as the medial hypothalamic defence circuit.

Downstream from the integration unit of the circuit is the output unit, located in the periaqueductal grey (PAG). Here the appropriate behavioural and homeostatic responses are triggered. Lesions of the PAG almost completely abolish defensive responses, while activation of the PAG is sufficient to trigger freezing and escape behaviour (Hunsperger, 1956). Different types of threat induce neural activation in the PAG, such as predator odours (Cezario et al., 2008), aggressive conspecifics (Motta et al., 2009) and electrical foot shock (Johansen et al., 2011).

Finally, there are other brain regions which provide further modulatory input. For instance, medial prefrontal cortex (mPFC) is also activated during exposure to predators (Staples et al., 2008) and it is thought to modulate responses to predator threat through its projections to the amygdala, hypothalamus and the PAG (Gabbott et al., 2005, Franklin et al., 2017).

While the main components of the circuit have been identified, it remains unclear how the information is integrated, how the appropriate defensive behaviour is selected, and what exact role each of the components plays in controlling responses to threat.

1.4 MEDIAL HYPOTHALAMIC DEFENCE CIRCUIT

Anatomical tracing studies have shown that the medial hypothalamic defensive circuit (MHDC) in rodents is composed of three heavily interconnected nuclei: the anterior hypothalamic nucleus (AH), the dorsomedial part of the ventromedial hypothalamus (VMHdm), and the dorsal premammillary nucleus (PMD)(Canteras et al., 1994). All of them show increased levels of c-Fos expression following exposure to predator odour (Canteras et al., 1997).

PMD shows the highest degree of c-Fos expression (Canteras et al., 1997). Lesions of the PMD almost completely abolish defensive behaviours, such as freezing and escape (Canteras et al., 1997), while local electrical stimulation triggers escape and freezing behaviour (Yardley and Hilton, 1986).

Similarly, optogenetic activation of the VMHdm can induce defensive behaviours such as avoidance, immobility and jumping (Kunwar et al. 2015; Wang et al. 2015, Viskaitis et al. 2017), while inactivation of the VMHdm reduces expression of defensive behaviours in the presence of natural predators (Silva et al., 2013). VMHdm is described in more detail in section 1.5.

Optogenetic activation of the AH induces jumping and avoidance (Wang et al., 2015). While AH has strong reciprocal connections with PMD and VMHdm, unlike the other two it contains mostly GABAergic neurons (Wang et al., 2015). Lesions of the AH increase the latency to elicit defensive behaviours through electrical stimulation of the VMHdm (Fuchs et al., 1985).

1.4.1 *Inputs*

Anatomical connectivity of the MHDC has been described in detail in a series of tracing studies using Phaseolus vulgaris leucoagglutinin (PHA-L) (Canteras, 2002; Cucchiaro and Uhlrich, 1990). While con-

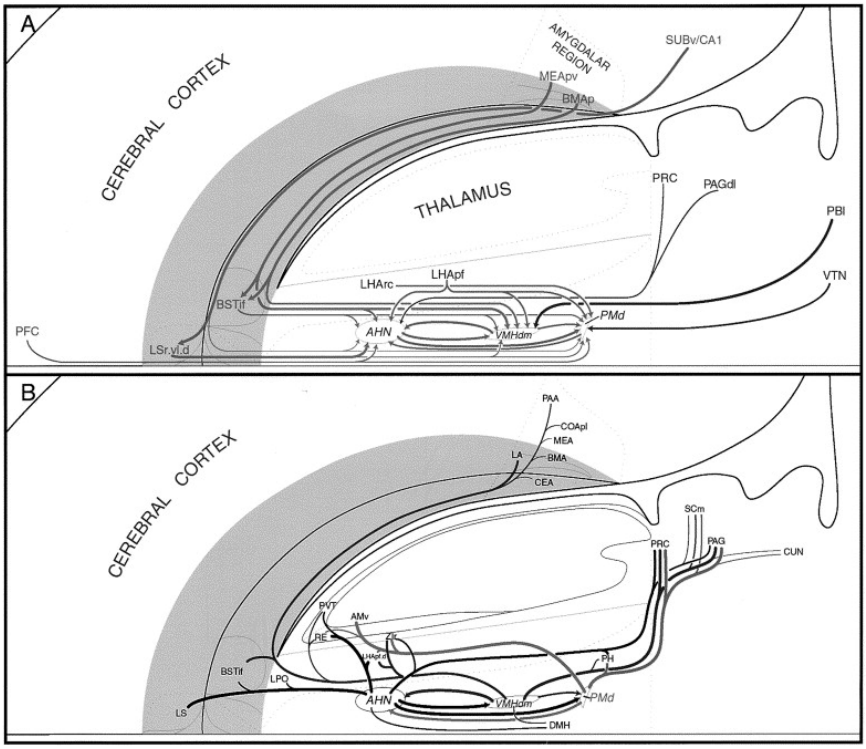

Figure 1.2: Inputs and outputs of the medial hypothalamic defence circuit. A. Inputs B. Outputs. Thickness of the line is proportional to the magnitude of the connection. Abbreviations: AHN—anterior hypothalamic nucleus; AMv—anteromedial thalamic nucleus, ventral part; BMA, p—basomedial amygdalar nucleus, posterior part; BSTif—bed nuclei of the stria terminalis, interfascicular nucleus; CA1—field CA1, Ammon's horn; CEA—central amygdalar nucleus; COApl—cortical amygdalar nucleus, posterolateral part; CUN—cuneiform nucleus; LA—lateral amygdalar nucleus; LHApf—lateral hypothalamic area, perifornical region; LHApfd—dorsomedial rostral perifornical region of the lateral hypothalamic area; LHArc—lateral hypothalamic area, retinoceptive region; LPO—lateral preoptic area; LS—lateral amygdalar nucleus; LS—lateral septal nucleus; LSrvld—lateral septal nucleus, rostral part, ventrolateral zone, dorsal region; MEApv—medial amygdalar nucleus, posteroventral part; PAA—piriform amygdaloid area; PAGdl—periaqueductal gray, dorsolateral part; PBl—parabrachial nucleus, lateral part; PFC—prefrontal cortex; PH—posterior hypothalamic nucleus; PMd—dorsal premammillary nucleus; PRC—precommissural nucleus; PVT—paraventricular thalamic nucleus; RE—nucleus reuniens; SCm—superior colliculus, medial region; SUBv—subiculum, ventral part; VMHdm—ventromedial hypothalamic nucleus, dorsomedial part; VTN—ventral tegmental nucleus; ZIr—zona incerta, rostral part. Figure from Canteras, 2002.

nectivity pattern of the circuit is fairly complex and in itself does not offer explanation for the function of each connection, it is necessary to consider inputs and outputs in order to understand the function of any brain region of interest. Figure 1.2A contains a visual overview of the inputs to the MHDC. VMHdm, PMD and AH are not only heavily interconnected, but also receive inputs from nearly the same brain regions. For this reason at this point inputs and outputs are considered for the MHDC in general, rather than for the individual components.

The main inputs to the MHDC come from amygdala, well known to be involved in expression of defensive behaviours (Blanchard and Blanchard, 1972). The inputs originate specifically in the posteroventral part of the medial amygdala (MEApv) and posterior part of the basomedial amygdala (BMAp). MEApv receives direct inputs from the accessory olfactory bulb (AOB) (Pro-Sistiaga et al., 2007) and is thought to transmit olfactory predator information (Dielenberg et al., 2001). BMAp on the other hand receives inputs from the basolateral amygdalar nucleus (BLA), which collects polymodal information from the olfactory, insular, and prefrontal cortices (Sah et al., 2003). A proportion of inputs from the amygdala comes to the MHDC through the bed nucleus of the stria terminalis (BNST)(Canteras et al., 1995). Fibre-sparing lesions of either MEA or BLA impair freezing in response to cat fur odour in rats (Takahashi et al., 2007). Similarly, temporary inactivation of the BNST impairs freezing in rats in response to cat urine (Xu et al., 2012).

Another set of inputs to the MHDC comes from the lateral septal nucleus (LSN). LSN is thought to modulate autonomic responses to threatening situations, in particular the cardiovascular responses (Kubo et al., 2002) and receives strong reciprocal inputs from the AH. Lesions of the LSN result in a hyperdefensive state, described as a "septal rage" (Albert and Chew, 1980), suggesting that LSN might be providing inhibitory inputs regulating expression of defensive behaviours.

Strong hypothalamic inputs come from the lateral hypothalamus (LH)(Comoli et al., 2000), an area involved in control of food intake and food aversion (Stuber and Wise, 2016), suggesting that MHDC might be involved in coordination of innate behaviours beyond just the defensive behaviour. This part of the LH also receives inputs from the retinal ganglion cells (Leak and Moore, 1997) and therefore could help choose appropriate behaviours depending on the visibility in the environment (Canteras, 2002).

A smaller set of inputs to the VMHdm comes from the parabrachial nucleus (PBN)(Bester et al. 1997), which relays information about the noxious stimuli (Bester et al., 1997). There is also a small projection to the AH from the precommissural nucleus, as well as the dorsolateral PAG (PAGdl), which being part of the output unit is likely to send feedback information to the MHDC through this projection. Finally, PMD receives inputs from the ventral tegmental area, involved in motivation and reward (Ranaldi, 2014), also positioned in close proximity to the medial mammillary nucleus, which could provide information related to spatial navigation (Sziklas and Petrides, 1998).

1.4.2 *Outputs*

Figure 1.2B contains an overview of the outputs of the MHDC. The main targets of the MHDC in the brainstem are the PAG and the neighbouring precommissural nucleus. Most of these projections originate in the VMHdm, although a proportion of inputs also comes from the PMD. The positioning of the inputs within the rostral PAG is mostly in the dorsomedial and dorsolateral parts, while caudally inputs can be found also in the lateral and ventrolateral parts. This pattern of projections in the PAG coincides with the patterns of c-Fos protein expression in the PAG following exposure to predators (Canteras and Goto, 1999b). A small projection can also be found in the cuneiform nucleus and the intermediate and deep layers of the su-

perior colliculus, which transmit information about the visual threats to the PAG (Redgrave and Dean, 1991).

The target of the MHDC projections in the telencephalus include previously mentioned lateral septal nucleus (LSN), which receives inputs from the AH, as well as the BNST and the lateral amygdala, which receive inputs from the VMHdm. Since these structures are reciprocally connected, these connections might also serve as a feedback system.

Dense projections can also be found in the nucleus reuniens, which in turn projects to the hippocampal formation. This pathway therefore could be involved in emotion based memory formation (Canteras, 2002). Another structure in the thalamus receiving dense projections, specifically from the PMD, is the ventral anteromedial thalamic nucleus, thought to be involved in attention related head and eye moments (Risold and Swanson, 1995). More ventrally, rostral part of zona incerta receives inputs from all MHDC nuclei (Canteras and Swanson, 1992; Canteras et al., 1994; Risold et al., 1994).

Within the hypothalamus, the MHDC projects to the posterior hypothalamic nucleus, which might be important for memory formation through its connection to the hippocampus (Vertes et al., 1995), as well as the control of visceral responses to threat, such as the blood pressure and heart rate (Di Micco and Abshire, 1987). AH and VMHdm also project to the dorsomedial hypothalamus, a densely connected structure implied in control of the neuroendocrine and autonomic output (Thompson and Swanson, 1998). AH sends projections to the lateral preoptic area, thought to modulate somatomotor responses associated with general arousal (Swanson, 1987; Swanson et al., 1984). Finally, all MHDC nuclei project to the dorsomedial rostral perifornical region, part of the lateral hypothalamus involved in control of feeding (Canteras et al., 1997).

1.4.3 *Function*

While the anatomical connectivity of the MHDC has been described in detail and provides us with insightful information regarding the type of inputs integrated by the MHDC, the exact functional importance of this circuit remains unknown. Moreover, few studies have looked at the connectivity of the circuit from an electrophysiological perspective and so little is known about the process and function of information integration by the circuit. Considering the source of inputs to the MHDC, it is likely to be a key integrator of threat levels, as determined not only by presence of a predator, but also the external environment, previous experiences and the internal state of the animal.

It is important to note that while medial hypothalamus has been shown to play an important role in controlling responses to predator threat, certain threatening stimuli can elicit defensive behaviours while bypassing the MHDC. For instance, visual stimuli are thought to elicit escape behaviour through a direct connection from the superior colliculus (SC) to the PAG (Zhao et al. 2014, Redgrave and Dean, 1991). Similarly, auditory stimuli are thought to be transferred directly from the inferior colliculus (IC) to the PAG (Xiong et al. 2015).

1.5 VENTROMEDIAL HYPOTHALAMUS

Ventromedial hypothalamic nucleus (VMH) is located within the medial hypothalamus. Cell densities are highest in the periphery of the nucleus, which is surrounded by a cell-free zone of passing fibres. It is conserved across species (Kurrasch et al., 2007, Shima et al., 2005) and thought to be involved in control of aggression, fear, feeding, thermoregulation and reproduction (review by King, 2006).

VMH can be divided into three main sections, based on the input and output projections, receptor expression and functional studies.

These sections are also anatomically separate and known as the larger ventrolateral (VMHvl), smaller dorsomedial (VMHdm), and the smallest central part (VMHc). VMHdm is thought to be involved mostly in control of fear and energy homeostasis (functions of the VMHdm are discussed in detail below), while VMHvl has been implicated in control of reproduction and aggression. VMHc is not associated with a specific function. VMHdm and VMHvl are part of largely parallel circuits controlling behaviours in response to predators and conspecifics, respectively.

Nr5a1:Cre mouse line

SF1 is a transcription factor expressed in neurons of the VMH, in particular VMHdm and VMHc, as well as the steroidogenic cells of the adrenal cortex, testes, ovaries and reticuloendothelial cells of the spleen (Ikeda et al., 1995). SF1, encoded by a gene called Nr5a1, is a nuclear receptor, which during development acts as a transcriptional regulator of enzymes involved in the synthesis of steroids (more specifically the cytochrome P450 steroid hydroxylases) (Lala et al., 1992). In the brain it is expressed in the developing ventral diencephalon, which eventually becomes the VMH. Image of the distribution of the Nr5a1 gene at the level of the VMH can be found in Figure 1.3.

Stallings et al., 2002 created a transgenic mouse in which eGFP is expressed using a fragment of the Nr5a1 gene promoter, thereby enabling identification of SF1 expressing cells in the VMHdm. Subsequently, a transgenic mouse expressing cre recombinase under the Nr5a1 promoter was created (Dhillon et al., 2006), allowing viral targeting of the VMHdm neurons. The majority of neurons in the VMHdm are SF1+ (Stallings et al., 2002) and a lot of the work on the VMHdm has since been done specifically on the SF1+ neurons

SF1 is also expressed in fish in a region analogous to the VMHdm (Kurrasch et al., 2007) and the promoter region of a gene regulating expression of SF1 is conserved across species, including humans (Shima et al., 2005).

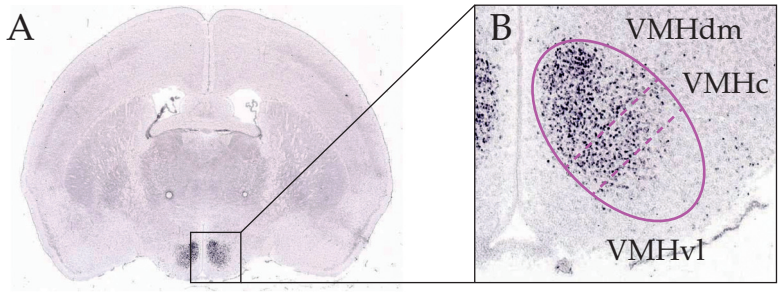

Figure 1.3: Nr5a1 expression in the VMH, ISH. Adapted from Allen Mouse Brain Atlas.

1.5.1 *Inputs*

Neuronal inputs to the MHDC have already been outlined in section 1.4. VMHdm receives particularly strong inputs from MEA and BMA, AH and the parabrachial nucleus (PBN) (Canteras, 2001). Smaller inputs come from the BNST, lateral septal nucleus and the lateral hypothalamus. There is also a small set of inputs from the VMHvl (Fahrbach et al., 1989). The exact nature of these inputs is largely unknown.

Apart from neuronal inputs, cells in the VMHdm also contain receptors which allow them to be modulated through hormones and neuromodulators. SF1+ neurons are known to express both leptin receptors (Dhillon et al., 2006) and insulin receptors (Klockener et al., 2011). It has been shown that insulin inhibits SF1+ neurons (Klockener et al., 2011; Sohn et al., 2016). The effect of leptin on SF1+ neurons is thought to vary depending on the position within the VMHdm, with more laterally positioned cells being inhibited by leptin (Sohn et al., 2016), although previously published studies reported only excitatory effects of leptin on SF1+ neurons (Dhillon et al., 2006). Cannabinoid type-1 receptors have also been found on the SF1+ neurons, and have been shown to be involved in regulating the effects of leptin (Cardinal et al., 2014). Another receptor expressed in the VMH is the thyroid receptor TRβ (Cook et al., 1992). It has been shown that TRβ knockdown in the VMH results in hyperphagia and reduced energy expenditure, causing severe obesity (Hameed et al., 2017). Evidence

suggests that the VMH is also intraconnected and it has been shown that activation of SF1+ neurons increases the frequency of IPSCs in the neighbouring SF1+ neurons (Jo, 2012). It is possible that this could be a feedback mechanism controlling levels of activity within the VMHdm.

1.5.2 *Outputs*

Using the Nr5a1:Cre mouse line injected with ChR2-EYFP, Wang et al., 2015 were able to map the projections of SF1+ neurons from the VMHdm. The major target of the VMHdm was the PAG, especially the dorsal PAG and more caudally also the ventral PAG. Dense projections were also found in the anterior hypothalamus (AH), particularly its ventral part. Moreover, by injecting a retrograde tracer cholera toxin b subunit (CTB) conjugated with a fluorescent dye in AH and the PAG, Wang et al., 2015 were able to estimate that two thirds of SF1+ neurons in the VMHdm project to either AH or the PAG, and over half of these send collateral projections to both.

Other targets of the VMHdm include periventricular nucleus (PVN), medial preoptic nucleus (MPN) and posterolateral part of the BNST. Smaller densities of fibres are found in the central amygdala, medial amygdala, posterolateral cortical amygdala and lateral amygdala. These findings are consistent with previously published studies (Canteras et al., 1994). Projection pattern was not found to vary along the rostrocaudal axis of the VMH (Canteras et al., 1994).

Sternson et al., 2005 also found that excitatory neurons from the medial part of the VMH project to the POMC neurons in the arcuate nucleus, which are known to inhibit feeding (Schwartz et al., 2000). Interestingly, when mice are food deprived, the strength of the connection between the VMH and POMC neurons decreases.

1.5.3 *Functions*

VMHdm has been implicated in control of defensive behaviours, feeding and metabolism (Xu et al., 2011, Gross and Canteras, 2012).

Involvement of the VMHdm in defensive behaviours has first been shown through electrical stimulation experiments. Lammers et al., 1988 recorded behaviour elicited from stimulation at multiple sites of the hypothalamus. They observed changes in locomotion and episodes of jumping during stimulation of the medial hypothalamus. This observation has since been replicated and optogenetic activation of SF1+ neurons has been shown to induce defensive behaviours such as avoidance, immobility and activity bursts (Wang et al., 2015, Kunwar et al., 2015, Viskaitis et al, 2017). Pupil dilatation, increase in the breathing rate and changes in the heart rate have also been observed (Wang et al., 2015), as well as termination of non defensive behaviours, such as feeding, aggression and mating (Wang et al., 2015, Kunwar et al., 2015). Low frequency of activation (5-10 Hz) tends to reduce locomotion and promote freezing, while high frequency of activation (20 Hz) tends to elicit jumping behaviour. Wang et al., 2015 have also shown that behaviour is context dependent. In presence of a hiding box, SF1+ neuron stimulation triggered escape towards the box, while in the absence it induced immobility and only occasional triggered running. In humans electrical stimulation of the VMH has been show to elicit panic attacks (Wilent et al. 2010).

Pharmacological inactivation of SF1+ neurons has been shown to reduce freezing and avoidance in mice in response to a rat (Silva et al., 2013). KO mice with a CNS specific deletion of SF1+ neurons have higher levels of baseline anxiety, reduction in the overall locomotor activity levels, and reduction in the levels of expression of several genes linked to anxiety (Kim et al., 2010, Zhao et al., 2008). Interestingly, these SF1+ KO mice are also obese.

VMH has long been implicated in control of feeding (King, 2006). Viskaitis et al., 2017 have shown that 2 Hz stimulation of SF1+ neurons suppresses feeding without affecting locomotion, autonomic activity or inducing avoidance. In general, stimulation below 4 Hz did not produce any aversion. Moreover, through pharmacological manipulation of SF1+ neurons Viskaitis et al., 2017 were able to show that activation of SF1+ neurons suppresses feeding in fasted mice, while inhibition of SF1+ neurons in fed mice increases their food intake.

Coutinho et al., 2017 noted that SF1+ neuron activation increases insulin mediated glucose uptake by skeletal muscle, heart and brown adipose tissue, thereby increasing energy expenditure. These findings are in line with the observations of the presence of leptin and insulin receptors on SF1+ neurons (Dhillon et al., 2006, Klockener et al., 2011). Furthermore, Garfield et al., 2014 characterised a projection from the PBN to SF1+ neurons, originating in glucose sensing cholecystokinin neurons, inhibited by glucose. Therefore low blood glucose can also increase the VMHdm activity through this projection from the PBN.

The exact function of the VMHdm in control of these behaviours remains unknown and is the subject of this thesis.

1.6 ELICITING DEFENSIVE BEHAVIOURS IN RODENTS IN THE LAB

Over the history of the innate defensive behaviour research, the majority of studies used a live predator to elicit defensive behaviours in rodents (Apfelbach et al., 2005). While it would seem advisable to use the most natural stimulus available, unfortunately an associated disadvantage is a huge variability of the stimulus, making it difficult to compare results from different studies. Moreover, live predator is a polymodal stimulus, which complicates the study of the function of individual brain regions, especially when they might be involved in integration of stimuli of different modalities.

In recent years a number of predator related stimuli has been identified, which can be used instead of a live predator to elicit innate defensive behaviours in the laboratory environment. They are more reproducible, often of a single sensory modality, and allow a more precise investigation of the function of selected parts of the circuit.

1.6.1 *Olfactory stimuli*

Defensive behaviours in rodents can be elicited using a range of olfactory predator stimuli, which can be either natural or synthetic. The natural stimuli used in published studies have been derived from a range of different species, such as domestic cat, lion, jaguar, python, sand boa, red fox, ferret, mongoose and stoat (review by Apfelbach et al., 2015). The exact sources of odour also vary and have included predator urine, faeces, anal gland secretions, fur, fragments of material rubbed against the fur, and fragments of bedding from the predator cage (Apfelbach et al., 2015).

The synthetic compounds used are much more limited and include 2,3,5-trimethyl-3-thiazoline (TMT), derived from fox urine (review by Fendt et al., 2005) and 2-phenylethylamine, derived from bobcat urine (Ferrero et al. 2011). Since their composition is constant, they allow precise control of the odour concentration, unlike the natural predator odour which is variable from one animal to another.

It is important to note that it is not simply the novelty of odour that triggers defensive behaviour. Courtney et al., 1968 showed that presence of cat odour in the arena significantly slows down rats in their pursuit for water, while presence of a deodorant smell does not. Similarly, Papes et al., 2010 showed that rabbit urine did not induce avoidance or risk assessment behaviours in mice, nor did it increase the ACTH levels, while rat, cat and snake derived odours did.

Cat

The vast majority of published studies in rodents have used cat odour as an olfactory predator stimulus, most commonly derived from a domestic cat (Apfelbach et al., 2015).

The first comprehensive study using cat odour was performed by Blanchard and Blanchard, 1989, where a range of defensive behaviours was observed in rats, including immobility, risk assessment, avoidance and reduction in non-defensive behaviours. Moreover, a real cat evoked much stronger responses than just cat odour, as odour alone elicited mostly risk assessment. While most studies have been conducted on rats, cat odour also induces avoidance in mice (Kavaliers et al., 1994).

Since then multiple sources of cat odour have been used: cat collar (Dielenberg et al., 2001), cloth rubbed against a cat (Blanchard et al. 2003c), cat bedding (Kavaliers et al., 1994), cat faeces (Dickman, 1992, Blanchard et al. 2003c) and cat litter (Williams and Scott, 1989). Not all sources of odour elicit the same behavioural response. Berton et al. 1998 showed that faeces from a carnivorous cat induced more anxiety in rats than faeces from a vegetarian cat. Blanchard et al. 2003c found that either cat faeces or a cloth rubbed against a cat could induce avoidance in rats, but not cat urine. Moreover, only the cloth was successful in producing contextual fear conditioning, suggesting that it was more anxiogenic than cat faeces. Certain odours, such as those found in urine or faeces, might be worse indicators of the presence of a predator than odours found on the fur of the animal.

Biological variability in responses exists even when exact same stimulus is used. Hogg and File, 1994 found that rats presented with cat odour could be divided into responders and non responders, with non responders spending significantly less time hiding in the shelter and more time in contact with the source of odour. The two groups did not differ when tested for the general anxiety levels in the elevated plus maze.

It is not clear from published literature whether responses to cat odour habituate. File at al., 1993 reported that avoidance of cat odour did not habituate, although corticosterone levels increased less over repeated exposures. Dielenberg and McGregor, 1999 measured the time rats spent hiding when exposed to cat collar and found that the hiding decreased over time. The anxiety reduction over multiple exposures was also tested on the elevated plus maze. Moreover, Staples et al. 2008 showed that c-Fos activity in different brain regions in rats decreased with multiple exposure to the same cat, although this effect dishabituated with exposure to a different cat.

Snake

A smaller number of studies have used shed snake skin as the olfactory stimulus. Papes et al. 2010 showed that mice exposed to snake skin display avoidance, risk assessment and increase in the ACTH levels. Moreover, Ishii et al., 2017 found an increase in c-Fos expression in the VMHdm in response to snake skin exposure.

Like in case of cat derived olfactory stimuli, published studies report conflicting results. Karen de Oliveira Crisanto et al. 2015 did not observe defensive responses in mice in the presence of snake odour, unlike in response to cat odour. Moreover, they found no changes in c-Fos expression in the medial hypothalamus following exposure to snake odour. The differences in results could be attributed to multiple factors. For instance, Karen de Oliveira Crisanto et al. 2015 used the bedding where the snake was previously residing, while Papes et al. 2010 used 5x5 cm pieces of skin shed by the snake, which might be higher in kairomone concentration. Moreover, the two groups used different snake species, as Karen de Oliveira Crisanto et al tested bedding used by Boa constrictor, while Papes et al. used skin shed by Pantherophis guttatus (cornsnake).

Synthetic compounds

The most commonly used synthetic odour is 2,3,5-trimethyl-3-thiazoline (TMT), derived from fox faeces (review by Rosen et al. 2015). It has been shown to induce avoidance (Blanchard et al. 2003c), however its use as a predator odour remains controversial and it has been suggested that it might be a noxious rather than fearful stimulus (Fendt and Endres, 2008). It has been shown that TMT upregulates c-Fos expression in regions which control gustatory responses, such as the parabrachial nucleus and the nucleus of the solitary tract (Day et al., 2004), but not in the AH or the VMHdm (Staples et al., 2008)

McGregor et al. 2002 showed that TMT does not elicit defensive behaviours in rats, unlike cat odour. Moreover, fibre-sparing lesions to either PMD, AH or VMH do not disrupt TMT-induced unconditioned freezing (Pagani and Rosen, 2009). Since TMT causes an increase in c-Fos expression in the MOB, but not in the AOB (Staples et al., 2008), this might explain why the response to TMT is different as compared to the responses to cat derived odours (Blanchard et al., 2003a; McGregor et al., 2002).

Less commonly used synthetic odours include 2-phenylethylamine derived from bobcat urine (Ferrero et al. 2011) and 2-propylthietane, the main component of weasel anal gland secretion, which has been shown to cause an increase in the plasma levels of ACTH and corticosterone in rats (Perrot-Sinal et al., 1999).

1.6.2 *Auditory stimuli*

A single ultrasound stimulus is sufficient to elicit defensive behaviours in naive laboratory mice (Mongeau et al. 2003). The stimulus used originally in this study included sine-wave sweeps between 17 and 20 kHz at 100 msec frequency and intensity of 85 dB, lasting for 2 seconds each. This frequency of sound it is similar to the frequency

of vocalizations emitted by rats when in a defensive state (Cuomo et al. 1992, Blanchard et al. 1992).

Preliminary experiments from this study, as well as our laboratory, have shown that even a continuous square pulse signal above a certain intensity threshold is sufficient to elicit defensive behaviours (unpublished data), however a sine wave is thought to be more effective at eliciting defensive behaviours (Mongeau et al. 2003). It is possible that the auditory stimulus might not necessarily be specific to a predator, but signal a general danger in the environment.

Behaviours induced by ultrasound include freezing and flight. Interestingly, the type of behaviour is dependent on the environmental conditions and previous experience of the animal. Animals exposed to ultrasound in their home cage respond predominantly with fleeing back to the shelter. In contrast, when placed in a novel environment or having received foot shock treatment beforehand, animals respond with freezing instead of fleeing. This suggests that the internal state of the animal, including the anxiety levels, might affect the behavioural choice, with the probability of freezing increasing with higher anxiety levels.

Ultrasound presentation not only induces defensive behaviours, but also reduces expression of non-defensive behaviours present during the habituation period, such as grooming and rearing. Moreover, it also causes an increase in the heart rate and blood levels of corticosterone. Since the stimulus not only triggers defensive behaviours, but also produces endocrine and physiological responses, it is likely to induce a state of anxiety rather than trigger a simple motor reflex response.

The study by Mongeau et al. 2003 also investigated the pattern of c-Fos mRNA expression across different brain nuclei following ultrasound exposure . They found that the expression was largely overlapping with the pattern of c-Fos expression following exposure to a natural predator.

1.6.3 *Visual stimuli*

Similarly to auditory stimuli, unimodal visual stimuli are sufficient to elicit defensive behaviours in mice (Yilmaz and Meister, 2013). The stimulus typically used is a dark expanding disc, presented overhead the animal, likely to represent a predator approaching from the overhead. It can reliably induce freezing or fleeing and the choice of behaviour is dependent on multiple factors, such as the contrast of the disc, environmental conditions and internal state of the animal.

Visual stimuli are thought to be transferred directly from the superior colliculus to the PAG. While VMHdm might be modifying responses to visual stimuli, it may not be necessary for the expression of the behaviour (Wei et al., 2015, Shang et al., 2015). For this reason I decided not to use visual stimuli in my experimental paradigm, but instead focus on the olfactory and auditory stimuli.

1.7 PREDATOR ODOUR DETECTION IN MICE

1.7.1 *Olfactory pathway overview*

Odours are first detected by two main sensory organs: the olfactory epithelium and the vomeronasal organ (VNO) (review by Dulac and Torello 2003, Stowers et al., 2013, Firestein, 2001). The VNO is specialised for detecting pheromones and projects to the accessory olfactory bulb (AOB), while the olfactory epithelium detects other odourants and projects to the main olfactory bulb (MOB). A third organ, the Grueneberg ganglion cells system, located in the nasal cavity, relays olfactory signals from injured conspecifics (Brechbühl et al. 2008). Since it has been shown that predator odours upregulate c-Fos expression in the AOB rather than MOB (McGregor et al., 2002), it has been postulated that predator odour is processed as a kairomone, a sub-

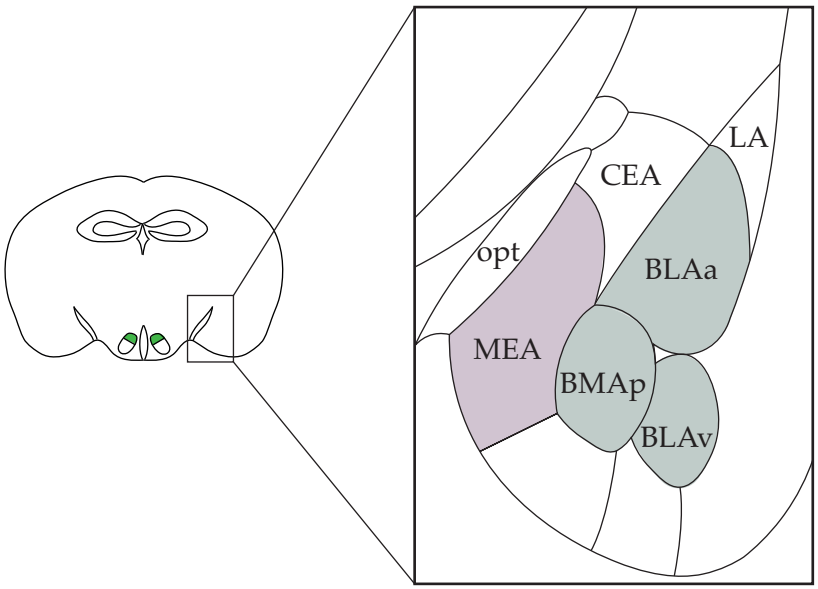

Figure 1.4: Illustration of the position of medial amygdala in relation to the neighbouring nuclei. On the left VMHdm marked in green. Abbreviations: CEA—central amygdala; BLAa—anterior part of the basolateral amygdala; BLAv—ventral part of the basolateral amygdala; BMAp—posterior part of the basomedial amygdala; LA—lateral amygdala; opt—optic tract. Figure adapted from Allen Mouse Brain Atlas and Fox et al., 2015.

stance released by one species which has an effect on another species (Dicke and Grostal, 2001).

The AOB projects primarily to the medial amygdala and the posterior lateral cortical amygdala, with an additional smaller projection to the piriform cortex (Kang et al., 2011). Importantly, cat odour has been shown to upregulate c-Fos expression in medial amygdala (Dielenberg et al., 2001; McGregor et al., 2004). MOB projects to multiple brain areas, including the piriform cortex, olfactory cortical regions, medial amygdala and cortical amygdala (Kang et al., 2011). It has been shown that activation of cortical amygdala can also induce defensive behaviours, while inhibition reduces defensive behaviours in response to TMT presentation (Root et al. 2014).

1.7.2 *Medial amygdala*

Medial amygdala (MEA) is a small amygdalar nucleus, which functionally can be further subdivided into posteroventral (MEApv), pos-

terodorsal (MEApd) and anterior (MEAa) parts. These are defined by different afferent and efferent connections, pattern of activation by different chemosignals, and cellular properties (Canteras et al., 1995; Meredith and Westberry, 2004; Choi et al., 2005, Keshavarzi et al., 2014). Importantly, it has been shown that predator and conspecific threats activate distinct parts of MEA, with MEApv being activated by predator threat and MEApd being activated by conspecific threat (Dielenberg et al., 2001, Choi et al., 2005). MEA activation has also been observed during restraint induced stress (Dayas et al., 1999).

Functionally, fibre sparing lesions with ibotenic acid in MEA reduce freezing when rats are exposed to cat odour and increase the number of contacts rats make with the source of odour (Li et al. 2004). Since MEA lesions do not impair freezing to foot shock conditioning (Nader et al., 2001), it is thought that MEA is involved in control of behaviours in response to innate rather than learnt threats. In vivo recordings in the amygdala in rats confirmed that MEA activity increases in the presence of cat odour (Govic and Paolini, 2015).

While overall 93% of cells in MEA are GABAergic, MEApv is made of 68% glutamatergic cells (Keshavarzi et al., 2014). Major inputs to MEA originate in the AOB, piriform cortex, CoA, BNST and hippocampus (Cádiz-Moretti et al., 2016). Major outputs include projections to parts of the defensive circuit described earlier, i.e. BNST, AHN and VMHdm, but also to other hypothalamic nuclei, the AOB and other amygdalar nuclei (comprehensive study by Pardo-Bellver et al., 2012; also Keshavarzi et al., 2014 and Canteras et al., 1995).

Bian et al, 2008 found that majority of VMH projecting neurons from MEA are glutamatergic and homogenous with regards to their morphological and intrinsic properties. Moreover, they found that these VMH projecting neurons receive direct excitatory inputs from the upstream sensory areas. Similarly, a study by Keshavarzi et al., 2014 has shown that only about 10% of VMHdm projecting neurons from MEApv are GABAergic.

Finally, amygdala stimulation in cats has been shown to reduce the latency of defensive behaviour in response to VMH stimulation (Stoddard-Apter and MacDonnell, 1980). It is not know how information from MEA is processed by the VMH.

1.8 AIMS OF THE PROJECT

Animals can respond to predator threat with a range of behaviours, such as fleeing, freezing, avoidance and inhibition of non-defensive behaviours. As described earlier, the stimulus, environment and internal state of the animal can all affect the behavioural response, for example by changing the probability of one response over the other (such as immobility versus escape) or modulating the strength of its expression.

Published evidence suggests that the VMHdm is important for control of innate defensive behaviours, yet it remains unknown what role it plays and how it contributes to decision making during predator encounter. It has been shown that activating SF1+ neurons in the VMH can elicit different behaviours, such as immobility and avoidance, and that increasing frequency or intensity can also produce jumping escape (Wang et al., 2015, Kunwar et al., 2015). However, it is not understood how different behaviours can be elicited from this one population of neurons. The questions addressed in this project were therefore the following:

1. How does activity in the VMHdm influence the choice of behavioural response to predator threat?

2. What determines the level of activity in the VMHdm in the presence of predator threat?

There are three main factors to consider when addressing these questions: properties of inputs, mechanism of input integration by the VMHdm, and the downstream effects of output projections. Wang et al., 2015 addressed the latter by showing that activity in the VMHdm-AH

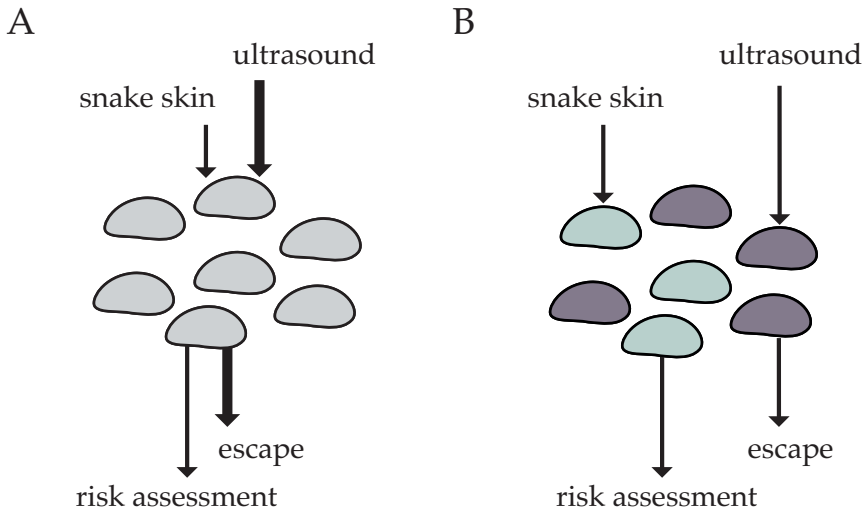

Figure 1.5: Working hypotheses. A. SF1+ neurons consisting of a homogenous population of cells. B. SF1+ neurons consisting of a heterogenous population of cells.

projections induces avoidance, while activity in the VMHdm-PAG projections promotes immobility. While this important finding helps explain how activity in SF1+ cells can elicit these two behaviours, it remains unclear what role the VMHdm has in choosing the most appropriate behaviour.

Experimental approach

I begun the project by conducting a behavioural study to describe behavioural responses to auditory and olfactory predator stimuli. Through these experiments I established conditions in which I could reliably induce defensive behaviours using stimuli of these two modalities, thereby creating a paradigm which allowed me to address the questions of the role of VMHdm in control of these behaviours. I also assessed the behaviour in response to optogenetic stimulation of SF1+ neurons (Chapter 3).

I hypothesised whether population of SF1+ neurons might in fact be heterogenous, consisting of subpopulations of cells with different electrophysiological properties. Such heterogeneity could explain how different populations of cells might be activated by increasing intensity or frequency of light stimulation in the optogenetic exper-

iments, thereby preferentially activating cells projecting to one area over the other, producing jumping escape at higher levels of stimulation.

I therefore performed a series of whole cell patch clamp recordings from SF1+ neurons in acute brain slices and characterised their electrophysiological properties. Using the same technique, in combination with optogenetics, I then characterised the excitatory connection from medial amygdala to SF1+ neurons in the VMHdm. I also studied the behavioural effects of activating this pathway by optogenetically stimulating it in vivo (Chapter 4).

Since I have not observed any differences in the electrophysiological properties of SF1+ neurons, I then questioned whether these cells might be receiving a heterogenous pattern of inputs. If that were to be true, cells receiving less threatening inputs might preferentially project to areas promoting avoidance, while cells receiving more threatening inputs project to areas eliciting escape. Illustration of the two possible models can be found in Figure 1.5.

Consequently, I used single cell in vivo calcium imaging to investigate whether auditory and olfactory predator stimuli activate different populations of cells in the VMHdm. I performed these recordings in freely moving mice, exposed to either ultrasound or snake skin. This allowed me to study the in vivo activity levels in the VMHdm and how this activity is correlated with predator stimuli and behavioural output (Chapter 5).

Part II

METHODS

2

METHODS

2.1 ANIMALS

All animal procedures were carried out under the UK Animals (Scientific procedures) Act of 1986 (PPL 70/7652). Genetically modified strains of mice were originally obtained from The Jackson Laboratory, bred and kept at the Biological Research Facility (BRF) at the MRC LMB and the SWC. Animals were housed in standard conditions on a 12h light cycle with ad libitum food and water and with environmental enrichment and were tested during the light phase.

All mice used for electrophysiological recordings were between 8-10 weeks old. Mice used in behavioural experiments, including calcium imaging experiments, were between 8 and 24 weeks old. All mice were female.

Table 2.1 shows a summary of the strains used for experiments and breeding. All genotyping was conducted by the MRC genotyping facility and TransnetYX, with help from the BRF.

2.2 VIRAL CONSTRUCTS

For optogenetic activation of medial amygdala projections in the VMHdm, both in slice electrophysiology (Chapter 4.2.3) and behaviour (Chapter 4.2.4), AAV2-CaMKIIa-hChR2(H134R)-EYFP (UNC Vector Core, 5.1 x10^{12}GC/ml) was used. The CaMKIIa promoter was used to target excitatory cells of the medial amygdala (Wang et al, 2013) in the Nr5a1::RYFP and Nr5a1-Cre mouse lines. The version of the ChR2 used has a mutation of histidine 134 changed to arginine, which was

LINE (JAX STOCK #)	BREEDING STRATEGY
Vglut2-ires-Cre (#016963)	heterozygote x C57BL/6J
Nr5a1-Cre (#012462)	heterozygote x C57BL/6J
VGAT-Cre (#016962)	homozygote x homozygote
tdTomato (#007914)	homozygote x homozygote
YFP (#006148)	homozygote x homozygote
Vglut2::YFP	Vglut2-ires-Cre (ho) x YFP (ho)
Nr5a1::YFP	Nr5a1-Cre (het) x YFP (het)
Vglut2::tdTomato	Vglut2-ires-Cre (ho) x tdTomato (ho)
VGAT::tdTomato	VGAT-Cre (ho) x tdTomato (ho)

Table 2.1: Summary of mouse lines used. het - heterozygote, ho - homozygote.

chosen because it has am increased ionic flow when the channel is open.

For control experiments, AAV2.CamKII0.4.eGFP.WPRE.rBG (Penn Vector Core, 5.8 $x10^{12}$GC/ml) was used to express eGFP instead of ChR2.

To target SF1+ cells in the VMHdm for in vivo optogenetic activation (Chapter 3.2.5), AAV9.EF1.dflox.hChR2(H134R)-mCherry. WPRE.hGHpA (Penn Vector Core, 5.8 $x10^{12}$GC/ml) was injected in the Nr5a1-Cre mouse line. This virus contains the hChR2(H134R)-mCherry coding sequence flanked between two recombination sites, thereby using a Cre-dependent flip-excision (FLEx) mechanism to limit virus expression to Cre-expressing neurons only (Atasoy et al. 2008). The EF-1 alpha promoter (Kim et al, 1990) was used to drive expression in the cells, while WPRE and hGHpA were used to further enhance the expression levels (Zufferey et al, 1999; Srivastava et al, 1983).

For calcium imaging experiments (Chapter 5) AAV9-CAG.Flex- GCaMP6s-WPRE (Penn Vector Core, 6.3 $x10^{12}$GC/ml) was used in the Nr5a1-Cre and Vglut2-ires-Cre mouse lines. The CAG promoter was used to drive expression of GCamP6s in the cre-expressing cells (Miyazaki et al. 1989). GCaMP6s was used instead of its faster variants GCaMP6m and GCaMP6f, because it produces the highest peak $\Delta f/F$ per action

potential (Chen et al, 2013). To answer the questions investigated in Chapter 5, improved signal to noise ratio was considered more important than the temporal resolution of the calcium signal.

All viruses used in this study were kindly ordered and aliquoted by Dr Li Jin and Dr Tulin Okbinoglu.

2.3 SURGICAL PROCEDURES

General surgery set up

A mixture containing ketamine (95 mg/kg) and xylazine (15.2 mg/kg) was injected intraperitoneally to anaesthetise the animals. Carpofen (5 mg/kg) was administered subcutaneously and animals were placed into a stereotaxic apparatus (Model 1900 and 963, David Kopf Instruments). The depth of anaesthesia was monitored throughout surgery and isoflurane (1-1.5% in O2, 1 l/min) was used for anasthesia maintenance.

A midline saggital incision was made to expose the skull and craniotomies were made using a 0.5 mm burr drill (Fine Science Tools) to allow virus injection or fibre implantation. Implants were attached to the skull using light-cured dental cement (RelyX Unicem 2, 3M). At the end of the surgery, the wound was sutured (6-0, Vicryl Rapide) and glued (Vetbond). Animals were injected subcutaneously with antisedan (0.08 ml) and allowed to recover in a heated cage at 27°C for 2 hours, after which they were transferred back to their come cage.

Experiments were started at two weeks after the surgery to allow enough time for viral expression and animal recovery.

Viral injections

Glass pipettes (10µl Wiretrol II) were pulled on a Sutter P-1000 puller. At the start of surgery, pipettes were backfilled with oil, mounted on an electrode holder coupled to a hydraulic micromanipulator (MO-10, 21 Narishige) on the stereotaxic frame and viral vectors were drawn

in through the pipette tip. During the surgery the pipette was slowly (3 mm/min) lowered through the brain tissue until the desired depth. The vectors were delivered at 10nl/min and pipette left in the same position for further 5 minutes to ensure the whole intended volume of solution has been left the pipette. VMHdm injection coordinates were AP: -1.6, ML: ±0.4, DV: -5.4. The medial amygdala (MEApv) injection coordinates were AP: -1.7, ML: ± 2.1, DV: -5.4.

Optic fibre implants

For optogenetic experiments, one optic fibre (200 m diameter, MFC-SMR; Doric Lenses Inc.) was implanted unilaterally immediately following the virus injection. The fibre was implanted at a speed of 3 mm/min, positioned 200 µm dorsal to the injection site and attached to the skull with dental cement.

GRIN lens implants

For calcium imaging experiments, a GRIN lens (SICL_V_500_80; Doric Lenses Inc.) was implanted following the virus injection. First a 23G (0.58 mm) needle with a cemented opening was slowly (1 mm/min) inserted 200um dorsal to the injection site, to minimise tissue compression during insertion of the cannula, and then slowly removed. The GRIN lens was then slowly (1 mm/min) inserted to the same depth as the injection site and attached to the skull with dental cement.

Head-fixed two photon imaging

For head-fixed two photon imaging, a craniotomy was performed to create a small cranial window. An outline of the cranial window (3 mm diameter) was shaved with a 0.5 mm burr drill until the bone in the middle could be lifted with forceps without causing any drilling. The exposed brain tissue was covered with a 3 mm diameter coverslip (Harvard Bioscience, Inc.). A 3D-printed metal headplate was then affixed to the skull using light-cured dental cement.

2.4 ELECTROPHYSIOLOGICAL RECORDINGS IN ACUTE BRAIN SLICES

Preparation of acute brain slices

All electrophysiological recordings were performed using the Nr5a1::RYFP strain. Animals were anaesthetised with isoflurane and rapidly decapitated. The tissue was immediately transferred to an ice cold oxygenated artificial cerebrospinal fluid (aCSF) containing (in mM): NaCl (119), $NaHCO_3$ (26), glucose (10), KCl (2.5), $CaCl_2$ (2), $MgCl_2$ (1), NaH_2PO_4 (1) (all chemicals purchased from Sigma-Aldrich), equilibrated with carbogen (95% O_2 and 5% CO_2). The brain was quickly removed and secured to the stage of the vibratome (VT1200, Leica) with superglue (Loctite). Coronal slices of 200 µm thickness were collected at the level of the VMH (-1.3 mm to -1.8 mm from bregma), allowed to recover at 35°C for 30 min and then stored at room temperature (19–23°C) for up to 6 hours in oxygenated aCSF.

Data acquisition

Brain slices were submerged in a recording chamber and secured in place under a nylon string grid stretched over a metal wire. Slices were perfused continuously with an oxygenated aCSF heated to 33°C, using a peristaltic perfusion system (PPS2, Multi Channel Systems) at rate of 1ml per min . Data from whole-cell patch clamp recordings was obtained with EPC 800 amplifier (HEKA), digitized at 20 kHz (PCI 6035E, National Instruments), filtered at 5kHz and recorded in custom software made in LabVIEW (2015 64-bit, National 12 Instruments; software created and maintained by Kostas Bestios).

Recording pipettes were pulled with a micropipette puller (P-1000, Sutter, USA) from borosilicate glass capillaries (Harvard Apparatus, 1.5 mm OD, 0.85 mm ID). Pipette resistance was 6-8 MΩ. Patch pipettes were backfilled with an internal solution containing (in mM): KGluconate (130), KCl (10), HEPES (10), Mg-ATP (2), Na-ATP (2), EGTA (1), Na2-GTP (0.3), 290mOsm.

SF1+ cells were identified by their EYFP fluorescence, using 490 nm LED illumination (pe-100, CoolLED), 4X dry objective (PLN-CY, 0.1 NA, Olympus) and 60X water-immersion objective (LUMPlanFL N, 1.0 NA, Olympus). Once a suitable, healthy looking cell was identified, the pipette was advanced towards the identified cell under positive pressure, which was released near the cell. A gentle suction was applied to form a GΩ seal, after which the membrane was ruptured with further suction to establish a whole cell configuration. The resting membrane potential was measured immediately in current clamp. Input resistance and series resistance were monitored throughout the experiment, and series resistance was compensated in current-clamp recordings. Only cells with series resistance <30 MΩ were used for analysis.

For a subset of experiments (Chapter 4.2.2), selective inhibitors have been added to the aCSF: the inhibitory inputs were blocked using 60 mg/l picrotoxin (Sigma-Aldrich), while excitatory inputs were blocked using 376 mg/l kynurenic acid (Sigma-Aldrich).

Optogenetic stimulation

In optogenetic activation experiments, ChR2 was stimulated with wide-field 490 nm LED illumination (pe-100, CoolLED). Synaptic inputs were evoked with LED light pulses over the area containing the recorded cell. The stimulation protocols used light pulses of 1 ms duration and varying number and frequency of the pulses.

Immunohistochemistry

At the end of the recording sessions, slices were fixed in 4% paraformaldehyde (PFA) in PBS for 20 mins at 4°C, after which they were rinsed in PBS and mounted on a glass slide slides in SlowFade Gold (S36938, Life Technologies). Slides were imaged using a Nikon TE2000 wide-field microscope.

2.5 BEHAVIOURAL PROCEDURES

General set up

Behavioural experiments were conducted in a rectangular arena (L: 60 cm x W: 20 cm x H: 40 cm) made of red tinted perspex placed inside a custom made sound and light isolated cabinet. An open ended shelter (L: 10 cm x W: 20 cm x H: 20 cm) was positioned at one end of the arena. Different shelter dimensions were tested to ensure the shelter was recognized a safe place by the animal, but not so safe that the exploratory drive was reduced.

Infra-red light in the cabinet was provided by six LED illuminators (TV6700, Abus). All behaviour was recorded at 50 frames per second with a near-IR GigE camera (acA1300-60gmNIR, Basler) positioned above the arena centre. Video acquisition and all stimulation protocols (auditory and optogenetic) were controlled with LabVIEW custom software and triggered using hardware-time signals controlled with a PCIe-6351 board (National Instruments) to allow synchronization. Animal position in the arena was tracked on-line in LabVIEW based on the centre of mass of the animal. Optogenetic and auditory stimuli were delivered when the animal entered a pre-defined ROI (L: 15 cm x W: 20 cm) at the end opposite to the shelter. The arena was washed with 70% ethanol in between the experiments.

Sensory stimuli

The auditory stimulus consisted of a sweep of increasing frequency from 17 to 20 kHz over 3 seconds (Mongeau et al. 2003) at a sound pressure level of 80 dB at the floor of the arena. Sound waveform files were created in MATLAB (Mathworks). The sound files were played from LabVIEW, amplified (QTX Sound PRO 240) and delivered through an ultrasound speaker (L60, Pettersson) suspended 60 cm above the arena, at the end opposite to the position of the shelter.

The olfactory stimulus consisted of a 0.20 g fragment of a shed snake skin (Bothrops jararaca). The snake skin was inserted and removed manually from the top of the arena. The snake skin was reused and in between the experiments stored in an air tight container at -20°C. The stock of snake skin was stored at -80°C.

To control for the stimulus of manual insertion and removal of the snake skin, as well as for the presence of a foreign object inside the arena, a transparent, clean petri dish (D: 35 mm, H: 10 mm, Falcon) was used in control experiments.

Optogenetic stimulation

Light was delivered by a 473 nm laser diode module (Stradus, Vortran), triggered by a sequence of pulses generated in LabVIEW. Laser intensity was modulated through an analogue input controlled by LabVIEW to achieve irradiance of 10 mW/mm² at the tip of the implanted cannula. Light transmission of each cannula was measured prior to surgical implantation. The laser diode was connected through an optic fibre (M72L02, Thorlabs) to a rotary joint (FRJ 1x1, Doric Lenses Inc.) positioned above the area, from which the light was transmitted by a magnetic patchcord (MFP_200/230/900-0.37_0.6m_FC-SMC, Doric Lenses Inc.) to the implanted cannula. The rotary joint allowed animal to move unrestrained around the arena. The stimulus consisted of 10ms light pulses of different frequencies.

Immunohistochemistry

At the end of each series of behavioural experiments, histology was performed to confirm the sites of injection and implantation. Animals were anaesthetised with Euthatal (0.1-0.2 ml of a 1:1 dilution in PBS) and transcardially perfused with 10-15 ml of ice-cold PBS with heparin (0.02 mg/ml) followed by 4% para-formaldehyde (PFA) in PBS. Brains were dissected out and fixed in 4% PFA overnight at 4°C, then washed once in PBS and and transferred to 30% sucrose solution in PBS for 48 hours. They were then embedded in the optimal

cutting temperature (O.C.T.) compound (Thermo Fisher Scientific), rapidly frozen on dry ice and 30 µm sections were cut using a cryostat (CM3050S, Leica). Brain sections were mounted on a glass slide using DAPI containing SlowFade Gold mounting medium (S36938, Life Technologies). Slides were imaged using a Nikon TE2000 widefield microscope.

2.6 CALCIUM IMAGING

Two-photon excitation microscopy

Two-photon imaging was performed using a resonant two-photon microscope (Neurolabware) and controlled through the Scanbox software.

The focus was first adjusted using an epifluorescence port camera. Fluophores were excited with 900 nm light produced by a titanium-sapphire laser (Spectra-Physics Mai Tai, average power 2.1 W, pulse width <100 fs, Newport), laser intensity regulated through a Conoptics Pockels Cell (302RM driver and 350-80-LA EO modulator) and controlled with shutter (LS6, Uniblitz).

Images were obtained by scanning at 512 lines per frame using an 8 kHz resonant scanner (Cambridge CRS) and a galvanometer scanner (Cambridge 6215H). The light was focused through a 16X water-immersion objective (Nikon, 0.8 NA). Emitted light was collected by two GaAsP detectors (H11706-40, Hamamatsu), allowing dual colour imaging. The images were acquired with a DHPCA-100 amplifier (Femto) and digitized at 80 MHz (ATS9440, AlazarTech).

Head-fixing

For the two photon imaging experiments, animals were first anaesthetised with isoflurane to minimise anxiety resulting from the process of transferring them over to the microscope. The animals where then placed inside a 3D printed tube in which they could sit com-

fortably (originally designed by Dr Edward Bracey and modified and printed by Martyn Stopps and Robb Barrett at the SWC Fablabs). The tube was printed in ASA production grade thermoplastic (Stratasys) and covered with flexible silicon coating (FSC05L, Electrolube).

Next to the tube there was a height adjustable headplate holder (Thorlabs). Both the tube and the headplate holder were attached to a platform fixed to a motorized linear translation stage (Thorlabs).

Single-photon excitation microscopy

Calcium imaging in freely moving animals was performed using a miniaturized head-mounted fluorescence microscope (Model L, Doric Lenses Inc.). The set up consisted of a fluorescence microscope driver (FMD_L), controlled through Doric Neuroscience Studio software. Trigger signals were sent to the connectorised LED (CLED), connected to a snap-in fluorescence microscope body (SFMB_L) through a rotatory joint (AHRJ-OE_PT_AH_12_HDMI) and two mono fibre-optic patch cords (MFP 200/230/LWMJ-0.48: 0.8m_FC-CM3 and 1m_FC_FC). A copy of the signal was send to a PCIe-6351 board (National Instruments) to allow synchronization with the custom LabVIEW data acquisition software. Images were acquired through an implanted snap-in imaging cannula (SICL_V_500_80; Doric Lenses Inc.) to which the microscope body was attached prior to each experiment. The microscope body containing a 0.5 NA objective lens, a dichroic beamsplitter, and a CMOS sensor was connected back to the microscope driver through an electrical cable.

Calcium imaging analysis

Fluorescence images were first corrected for movement artifacts in Doric Neuroscience Studio. All following image processing was performed in Fiji. Images were first background-subtracted (rolling ball radius 50 pixels), ROIs were manually drawn and mean intensity traces were extracted for each ROI. The traces were then interpolated

with the behavioural data in LabVIEW using custom written scripts in Python 2.7.

The behavioural videos were manually annotated to mark specific behavioural events and correlate them with the calcium transient activity. The behaviour tagging included: detection of the auditory stimulus (head turn), onset of the turn prior to the escape, initiation of the escape, insertion of the snake skin/petri dish, removal of the snake skin/petri dish, sniffing of the snake skin/petri dish.

2.7 DATA ANALYSIS

Analysis was performed using custom-written scripts in Python 2.7. Statistical analysis was performed in GraphPad Prism. Statistical significance was defined at 95% confidence limit (p-value <0.05). Same size pair-wise comparisons were analyzed using parametric paired or unpaired two-tailed Student's t-test, samples of unequal sizes were analyzed using Welch's t-test. All data are reported as mean ± standard deviation (SD) unless stated otherwise. Plots were created using custom-written scripts in Python 2.7 and GraphPad Prism.

Part III

RESULTS

3

INDUCING DEFENSIVE BEHAVIOURS

3.1 INTRODUCTION

When exposed to predators or predator-related stimuli, mice innately respond with defensive behaviours. These behaviours have been studied extensively across a variety of mouse species, in different experimental conditions and using a range of predator stimuli. Some of those published studies are described in Chapter 1.

Mice can display a variety of defensive behaviours. Genetic background, subtle differences in experimental conditions, nature of the predator stimulus - all of these affect the behavioural outcome. Before starting to investigate how this choice of behaviour is made at a neuronal level, it is necessary to create a behavioural paradigm in which these behaviours can be elicited in the laboratory. I therefore started the project by characterising defensive behaviours elicited by auditory and olfactory stimuli, specifically by ultrasound and snake skin. I observed a number of similarities and differences in behaviours elicited by these two stimuli, the results of which are presented in this chapter.

I next assessed the behavioural effects of optogenetically activating SF1+ neurons in the VMHdm. In accordance with published results (Wang et al., 2015, Kunwar et al., 2015, Viskaitis et al, 2017), I observed that different behaviours could be elicited through activation of SF1+ neurons depending on the frequency of activation.

Taken together, these results show that mice express behaviours appropriate for a given type of stimulus. They also establish a paradigm for investigation of the role of the VMHdm in choosing the most appropriate behavioural response, addressed in the following chapters.

3.2 RESULTS

3.2.1 *Quantifying defensive behaviours*

There are many ways to quantify defensive behaviours, some of which have been described in Chapter 1. In this project defensive behaviours were quantified mostly based on the position of the animal in the arena, from which the speed of movement, avoidance and risk assessment were quantified.

The animal was placed in the arena and behaviour was recorded throughout the experiment. The centre of mass of the animal was tracked over time in form of xy coordinates. Each experiment lasted 20 minutes. During the first 10 minutes mouse was allowed to habituate to the arena, while in the second 10 minutes it was exposed to the test stimulus which was presented in the region of interest (ROI).

The path travelled by the animal over time was first plotted, providing a quick visual overview of the animal's locomotion and exploration of the arena. An example of movement of the animal over a period of 10 minutes can be found in Figure 3.1. The two graphs illustrate the movement over the first (3.1C) and second (3.1D) half of the experiment. This is a visual representation of the motility of the animal and it can give an indication of the internal state of the animal. Reduced or increased motility can be suggestive of an altered internal state, which can be due to factors such as anxiety or hunger. In this case there was no stimulus introduced in the second half in order to assess whether movement and exploration change over time.

To quantify the animal's preference for a given area we can measure the time the animal spends in this area. This can be presented either as the proportion of total time spent in the area (Figure 3.1E and G) or by calculating the place preference index (Figure 3.1F and H). In this case the area of interest (shelter or ROI) constituted 1/5th of the total area, therefore the place preference index was calculated from

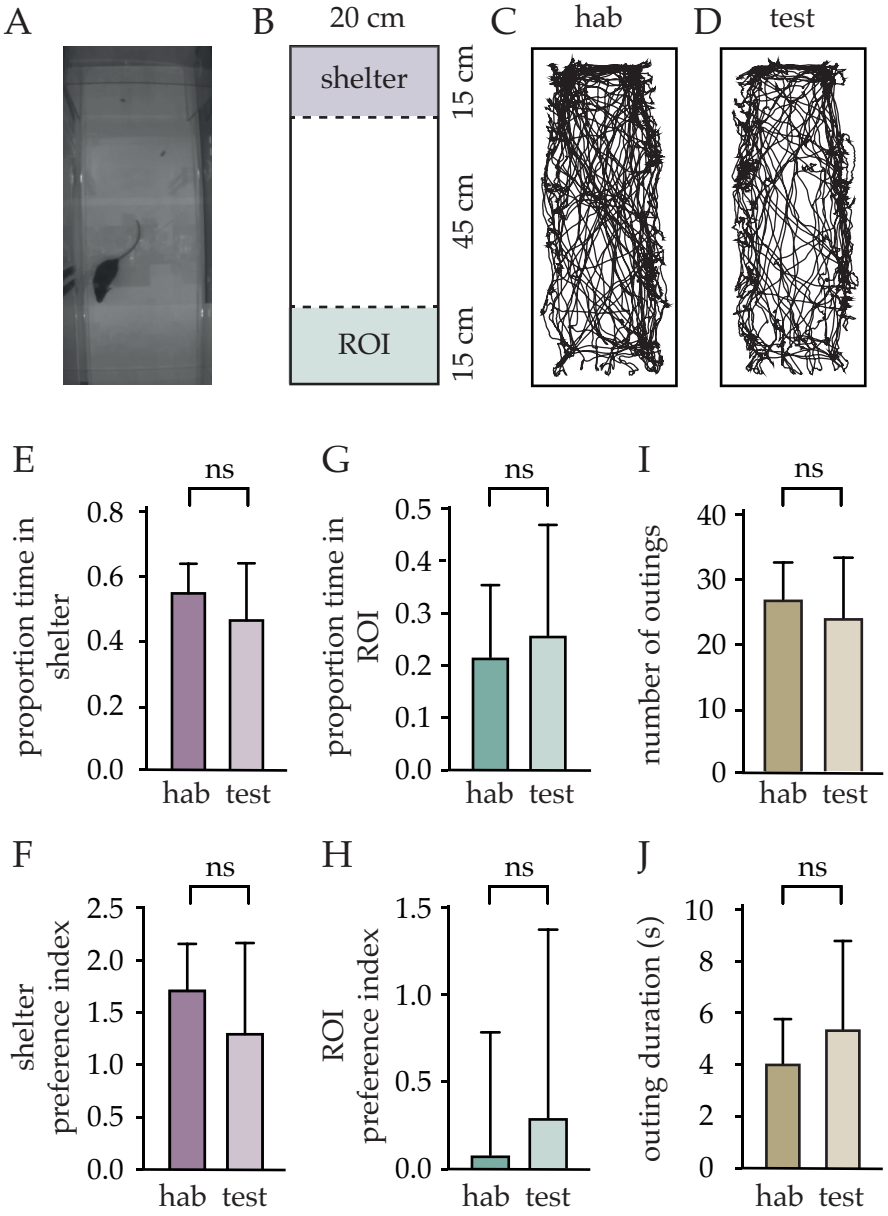

Figure 3.1: Overview and quantification of the behavioural experiments. A. Photo of the arena with a mouse B. Sketch of the arena C. Path travelled by the animal during the habituation period (10 mins) D. Path travelled by the animal during the test period (10 mins) E. Proportion of the time spent in the shelter F. Shelter preference index G. Proportion of the time spent in the ROI H. ROI preference index I. Number of outings J. Duration of each outing. hab – habituation, 0-10 mins, test – 10-20mins. n=6

the equation (p-0.2)/0.2, where p is the proportion of total time the animal spent in that area (adapted from Takahashi and Tsuboi, 2017). If the animal had no preference for the area, it would spend 1/5th (i.e. 0.2) of the total time there, thereby giving an index of approximately 0. Therefore positive values indicate place preference, while negative values place avoidance. Index of -1 illustrates complete avoidance (animal spends no time in that area), while index of 4 means that the animal spends all the time there. The preference index gives a better visual representation of the animal's place preference and therefore has been used in the subsequent analysis instead.

Using the above methods we can measure the animal's preference for the shelter (Figure 3.1E and F). The mean proportion of time spent in the shelter was 0.55 ± 0.09, while the place preference index for the shelter was 1.73 ± 0.45. Both values are significantly different as compared to the values expected in absence of any preference, namely 0.20 and 0 respectively ($p<0.0001$). Therefore the animal had a preference for the shelter, suggesting that the shelter was considered to be the safest or the most comfortable place in the arena, most likely due to the enclosure it provided. This preference for the shelter is determined by a balance between factors such as the desire to explore, for instance in order to search for food, and the anxiety of encountering danger.

We can use the above measures to investigate the effect of a stimulus which is later presented in ROI. First we can quantify the place preference for ROI during the habituation period. The proportion of time spent in ROI was 0.22 ± 0.14, which corresponds to ROI preference index of 0.08 ± 0.68. These are not significantly different from the expected values of 0.20 and 0 respectively ($p=0.79$).

While mice prefer to stay in the shelter, they periodically leave the shelter to explore the arena. They do so mostly for the purpose of foraging. Since animals try to minimise the risk of exposure to predators, this foraging behaviour is usually seen in the form of short exploratory trips from the shelter. Therefore the number of these exploration

trips and the duration of each trip can also be used to assess the internal state of the animal. There are many reasons for why the length of these trips could vary. One assumption is that a more anxious animal should be more likely to stay in the shelter, although multiple other factors can play a role. During the period of habituation the number of exploration trips was equal to 26.3 ± 5.6 (Figure 3.1I), while the mean length of each trip was equal to 4.1 ± 2.3 s (Figure 3.1J).

Paired t-test was used to analyse the differences in the shelter and ROI preference, as well as the number of trips. Welch's t-test was used to analyse the differences in duration of the trips.

Behavioural changes over time

Since the internal state of the animal is not constant, the pattern of movement and exploration can change over time. As the animal becomes more familiar with the environment, the anxiety of being in new surroundings decreases, which might increase exploration. Other factors can also change, such as hunger or energy levels. It is therefore important to consider the influence of the time factor in assessing the effect of a stimulus on the behaviour.

Figure 3.1 illustrates changes in the behaviour between the first (habituation) and second (experimental) half of a 20 minute long experiment. There was no significant change in the place preference over time, neither in the shelter preference index (decrease to 1.31 ± 0.87, p=0.32) nor the ROI preference index (increase to 0.29 ± 1.05, p=0.69). There was also no significant difference in the number of trips the animal took over that period (decrease to 23.5 ± 9.1, p=0.53). However, there was a slight increase in the duration of each exploration trip (increase to 5.4 ± 4.0 s, p=0.0003). This might reflect reduced anxiety of the animal as it became more comfortable in the new environment. It could however also reflect an increase in the motivation to explore, perhaps in order to find food or water.

Having observed the behaviour in the absence of any stimuli, I next tested the effects of olfactory and auditory predator stimuli.

3.2.2 *Behavioural responses to olfactory predator cues*

Multiple olfactory stimuli have been used in published studies to elicit defensive behaviours, as outlined in subsection 1.6.1. However, often stimuli of seemingly similar origin elicit behaviours in one study but not in another (Karen de Oliveira Crisanto et al. 2015, Papes et al. 2010). This can be due to subtle differences in stimulus presentation, kairomone concentration, experimental set up, genetic differences in the test subjects, and many others.

At the beginning of the project I performed preliminary testing of a variety of olfactory stimuli, which included bobcat urine (PredatorPee), fox urine (PredatorPee), 4-methylthiazole (Sigma-Aldrich), TMT (Sigma-Aldrich), isoamyl acetate (Sigma-Aldrich), cat collar, cat fur, shed snake skin, rat fur, rat bedding, and an anaesthetised rat.

While volatile compounds triggered freezing and avoidance, they were also very pungent and it was not clear whether the behaviour was a result of fear or simply aversion of a painfully unpleasant olfactory stimulus (Fendt and Endres, 2008). Out of all the natural predator stimuli I tested, snake skin elicited most reliable and strongest responses in the form of risk assessment and avoidance. Therefore all the following experiments were conducted using snake skin as the olfactory predator stimulus.

Behavioural responses to snake skin

The animal was placed in the arena and given 10 minutes to explore and habituate to the environment. After that time, snake skin was manually inserted from the top of the arena and placed on the ground inside ROI. The animal was free to explore the arena for the following 10 minutes, including the region with the snake skin, after which the snake skin was manually removed.

Behavioural responses to snake skin can be broadly divided into two categories, based on whether snake skin produced an increase or decrease in the ROI preference index. The majority of mice (4/6),

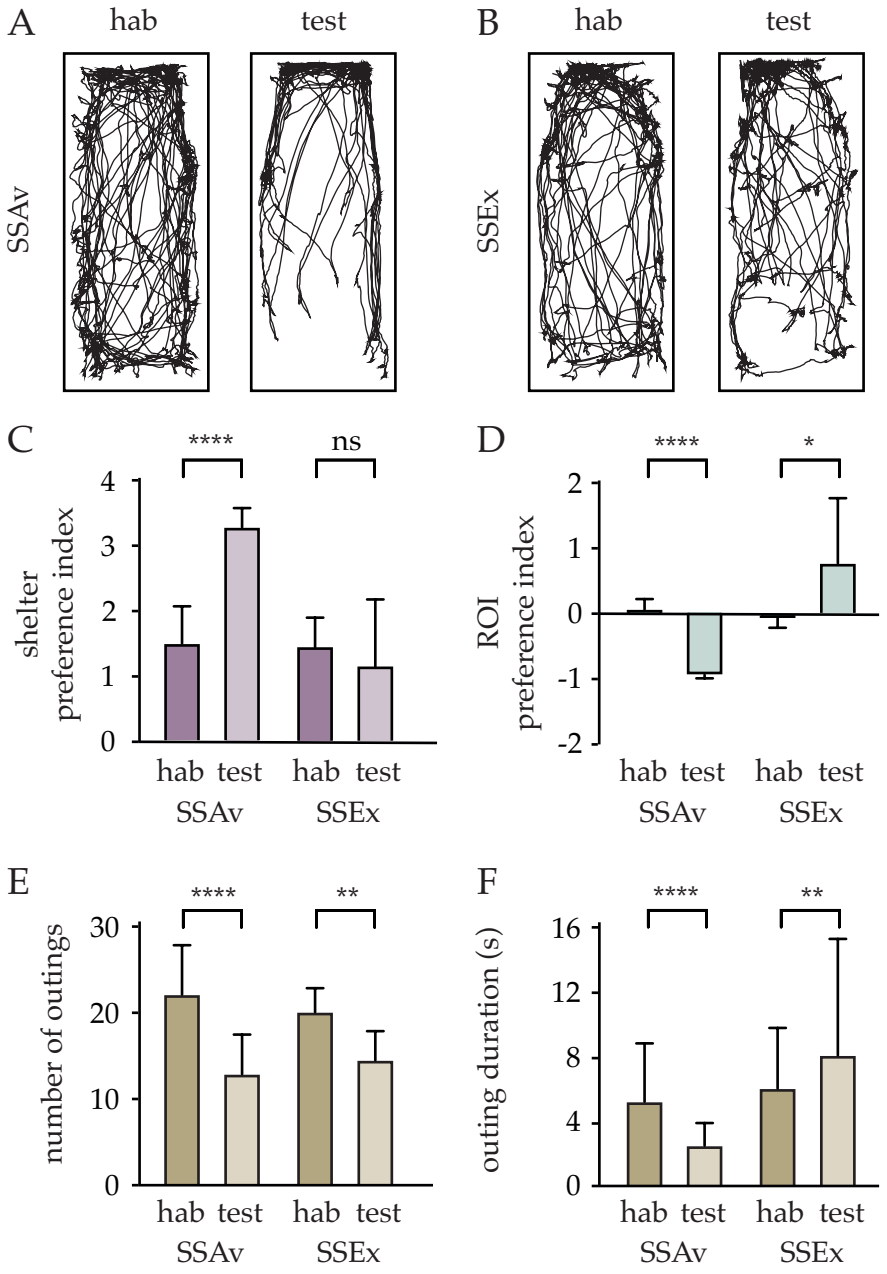

Figure 3.2: Behavioural responses to snake skin. A. Path travelled during the habituation period (left) and exposure to snake skin (right), SSAv B. Path travelled during the habituation period (left) and exposure to snake skin (right), SSEx C. Shelter preference index D. ROI preference index E. Number of outings F. Duration of each outing. hab – habituation, 0-10 mins, test – 10-20mins. n=6

which I will refer to as SSAv (snake skin avoiders), showed a marked ROI avoidance and risk assessment of snake skin. The risk assessment consisted of slow approach towards the snake skin, stretch posture combined with sniffing, and a quick retraction back to the shelter. Figure 3.2A illustrates this type of behaviour. A smaller proportion of mice (2/6), referred to as SSEx (snake skin explorers), did not show this stereotypical risk assessment, but instead showed an active interest in the snake skin, as observed by an increase in the ROI preference index, occasionally even attempting to bite the snake skin and drag it towards the shelter (Figure 3.2B).

SSAv showed a significant avoidance of the area with the snake skin as compared to the habituation period (from 0.05 ± 0.16 to -0.93 ± 0.05, $p<0.0001$), as well as an increased place preference for the shelter (from 1.50 ± 0.58 to 3.30 ± 0.30, $p<0.0001$), which is indicative of increased fear. Note the small standard deviation in the place preference indices, illustrative of low variability within this group of animals. SSAv also had a reduced number of outings (from 22.3 ± 5.8 to 13.0 ± 4.6, $p<0.0001$) and a significantly reduced duration of each outing (from 5.1 ± 3.6 s to 2.4 ± 1.4 s, $p<0.0001$). This short outing duration and low standard deviation illustrates the risk assessment behaviour. Since every trip out of the shelter led to a single risk assessment, the number of risk assessment episodes over the 10 minute period is equal to the number of outings. It is a significant increase as compared to no risk assessment episodes in the habituation period ($p<0.0001$).

The escape speed from snake skin was 62.8 ± 6.1 cm/s, slightly higher as compared to the speed of return to the shelter in the absence of any stimuli (54.9 ± 7.0 cm/s, $p=0.0011$). It is important to note that animals often escaped back to the shelter before reaching the snake skin, therefore it is possible that in some cases animals did not achieve their maximal escape speed.

A smaller proportion of mice, SSEx (snake skin explorers) did not show this stereotypical risk assessment. Instead, they showed an in-

creased interest in the object, as illustrated by the increased ROI place preference (from -0.03 ± 0.15 to 0.74 ± 0.98, p=0.0429) and no change in the shelter place preference (from 1.45 ± 0.46 to 1.15 ± 1.05, p=0.4709). The number of outings from the shelter was decreased (from 20.3 ± 2.8 to 14.6 ± 3.4, p=0.0029). The duration of each outing was slightly increased (from 6.0 ± 3.7 s to 8.0 ± 7.1 s, p=0.0054), which could explain the reduction in the number of outings, especially considering the very large standard deviation.

Similar variability in responses to predator olfactory cues was observed by File at al., 1993. Based on the responses to cat odour, the rats they observed could be divided into responders and non responders. Interestingly, the two groups did not differ when tested for the general anxiety levels on the elevated plus maze. The neural basis of these differences in responses has not been investigated in the published literature.

Adaptation

In order to assess whether defensive responses change over time, either due to increased aversion of ROI or adaptation to snake skin, I repeated the experiment in SSAv over four sessions on separate days. The behaviour was consistent across the sessions, showing no signs of adaptation to snake skin (Figure 3.3). There was no change in the ROI preference index (RM one way ANOVA, p=0.9357) nor in the shelter preference index (RM one way ANOVA, p=0.2312). This is in line with other studies showing lack of adaptation of responses to cat odour (Zangrossi and File, 1994).

During the habituation period there was a slight aversion of ROI from the previous sessions, as measured by a decrease in the ROI preference index (RM one way ANOVA, p=0.0133) and an increase in the shelter preference index (RM one way ANOVA, p=0.0003). Zangrossi and File, 1994 showed that contextual fear development can be dependent on the duration of exposure to the odour.

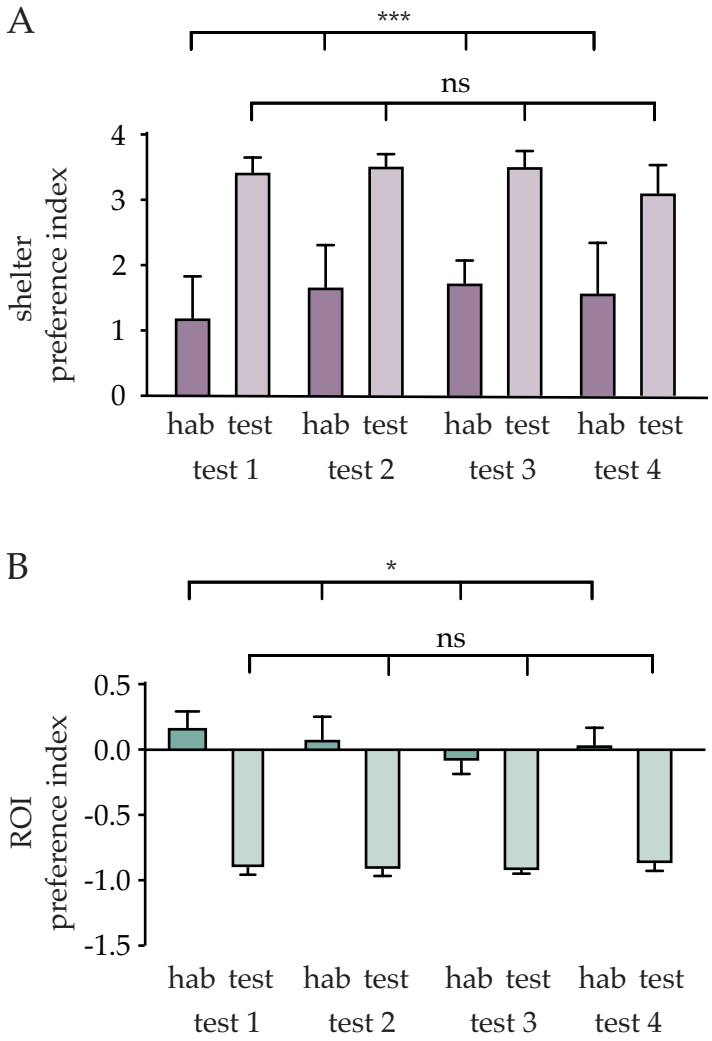

Figure 3.3: Adaptation of the behavioural responses to snake skin in SSAv, measured over 4 testing sessions. A. Shelter preference index B. ROI preference index. n=4

In order to test whether the behavioural responses were induced specifically by snake skin or more generally by the presence of a novel object, mice were also exposed to a petri dish in a separate set of experiments.

Behavioural responses to a novel object

Mouse was placed in the arena and given 10 minutes to explore and habituate to the environment. After that time, a clean 3 cm petri dish was placed on the ground at the end opposite to the shelter. The animal was free to explore the arena, including the region with the petri dish, for the following 10 minutes, after which the petri dish was removed.

Unlike in case of snake skin, mice did not show a significant increase in the number of risk assessment episodes over the 10 minute period when the petri dish was in the arena (from 0 to 1.3 ± 1.5 episodes, p=0.0822). Moreover, risk assessment happened only at the beginning of the 10 minute period and animals quickly adapted to the presence of the petri dish, after which the risk assessment behaviour stopped. Half of mice did not show any risk assessment at all. Animals did not show a significant change in the ROI place preference index (from 0.00 ± 0.37 to -0.17 ± 0.54, p=0.5099) nor in the shelter preference index (from 1.42 ± 1.01 to 2.09 ± 1.29, p=0.1552). However, the number of outings from the shelter was significantly decreased (from 24.5 ± 6.8 to 14.7 ± 7.9, p=0.0011). The duration of each outing was not significantly different (from 4.8 ± 3.4 s to 5.9 ± 5.2 s, p=0.0742).

The escape speed back to the shelter following risk assessment was 57.2 ± 10.2 cm/s, which is not significantly different from the average speed of return to the shelter during foraging (p=0.4272), but neither from the escape speed from snake skin (p=0.0578).

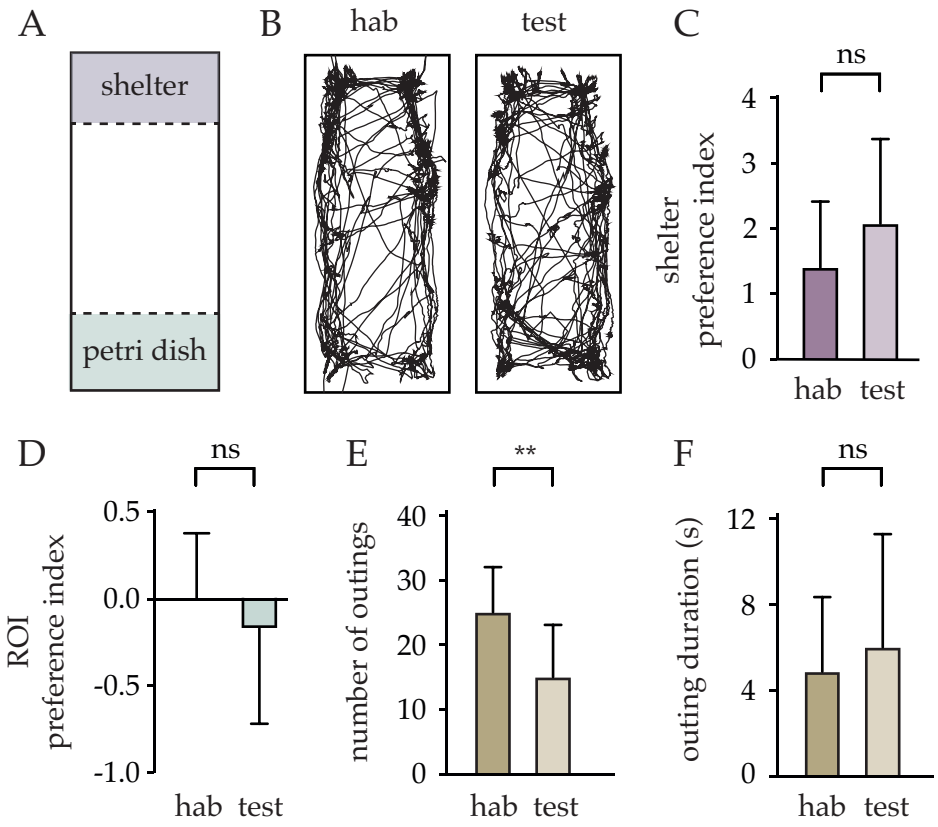

Figure 3.4: Behavioural responses to a novel object (petri dish). A. Illustration of the arena B. Path travelled during the habituation period (left) and petri dish presentation (right) C. Shelter preference index D. ROI preference index E. Number of outings F. Duration of each outing. hab – habituation, 0-10 mins, test – 10-20mins. n=6

3.2.3 *Behavioural responses to auditory predator cues*

The animal was placed in the arena and given 10 minutes to explore and habituate to the environment. After that period, when the animal entered ROI, a single 3-second-long 17-20 kHz sweep of ultrasound was triggered. Each animal was exposed to three presentations of ultrasound, separated by at least one minute to allow the animal to revisit ROI at least once and reduce the risk of developing aversion.

All animals clearly detected the ultrasound and responded with a head turn. On virtually all trails the animals fled towards the shelter (17 out of 18 trials), although in some cases the animals fled towards the shelter without fully entering it. The maximum speed of escape was 78.6 ± 16.0 cm/s, significantly higher than the speed of return to the shelter in the absence of any stimuli ($p<0.0001$).

There was a significant increase in the shelter preference index (from 0.90 ± 0.47 to 2.38 ± 0.60, $p=0.0007$), indicative of fear. There was also a significant decrease in the ROI preference index (from 0.15 ± 0.22 to -0.42 ± 0.20 $p<0.0001$), illustrating avoidance. The number of outings also decreased (from 26.7 ± 7.6 to 16.3 ± 9.4, $p=0.0048$), however the length of each outing did not change (from 5.4 ± 4.0 s to 4.5 ± 3.3 s, $p=0.0953$).

Comparison of responses to ultrasound and snake skin

The shelter preference index during the test phase was higher in case of exposure to snake skin as compared to ultrasound ($p=0.0113$) and the ROI preference index was more negative ($p=0.0015$), suggesting that animals were more scared in the presence of snake skin and were avoiding the area more than when exposed to ultrasound. The number of risk episodes was also significantly higher during snake skin presentation ($p<0.0001$), as there were no risk assessment episodes following ultrasound stimulation. The speed of escape from ultrasound was significantly higher as compared to the speed of escape from snake skin ($p=0.0006$), although the distance travelled back to

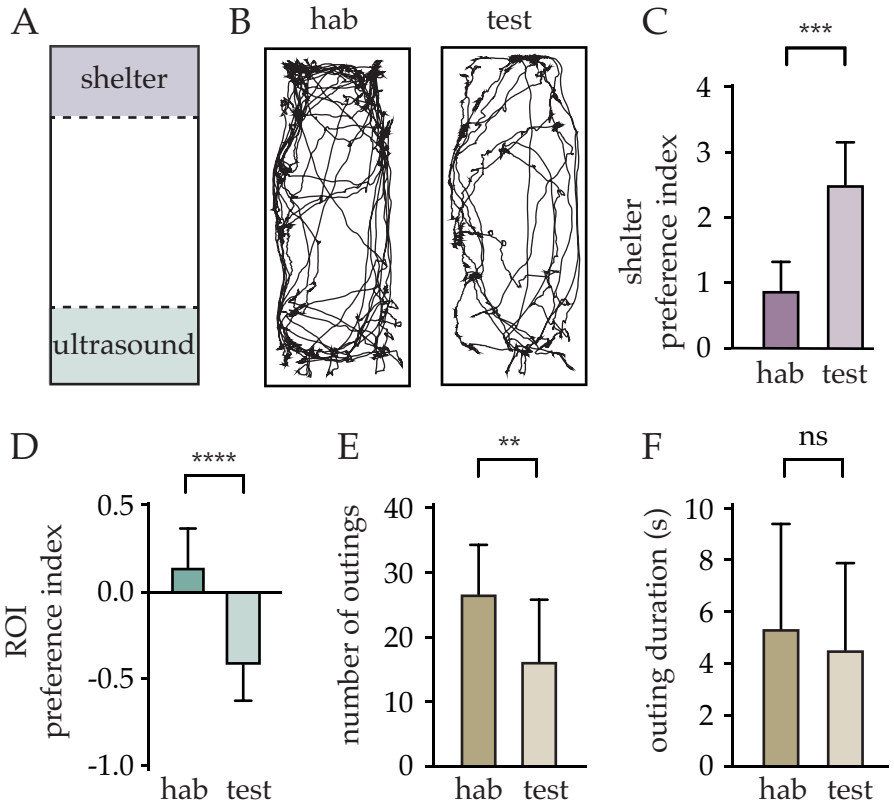

Figure 3.5: Behavioural responses to ultrasound. A. Illustration of the arena B. Path travelled during the habituation period (left) and ultrasound stimulation (right) C. Shelter preference index D. ROI preference index E. Number of outings F. Duration of each outing. hab – habituation, 0-10 mins, test – 10-20mins. n=6

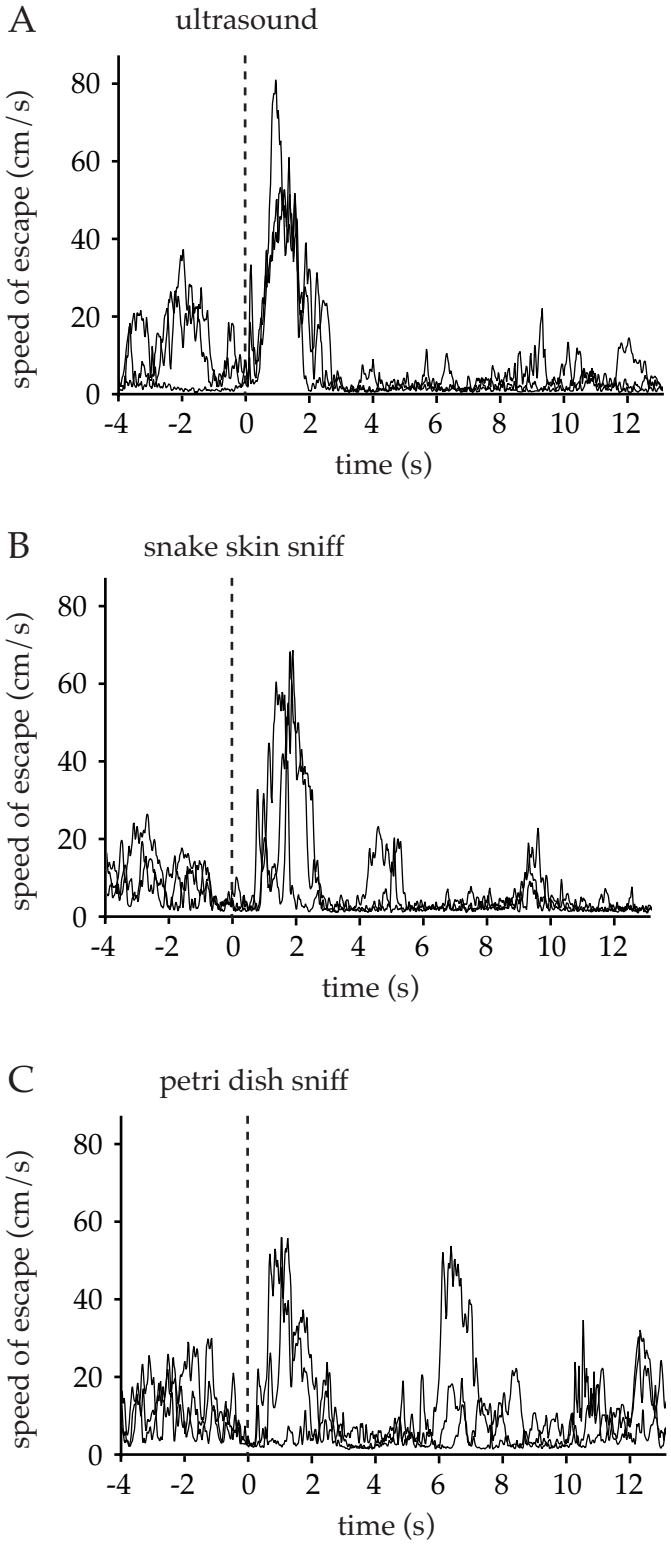

Figure 3.6: Speed of escape from different stimuli, individual trials. A. Speed of escape from ultrasound, aligned to the onset of ultrasound B. Speed of escape from snake skin, aligned to tagged sniff C. Speed of escape from petri dish, aligned to tagged sniff.

the shelter was shorter in case of snake presentation. Examples of speed change over time in response to stimulation by ultrasound, snake skin and petri dish can be found in Figure 3.6. These differences and similarities are discussed further in subsection 3.3.2.

3.2.4 *Optogenetic stimulation of SF1+ neurons induces a range of defensive-like behaviours*

A few studies have been published which comprehensively described the behavioural effects of in vivo optogenetic activation of SF1+ cells in the VMHdm (Wang et al., 2015, Kunwar et al., 2015, Viskaitis et al., 2017). My results confirm that different frequencies of SF1+ neurons stimulation can trigger different behaviours. Figure 3.7 shows a trace of movement in response to 5 Hz and 40 Hz stimulation. In general, high frequency stimulation (20 Hz) increased the speed of movement and triggered jumping escape behaviour (from 0 to 1.03 ± 1.05 jumps during 10 s stimulation). Low frequency stimulation slowed down the movement, although a prolonged 10 Hz stimulation for over 1 min occassionally also triggered jumping escape behaviour, suggesting some form of accumulation of activity.

Stimulation with either low (5 Hz) or high (40 Hz) frequency resulted in place avoidance of the area where the animal received stimulation. Interestingly, the time spent in ROI (i.e. the duration of optogenetic stimulation) before the animal escaped depended on the frequency of stimulation. 40 Hz stimulation resulted in escape from ROI within 1.3 ± 0.4 s (equal to 51.9 ± 17.1 light pulses), significantly faster as compared to the escape from ROI in the control condition (6.7 ± 4.2 s, $p<0.0001$) in which the animal received no laser stimulation. 5 Hz stimulation resulted in escape within 5.1 ± 1.7 s (equal to 25.4 ± 8.5 light pulses), also significantly faster than control ($p=0.0243$).

This is interesting for two reasons. Firstly, the difference in latency to escape suggests accumulation of activity by the circuit, in line

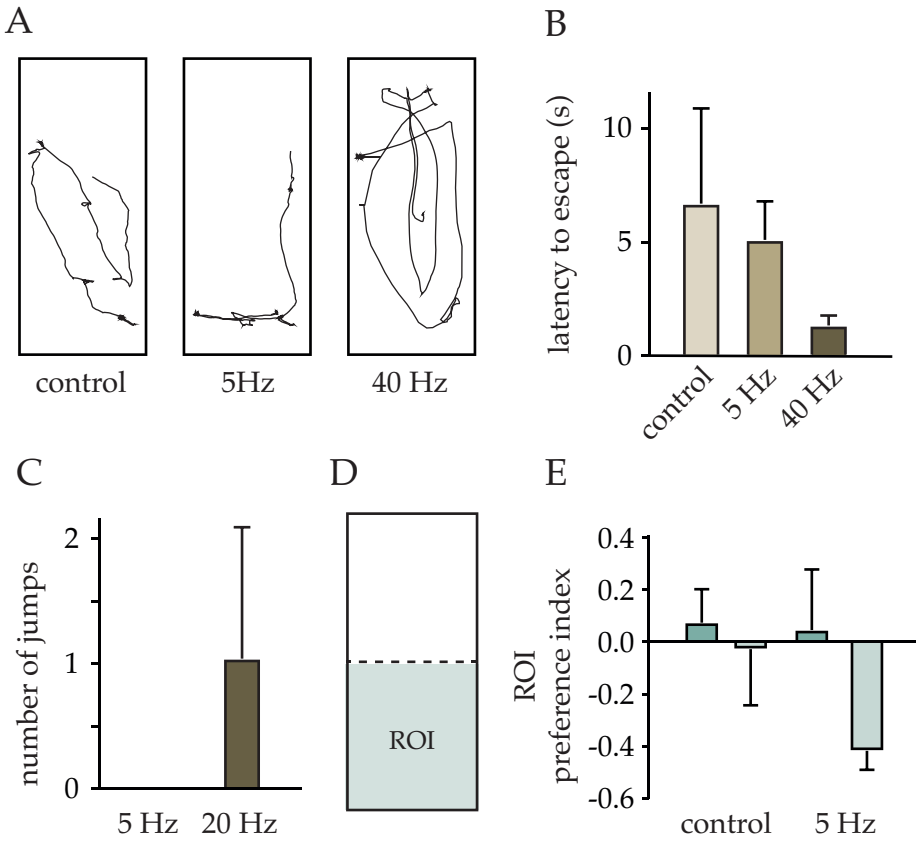

Figure 3.7: Behavioural responses to optogenetic activation of SF1+ cells in the VMHdm A. Movement of the animal during 20 seconds of stimulation B. Latency to escape from ROI to shelter, average from a 15 minute experimental period C. Average number of jumps during 20 seconds of SF1+ activation D. Illustration of the avoidance test paradigm (no shelter) E. ROI preference index (10 minute habituation period and 10 minute stimulation in ROI)

with the earlier observations that even low frequency of stimulation can lead to jumping if the stimulation is long enough. Secondly, the latency to escape from stimulation of SF1+ neurons is very long, even in case of very high frequency of stimulation (1.3 ± 0.4 s). This latency is much longer than during naturally evoked escape, for instance by ultrasound (reaction time around 200 ms, Vale et al., 2017). This prompts a question of the role of SF1+ neurons in triggering defensive behaviours, which is further considered in the discussion.

3.3 DISCUSSION

In this study I elicited mouse defensive behaviours using auditory and olfactory predator stimuli, as well as through optogenetic activation of SF1+ neurons in the VMHdm.

3.3.1 *Reproducing defensive behaviour in the lab*

In this chapter I showed that defensive behaviours could be reliably elicited in the laboratory using predator stimuli of a single modality, either auditory or olfactory. The defensive behaviours were quantified by measuring ROI avoidance, shelter preference, exploration pattern, risk assessment, as well as the speed of fleeing from the stimulus.

There was variability in the behavioural response between different mice, illustrated by a relatively large standard deviation in all parameters measured. This variability might be due to differences in the initial state of the animal, depending on factors such as hunger and anxiety. These factors are hard to control for, which means that a larger number of subjects may be required to observe more subtle differences in behaviour.

3.3.2 *Behavioural responses to different stimuli*

Both ultrasound and snake skin elicited defensive behaviours in mice. While these behaviours were largely similar, they did show subtle differences. Before the behaviours are compared, it is important to mention the differences between the olfactory and auditory stimuli themselves. Snake skin as a stimulus was constantly present during the test period, while ultrasound was only presented periodically. Moreover, snake skin was not a purely olfactory stimulus, but also a visual one. In the future experiments these differences could be accounted for by placing a petri dish in ROI also during the ultrasound stimulation experiments, rather than as a separate control experiment. Finally, the relative strengths of each stimulus are not known, since they act via different sensory pathways.

While both stimuli elicited defensive behaviours, the responses to ultrasound were less variable than to snake skin. Ultrasound elicited fleeing on nearly all trials, while snake skin responses could be divided into two types, based on whether mice avoided the snake skin or investigated it, as measured by the change in the ROI preference index. The second type of responses to snake skin was less common and these mice showed an exploratory interest in the snake skin. There was no change in the ROI preference index when mice were exposed to a petri dish, suggesting that these effects were not due to the presence of a novel object in the arena.

In terms of similarities, both ultrasound and snake skin elicited avoidance, as seen by a decrease in the ROI preference index, as well as an increase in the shelter preference index, indicating fear. Both shelter preference and ROI avoidance were larger in case of snake skin presentation, which could be because snake skin as a stimulus was continuously present in the arena. Importantly, snake skin also elicited risk assessment behaviour, which was not observed in case of ultrasound stimulation. This was one of the most striking differences

in behaviour, which could also be explained by the fact that snake skin was continuously present in the arena.

The speed of fleeing from ultrasound was significantly higher as compared to the escape speed from snake skin. However, distance travelled during escape from snake skin was shorter than during escape from ultrasound, even though snake skin was in the same ROI as ultrasound stimulation. This was because the animals often travelled only half way through the arena when risk assessing the snake skin, after which they turned around and run back to the shelter. It is possible that the odour was already detectable at that point. The animals therefore they had a shorter distance back to the shelter and they might not have reached their maximum speed of escape before reaching the shelter. To compare the speed of escape it would be necessary to use a longer arena, where small differences in the distance to travel would not affect the top speed reached. The outing duration also decreased significantly in the presence of snake skin, illustrative of the risk assessment behaviour, while it did not decrease significantly in case of ultrasound presentation. The number of outings decreased both in case of ultrasound and snake skin presentation.

In summary, ultrasound and snake skin both elicited avoidance, triggered escape from the stimulus, and increased the time the animals spent in the shelter. However, avoidance was larger in the condition of snake skin presentation, while fleeing was faster when animal was stimulated with ultrasound. Moreover, snake skin elicited risk assessment behaviour, absent in case of ultrasound stimulation. How each stimulus affects the choice of behaviour and its level of expression is addressed in the following chapters.

3.3.3 *Eliciting behaviour with VMHdm stimulation*

Optogenetic activation of SF1+ neurons elicited a range of behaviours, in accordance with previously published studies (Wang et al., 2015,

Kunwar et al., 2015, Viskaitis et al., 2017). The type of behaviour elicited was dependent on the frequency of stimulation, with lower levels of activation reducing locomotion and higher levels of activation increasing locomotion and triggering jumping escape behaviour. Both high and low levels of activation elicited avoidance.

While optogenetic activation of SF1+ neurons could trigger behaviours like avoidance and escape jumping, this elicited behaviour had a much longer latency from the onset of the stimulation as compared to the naturally evoked behaviours. This has not been highlighted in the published studies (Wang et al., 2015, Kunwar et al., 2015) and puts into question the role of the VMHdm in eliciting behaviour under physiological conditions.

Very recently another paper has been published, which investigated the effects of very low frequency stimulation of SF1+ neurons (Viskaitis et al., 2017). In this study the effects of frequencies between 1 and 5 Hz were investigated. The results showed that activation below 4 Hz did not induce avoidance or changes in locomotion, but it had an effect of inhibiting feeding behaviour. These findings are further interpreted in Chapter 6.

Based on my own findings and studies published at the time (Wang et al., 2015, Kunwar et al., 2015), I begun to question how activity in one brain area could elicit different behaviours, such as avoidance or jumping escape, and speculated that SF1+ neurons might exhibit some kind of heterogeneity.

As discussed in chapter 1, there are three main factors to consider when addressing the question of heterogeneity of a brain structure: input pattern, input integration, and projection pattern. Wang et al., 2015 already addressed the latter by investigating the effects of stimulating specific projections of the SF1+ cells. They have established two main targets of SF1+ neurons, namely the anterior hypothalamus (AH) and the periaqueductal gray (PAG) and showed that activity in the VMHdm-AH projections induces avoidance, while activity in the VMHdm-PAG projections promotes immobility.

While this important finding helps explain how activity in SF1+ neurons can elicit different behaviours, it remains unclear what role VMHdm plays in choosing the appropriate behaviour. How the level of activity in SF1+ neurons is determined in vivo and how it affects the choice of behaviour is addressed in the following chapters.

Limitations

While optogenetics is a very useful tool for investigating functions of a population of cells, it is important to remember the associated limitations. First and foremost, optogenetic activation results in a synchronous activation of the whole illuminated region. VMHdm is heavily interconnected with other medial hypothalamic circuit areas and it is likely that with prolonged stimulation multiple other brain regions are also activated. Moreover, the whole population of VMHdm SF1+ neurons is activated, which might not reflect the physiological state of activation by natural stimuli. Finally, it is known that ChR2 can produce artefacts and result in either synaptic depression or facilitation, depending on the cell type it is expressed in (Jackman et al., 2014).

3.3.4 *Conclusions*

The results from this chapter show that a range of defensive behaviours can be elicited in mice, either by presenting natural stimuli, such as ultrasound and snake skin, or by optogenetically activating SF1+ neurons in the VMHdm.

Ultrasound and snake skin elicited overlapping but not identical behaviours. Both stimuli elicited avoidance, escape from the stimulus, and fear, as measured by the increase in the time spent in the shelter. Snake skin resulted in larger avoidance than ultrasound, while ultrasound triggered faster fleeing than snake skin. Moreover, snake skin elicited risk assessment which ultrasound did not.

Similarly, optogenetic activation of SF1+ neurons at different frequencies elicited different behaviours, with lower frequencies reducing animal mobility and higher frequencies producing jumping behaviour. It is not known what role SF1+ neurons play in choosing the most appropriate behavioural response in vivo.

I first hypothesised that there might exist differences in the electrophysiological properties within the population of SF1+ cells, which could result in subpopulations of cells being activated by different frequencies of light, thereby preferentially activating cells projecting to one area over the other. To investigate these properties, I performed a series of electrophysiological recordings in brain slices (chapter 4). Following from the results of these experiments, I next investigated the possible heterogeneity of the input pattern onto SF1+ neurons and recorded calcium transients in the VMHdm in vivo in the presence of olfactory and auditory stimuli (chapter 5).

4

INPUT PROCESSING BY THE VMHDM

4.1 INTRODUCTION

The results from Chapter 3 alongside published data (Wang et al., 2015, Kunwar et al., 2015, Viskaitis et al, 2017) show that optogenetic activation of SF1+ neurons can trigger defensive behaviours. Moreover, the type of behaviour elicited depends on the frequency and intensity of stimulation. Low frequency or intensity of stimulation tends to reduce mobility, while high frequency or intensity of stimulation promotes activity bursts. How can activity in one population of cells elicit such different behaviours?

There are three main factors to consider - heterogeneity of the input pattern, input integration, and the output projections. The first factor I decided to study was input integration by SF1+ neurons. I hypothesised whether the electrophysiological properties of the population of SF1+ cells in the VMHdm might be in fact heterogenous, with different subpopulations of cells being activated by different frequencies or intensities of the light stimulation. To find out whether this was the case, I first investigated the electrophysiological properties of SF1+ neurons by performing whole cell patch clamp recordings from acute brain slices. While studies have reported certain electrophysiological properties of the VMHdm neurons (Dhillon et al, 2006; Branco et al, 2016, Sohn et al., 2016, Viskaitis et al, 2017), no study has comprehensively described the electrophysiological properties of SF1+ neurons in the VMHdm.

In order to investigate further how SF1+ neurons integrate the inputs they receive, I next studied the integration of excitatory inputs from the medial amygdala (MEA) using a combination of slice electro-

physiology and optogenetics. While there exists anatomical evidence that MEA neurons project to the VMHdm (Bian et al, 2008), there is no published study describing the physiology or the behavioural importance of this connection. Finally, I investigated the functional importance of the activity in this pathway by measuring changes in behaviour while optogenetically activating MEA inputs in the VMHdm in vivo.

Taken together, these results advance our understanding of the mechanism of input integration by SF1+ neurons in the VMHdm, the contribution of the MEA inputs for eliciting defensive behaviours, and the role of VMHdm in controlling innate defensive behaviours.

4.2 RESULTS

4.2.1 *Electrophysiological properties of SF1 neurons*

To characterise the electrophysiological properties of SF1+ neurons I performed whole cell patch clamp recordings in acute brain slices from different areas of the VMHdm. While I aimed to record from cells across the VMHdm (anterior - posterior, ventral - dorsal and medial - lateral), the majority of cells were in the dorsomedial region to avoid recording from the VMHc.

Table 4.1 contains definitions of the properties measured and Figure 4.1 an illustration of the methods used to calculate them. The main properties of SF1+ cells are summarised in Table 4.2. All the values are given as mean ± SD, unless stated otherwise.

General electrophysiological properties

The resting membrane potential (Vm), determined in cells with a stable seal of at least 1 GΩ immediately after establishing a whole cell patch clamp configuration, measured -49.2 ± 6.1 mV, consistent with previous reports (Dhillon et al, 2006; Sohn et al., 2016, Viskaitis

PROPERTY	DEFINITION
AP threshold	The voltage point where the first derivate (speed of AP) reaches 5% of its maximal value
AHP	The voltage difference between AP threshold and the lowest voltage reached during the hyperpolarization phase
AP height	The maximum membrane voltage reached during AP
AP amplitude	The voltage difference between the AP threshold and the AP peak
Input resistance (Ri)	Calculated from Ri=I/V by measuring the steady-state voltage change in response to a 10pA current injection
Membrane time constant	Time for the membrane potential to reach 63% of its absolute final value after injection of 10 pA of current
Spike half-width	Duration of the AP between the membrane voltage at a value halfway between AP threshold and AP peak
Resting Vm	Membrane potential as measured immediately after achieving a whole cell recording
Maximum firing rate	The highest frequency of AP firing as determined by 500 ms long step injections of current
Rise time	The time required for a value to rise from 10% to 90% of its peak amplitude

Table 4.1: Definition of electrophysiological properties measured

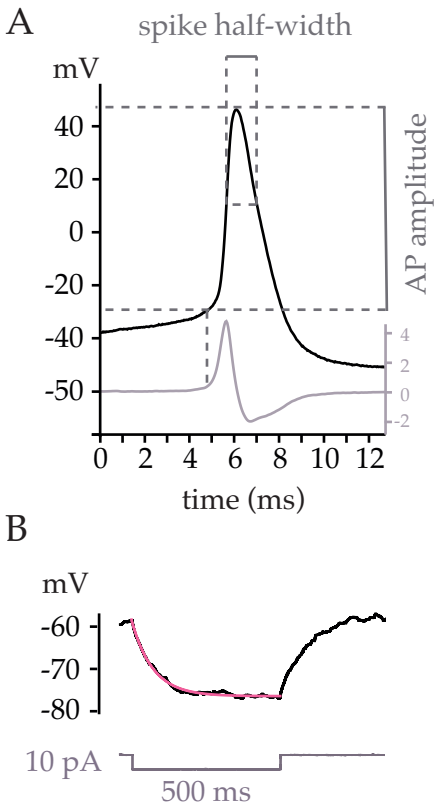

Figure 4.1: Overview of action potential measurements. A. In black – voltage changes during an action potential; in grey – first derivate of the voltage changes B. In black – membrane hyperpolarization in response to a -10 pA current injection; in pink – a single exponential curve fitted to allow measurement of the time constant of the voltage change.

PROPERTY	MEAN ± SD
Resting Vm (mV)	-49.2 ± 6.1
Input resistance (GΩ)	2.0 ± 1.0
Membrane time constant (ms)	57.0 ± 23.3
AP threshold (mV)	-33.5 ± 3.0
AHP (mV)	19.4 ± 4.5
AP amplitude (mV)	107.4 ± 8.5
AP height (mV)	19.4 ± 4.5
AP half-width (ms)	1.45 ± 0.20
Max firing rate (Hz)	41.7 ± 14.1

Table 4.2: Electrophysiological properties of SF1+ neurons. n=45

et al., 2017). A proportion of cells (58%) were tonically firing in current clamp (6.4 ± 4.6 Hz).

The membrane time constant was calculated from a 500 ms injection of -10 pA in current clamp at holding potential of -60 mV. A single exponential curve was fitted to describe the membrane hyperpolarization from the holding potential until it reached a stable value (illustration in Figure 4.1B). The time constant was measured as the time it takes for the value of the membrane potential to reach 63% of its absolute final value. The value of the membrane time constant was variable between the cells, with a mean of 57.0 ± 23.3 ms. This relatively large value suggests that these cells are more suited to accumulating information over a period of time, rather than acting as coincidence detectors with high temporal precision. Since the membrane time constant is a measure of the passive properties of the membrane and depends on the membrane resistance and the membrane capacitance, as described by the equation tau = Cm.Rm, the variability between the cells could be attributed to the process of tissue preparation, with different lengths of neuronal membrane being cut during slicing, thereby changing membrane capacitance and resistance.

The input resistance (Ri) is a measure of the neuronal responsiveness to current input, described by the equation Ri=I/V. Here it was calculated by measuring the amplitude of voltage change in response

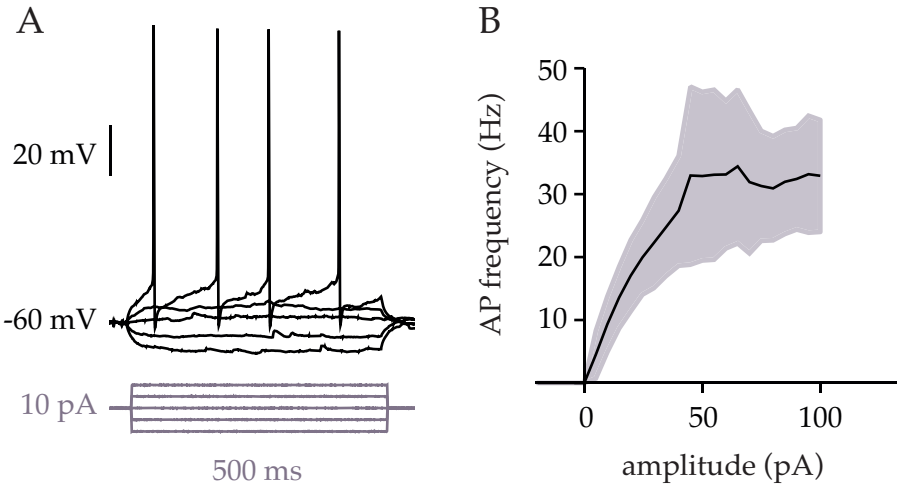

Figure 4.2: Firing properties of SF1+ neurons. A. An example trace of membrane potential changes in response to 10 pA current injections B. Relationship between the amount of injected current and the frequency of action potential firing (mean and SD, n=18)

to an injection of -10 pA of current (illustration in Figure 4.1). The mean value of Ri was 2.0 ± 1.0 GΩ, a value relatively high in comparison to other brain regions (for example the pyramidal cells of the olfactory cortex, with Ri equal to 55 MΩ, Suzuki and Bekkers, 2011). Ri is reflective of the sensitivity of the cells to current input and high Ri means that small current inputs cause a relatively large change in membrane potential. High Ri partly accounts for the long membrane time constant described earlier.

The effects of high Ri are reflected by the high spike rate output in response to current injections. This can be illustrated by plotting the frequency response (F) per injected current (I), known as the F-I curve. As seen in Figure 4.2, an input of 5-10 pA is already sufficient to trigger action potential firing in most cells.

Action potential properties

This brings us to the properties of the action potential (AP) itself. See Figure 4.1 for visual explanation of the AP properties measured. The main AP properties are summarised in Table 4.2.

The threshold for AP firing was calculated from a train of APs evoked by 15 pA current injection. It was taken as the value of the

membrane potential at the time when the first derivative of the voltage reached 5% of its maximal value (illustration in Figure 4.1). The value of the AP threshold was -33.5 ± 3.0 mV, around 15 mV above the resting Vm.

The maximum firing rate was measured by injecting current in 5 pA steps, until the point when the cell started to fail to produce a series of APs. While some cells saturated at frequencies as low as 20 Hz, a small number of cells was capable of firing up to 70 Hz. The mean maximum firing rate was 41.7 ± 14.1 Hz.

The maximum firing rate can dependent on the properties of the AP itself. It has been shown that increasing the afterhyperpolarization potential (AHP) length and AP half width can lower the maximum firing rate by prolonging the inter-spike interval (Cloues and Sather, 2003). The AHP of SF1+ neurons, measured as the difference between the AP threshold and the lowest hyperpolarization potential reached by the neuron, was 19.4 ± 4.5 mV. AP half-width, measured as the duration of the AP at the membrane voltage equal to half of the AP amplitude, was 1.45 ± 0.20 ms, a fairly average value in comparison to other brain areas (neuroelectro.org, Tripathy et al., 2014).

The in vivo probability of AP firing is regulated by the balance of the spontaneous excitatory and inhibitory currents (EPSCs and IPSCs). Measuring these currents can also give additional information about the properties of the excitatory and inhibitory synapses on a neuron and allow comparison with evoked currents. To gain a further understanding of the properties of SF1+ neurons, I next isolated and recorded these spontaneous currents with the aid of selective blockers of excitation and inhibition.

4.2.2 *Spontaneous excitatory and inhibitory inputs*

Spontaneous excitatory and inhibitory events happen as a result of presynaptic vesicle release, which can be both action potential de-

pendent and independent. Analysing these events can give us different types of information about the synapses, such as the proportions between the excitatory and inhibitory inputs, which help explain the integrative properties of the neuron. We can also compare these spontaneous events with evoked inputs (optogenetically or electrically triggered) to describe the synapses studied in relation to the whole population of synapses on the neuron.

The inhibitory and excitatory events measured occurred at relatively low frequencies and as discrete, individual events rather than in bursts. They were recorded separately in the presence of pharmacological blockers of either excitation or inhibition.

Spontaneous excitatory events

Excitatory post synaptic currents (EPSCs) and potentials (EPSPs) were measured at -60 mV in the presence of picrotoxin (60 mg/l), GABA-A receptor antagonist. The average waveform and the properties of EPSCs and EPSPs can be found in Figure 4.3 and Figure 4.4. Distributions of these properties from one sample cell are illustrated on the histograms. The mean and standard deviation were calculated from the distribution of mean values calculated for each individual cell.

The mean frequency of EPSCs was 2.0 ± 0.9 Hz, while the amplitude was 12.1 ± 7.9 pA. Since the frequency depends on the release probability at the presynaptic terminals and the number of active synapses, and at this stage it was not possible to estimate the relative contribution of each of these. Considering the high input resistance and large membrane time constant of these cells, these currents resulted in large depolarisations of the membrane, contributing significantly to the probability of AP firing.

The rise time of EPSCs was 2.1 ± 1.1 ms. Plotting the amplitude against the rise time shows that the events of a smaller amplitude tend to have a longer rise time, suggesting that these synapses might be placed further away on the dendritic tree and the currents subjected to filtering. The decay time was 6.8 ± 3.1 ms.

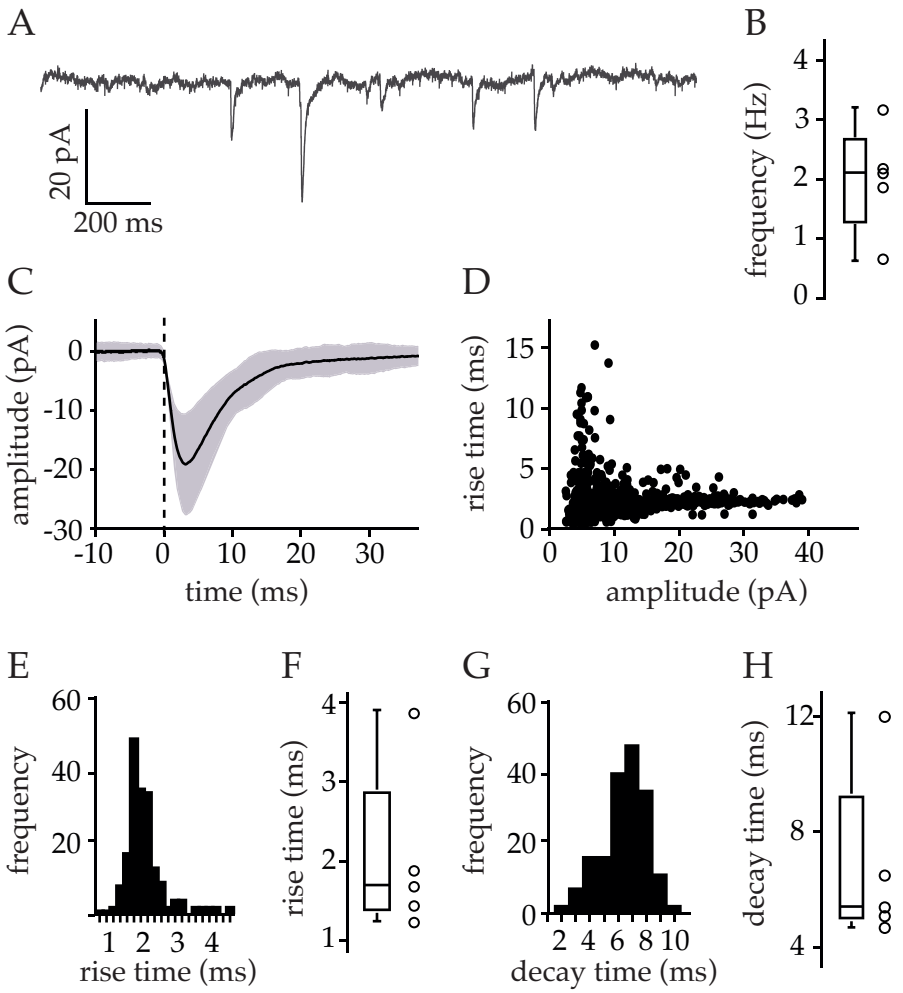

Figure 4.3: Properties of EPSCs. A. An example trace of EPSCs in voltage clamp, -60 mV B. Mean frequency of EPSCs C. A trace of EPSCs from a single cell (mean and SD). Dashed line marks the onset of the event. D. Plot of rise time against amplitude, each dot represents an individual ESPC measurement. E. Histogram of rise time of all EPSCs from one single cell, 1 ms bins. F. Mean rise time of EPSCs from all recorded cells. G. Histogram of decay time time of all EPSCs from one single cell, 1 ms bins. H. Mean decay time of EPSCs from all recorded cells.

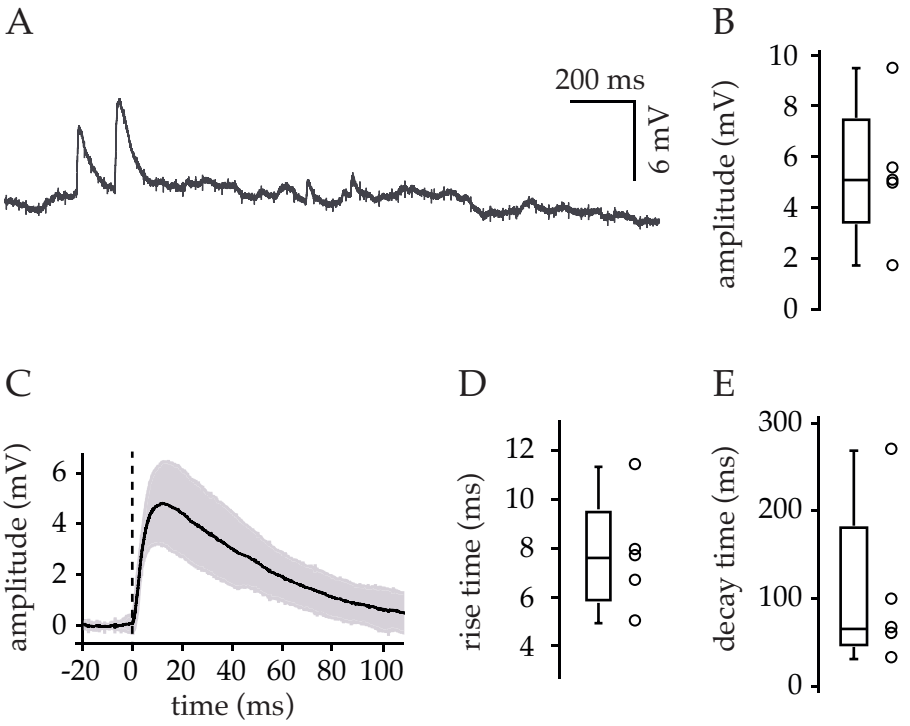

Figure 4.4: Properties of EPSPs. A. An example trace of EPSPs in current clamp, -60 mV. B. Mean amplitude of EPSPs from all recorded cells. C. A trace of EPSPs from a single cell (mean and SD). Dashed line marks the onset of the event. D. Mean rise time of EPSPs from all recorded cells. E. Mean decay time of EPSPs from all recorded cells.

The amplitude of the resulting evoked potentials, EPSPs, was 5.2 ± 2.8 mV. The rise time was 7.7 ± 2.3 ms. The decay time was very variable between the cells, with the mean equal to 62.1 ± 27.8 ms. The EPSP decay time is in line with the data published (Branco et al., 2016). The Ri in the presence of picrotoxin was 1.9 ± 0.7 GΩ, not significantly different to Ri measured in the absence of inhibitors (p=0.6139, Welsch's t test).

Spontaneous inhibitory events

Inhibitory post synaptic potentials (IPSPs) were measured at -60 mV in the presence of kynurenic acid (376 mg/l), glutamate receptor antagonist. Since these currents were smaller and harder to measure, they were recorded with internal solution containing a high Cl^- concentration (155 mM KCl) to increase the driving force for Cl^- and therefore increase the amplitude of the events.

The frequency of IPSCs was 0.8 ± 0.7 Hz, roughly half of that of the EPSCs. The average waveform and the properties of IPSCs can be found in Figure 4.5.

The rise time of IPSCs was 2.2 ± 0.8 ms. Like in case of EPSCs, plotting amplitude against the rise time shows some filtering of these inputs along the dendritic tree. The decay time was 49.6 ± 31.1 ms.

Having measured the properties of spontaneous inputs in SF1+ cells, I next investigated integration of evoked activity coming from the medial amygdala.

4.2.3 *Excitatory inputs from the medial amygdala to SF1+ neurons in VMHdm*

In order to investigate the evoked input integration by SF1+ cells, ChR2 expressing axons of MEA neurons present in the VMH were optically activated with 1 ms pulses of light. The resulting currents

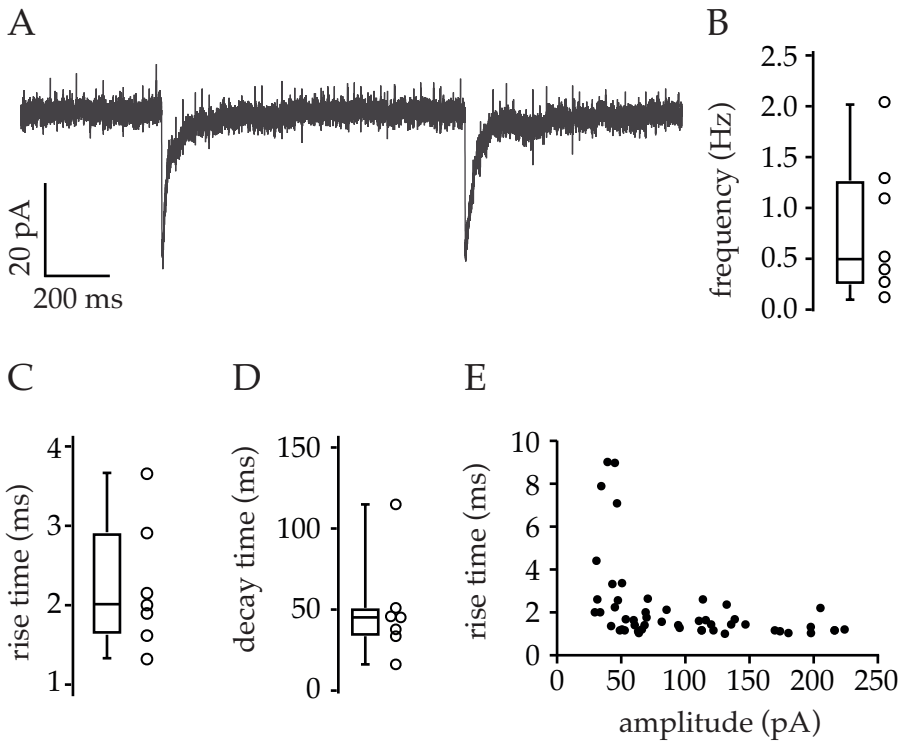

Figure 4.5: Properties of IPSCs. A. An example trace of IPSCs in voltage clamp, -60 mV. B. Mean frequency of IPSCs. C. Mean rise time of IPSCs from all recorded cells. D. Mean decay time of IPSCs from all recorded cells. E. Plot of rise time against amplitude, each dot represents an individual ISPC measurement.

in SF1+ neurons were recorded in both voltage and current clamp at different holding potentials.

The initial experiment confirmed presence of both excitatory and inhibitory inputs from the MEA. Since it was the activation of SF1+ cells that produced defensive behaviours as described in Chapter 3, and majority of VMH projecting MEA neurons are glutamatergic (Bian et al, 2008), I decided to focus primarily on the excitatory inputs. The following experiments were therefore performed with ChR2 expressed selectively in the glutamatergic cells under CaMKII promoter.

Evoked currents

An example of the light evoked current measured in voltage clamp at -60 mV holding potential can be found in Figure 4.6. The amplitude of the current was 40.4 ± 31.8 pA, a value relatively large considering the high input resistance of the SF1+ cells. The rise time was 2.5 ± 1.0 ms and the decay time 17.8 ± 6.4 ms, both likely prolonged due to the presence of multiple synapses activated at slightly different times, in contrast to spontaneous EPSCs which consisted largely of unitary events.

The connectivity rate between MEA and VMH was 80% (n = 65). The reliability of each connection was high, with the failure rate of 12.9 ± 4.9 % (SEM).

The latency between light stimulation and onset of current inflow was 8.9 ± 3.4 ms (n=16). There was a high variability in latency between cells but low variability between recordings for an individual cell (mean standard deviation equal 1.83 ms), indicating a monosynaptic connection.

Evoked potentials

The large amplitude of evoked currents, combined with the high input resistance described in subsection 4.2.1, meant that a single 1ms light pulse was often sufficient to trigger an action potential in current clamp (Figure 4.7). The amplitude of the membrane voltage change,

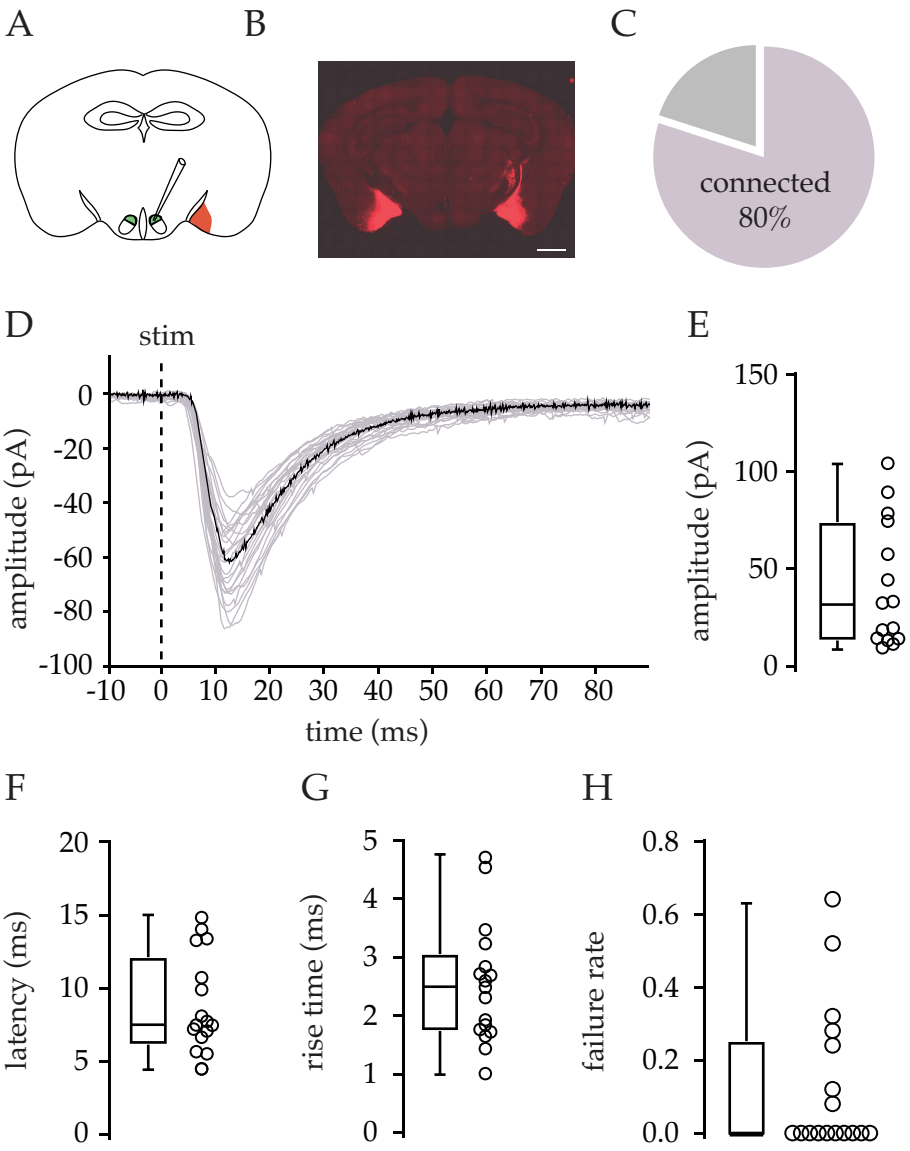

Figure 4.6: Light evoked MEA currents in SF1+ cells in response to a single 1 ms light stimulation. A. Illustration of a coronal brain section containing ChR2 injection in MEA in red and the VMHdm in green. B. Histology of the coronal brain section containing ChR2 injection in MEA in red. scale bar, 1 mm. C. Proportion of all recorded cells which received light evoked currents. D. Current inflow in a SF1+ cell in response to ChR2 stimulation at t = 0, -60 mV. E. Mean amplitude of evoked currents across all recorded cells. F. Mean latency from stimulation to the onset of the evoked current. G. Mean rise time of the evoked currents. H. Failure rate to evoke current inflow in each cell over multiple light stimulation trials.

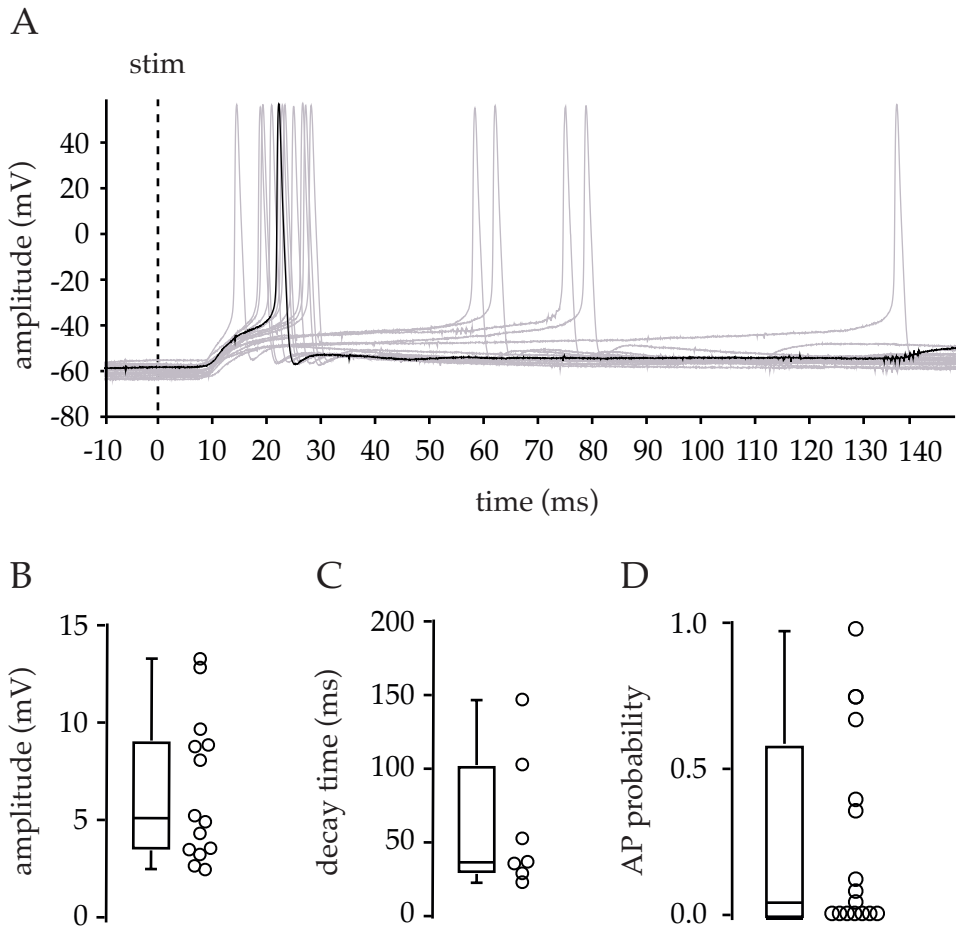

Figure 4.7: Light evoked MEA voltage changes in SF1+ cells in response to a single 1 ms light stimulation. A. Voltage changes in a SF1+ cell in response to ChR2 stimulation at t = 0. B. Mean amplitude of evoked voltage changes. C. Event decay time. D. Mean probability of action potential firing.

calculated from trials in which action potential was not elicited, was on average 6.6 ± 3.7 mV, although in some cells the voltage change was as high as 20 mV. The probability of evoking an action potential was variable, with mean of 26.3 ± 8.7% (SEM) and some cells showing a trial to trial probability of 100%.

Repeated stimulation

Since low failure rate can reflect either a high release probability of each synapse or a large number of synapses, I next presented a series of 1 ms light pulses at a frequency of 10 Hz in order to calculate the paired pulse ratio (PPR), another measure of the release probability. The PPR is the ratio between the current amplitude induced by the

second and first pulse in a train of pulses, where ratio values below 1 indicate synaptic depression and above 1 synaptic facilitation. Interestingly, at 10 Hz stimulation all recorded cells had PPR lower than 1, with the mean PPR of all cells equal to 0.58 ± 0.18. The low PPR, together with a low failure rate and high amplitude of the evoked currents are all suggestive of a high release probability of these synapses.

In accordance with the voltage clamp recordings of 10 Hz stimulation, current clamp recordings showed that the cells failed to initiate multiple action potential firing upon a high frequency stimulation. Out of the cells which had a probability >0 of action potential firing in response to light stimulation, there was only a 5.6 ± 3.7% (SEM) probability of evoking more than 3 action potentials from a series of 10 pulses at 10 Hz. As seen in Figure 4.8D, the cumulative probability of action potential firing did not increase significantly over the subsequent pulse stimulations.

Having shown the presence of a physiological connection between MEA and VMHdm, I next wanted to see how optogenetic activation of this pathway in vivo might affect the animal's behaviour. This was particularly interesting considering the depressing nature of the synapses, but also the reciprocal connectivity between VMHdm and MEA as well as between other medial hypothalamic areas, absent in the slice, which might influence the way these inputs are integrated in vivo.

4.2.4 *Optogenetic activation of MEA inputs in the VMH induces place avoidance*

In order to investigate the behavioural effects of activating the MEA-VMHdm pathway, I injected ChR2 in the MEA and implanted an optical fibre above the MEA projections in the VMHdm. Interestingly, even long duration (1 min) 20 Hz stimulation did not cause jumping

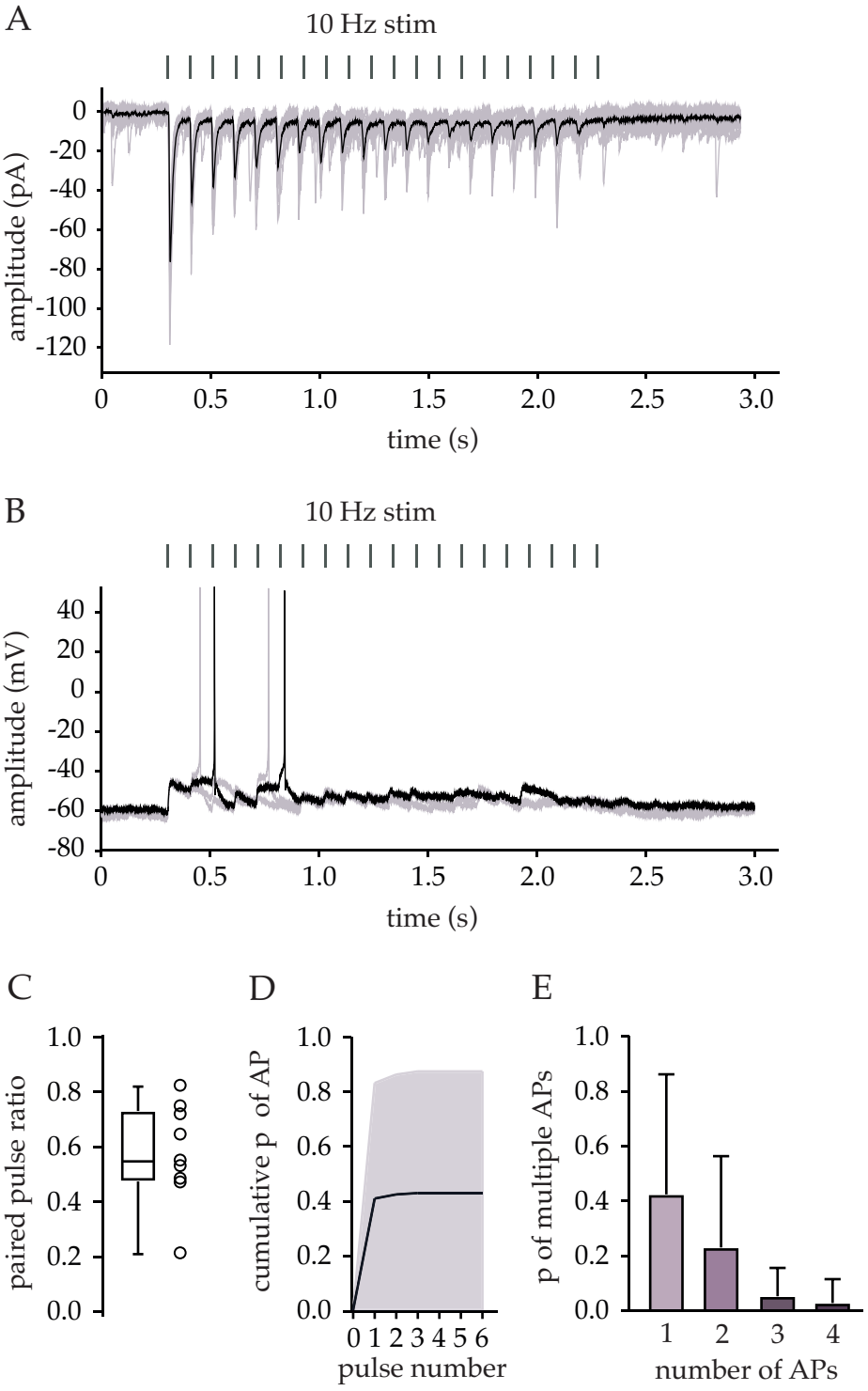

Figure 4.8: Current and voltage changes in SF1+ neurons in response to 10 Hz stimulation of MEA inputs. A. Evoked currents, -60 mV. B. Evoked voltage changes. C. Paired pulse ratio D. Cumulative probability of action potential firing over subsequent light pulses. E. Probability of evoking multiple action potentials during the course of stimulation.

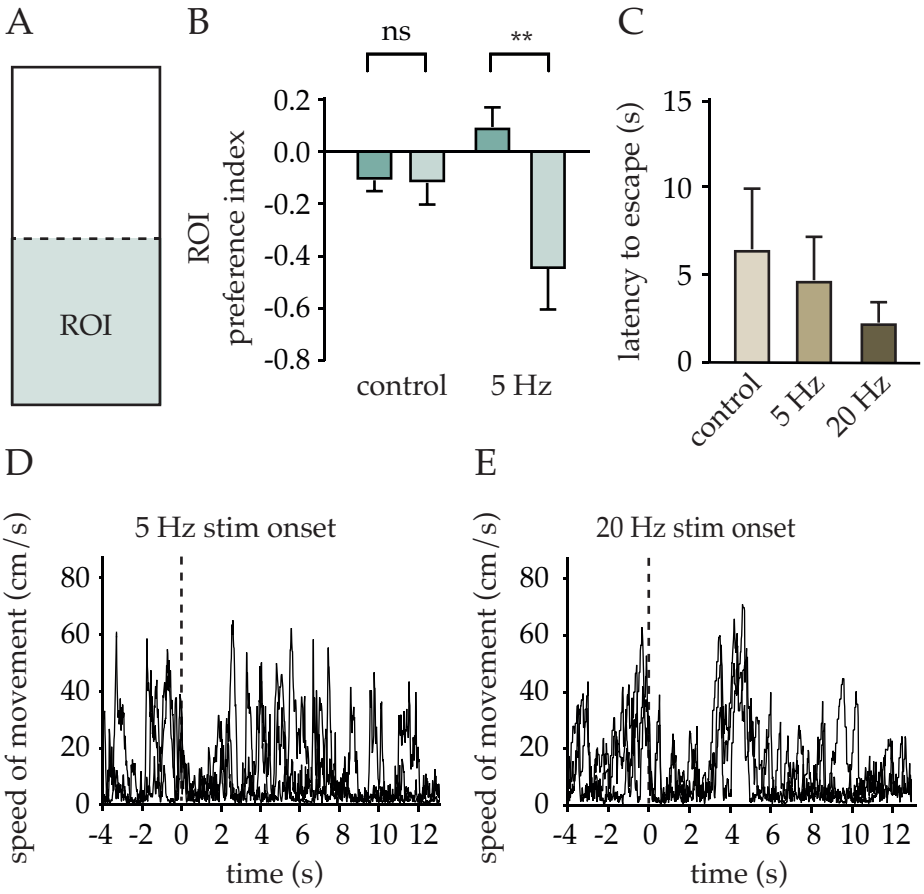

Figure 4.9: Behavioural effects of stimulation of MEA projections in the VMHdm. A. Illustration of the avoidance paradigm. B. Place preference index for the ROI, prior to and during the stimulation period. C. Latency to escape from ROI during stimulation. D. Speed of escape from 5 Hz stimulation, aligned to the onset of stimulation. E. Speed of escape from 20 Hz stimulation, aligned to the onset of stimulation

behaviour. This is in contrast to the effects of direct VMHdm stimulation, where even a couple seconds of stimulation was sufficient to trigger jumping behaviour. There was however a difference in the time to escape at 5 Hz stimulation as compared to 20 Hz stimulation (Figure 4.9C).

In order to further quantify the aversion of the stimulus, I used the place avoidance paradigm described in Chapter 3. The arena was divided into two halves, with one half marked as the region of interest (ROI). The animal was placed in the arena and allowed 10 minutes of habituation, followed by 5 Hz light stimulation upon entering the

ROI. The relative time the animal spent in each half was measured during the habituation period and during the stimulation.

As shown in Figure 4.9B, the animals showed significant place avoidance of the area where they received 5 Hz stimulation. The avoidance was similar to that produced during direct VMH stimulation.

This behavioural data supports the electrophysiological findings discussed earlier. Activating MEA inputs in the VMHdm increases the defensive state of the animal, as shown by the place avoidance in response to stimulation. High frequency stimulation however is not capable of eliciting jumping behaviour, which could be explained by synaptic depression limiting the level of activity in the VMHdm. The limitations and implications of these findings are discussed in the following section as well as in Chapter 6.

4.3 DISCUSSION

SF1+ neurons in the VMHdm are known to be involved in innate defensive behaviours, however it has not been shown before how these neurons integrate synaptic inputs. By using electrophysiological recordings in slices combined with optogenetics, I described the physiological properties of SF1+ neurons in the VMHdm, integration of the inputs they receive from the MEA, and the behavioural effects of activating these projections from MEA to VMHdm in vivo.

4.3.1 *Properties of SF1+ cells*

The population of SF1+ neurons in the VMH appears to be homogenous however there exists variability in certain properties, such as the maximum firing rate, input resistance and resting Vm. While this variability could be explained by artefacts due to the recording technique (for example some cells having their dendritic tree cut at different

places during the slice preparation), it cannot be excluded that the cells are indeed heterogenous, but on a more continuous scale.

The most remarkable electrophysiological property of SF1+ cells is their high input resistance. In combination with the large membrane time constant, these cells are efficient integrators of current inputs. Since a small number of synaptic inputs is sufficient to trigger an action potential, it can be interpreted that these cells have a high sensitivity, with each input carrying significant weight. It is interesting to consider this in relation to the relatively low frequency of spontaneous inputs. Considering only 15 mV difference between Vm and action potential threshold together with the high input resistance, these spontaneous inputs can have a significant effect on the probability of action potential firing.

These findings pose a few interesting questions regarding the in vivo properties of the circuit. What is the baseline firing rate of SF1+ cells and of the brain regions of the brain projecting to these cells, such as the medial amygdala? Given the high sensitivity of SF1+ cells, one would expect the upstream regions to be largely silent. Indeed, in vivo recordings from MEA in rats (Govic, Paolini 2015) confirm this prediction, showing that the baseline firing rate of MEA ranges between 0 Hz and 1 Hz and that of the BMA between 0 and 1.5 Hz. Similarly, one would expect SF1+ cells to have a low level of baseline activity. There are no published data looking at the in vivo activity of SF1+ cells and this question is addressed in Chapter 5, where I describe my results from in vivo Ca^{2+} imaging in the VMHdm.

The relatively long membrane time constant suggests that the precise timing of the stimulus might be of a lesser importance, i.e. these cells are unlikely to be acting as coincidence detectors, in contrast to for example neurons in the cochlear nucleus, with membrane time constant of 1 ms (Wang, Manis 2005). Instead, they are able to accumulate inputs over a longer period of time, thereby ensuring that none of the incoming inputs are neglected.

Naturally, interpreting results from recordings in slices has to be done cautiously, as the tissue preparation is likely to introduce artefacts despite the best efforts to minimise them. For instance, Bindman et al., 1988 showed that the Ri of neurons in the rat neocortex was twice as large when measured in slices as compared to in vivo, which authors attribute to the reduction in membrane surface area of neurons in slice preparation. Moreover, the technique of patch clamp electrophysiology also has its limitations, since the measurements are taken in the soma and the current and voltage changes happening in far away dendrites can be easily lost. Ideally this characterisation should be performed with in vivo patch clamp recordings, which would also allow recording of activity upon presentation of predator stimuli. While not providing us with the same answers, instead of in vivo electrophysiology I performed in vivo Ca^{2+} imaging, results of which I describe in the next chapter.

Findings in relation to published recordings from the VMHdm

While there has been no comprehensive study of the electrophysiological properties of SF1+ neurons, a handful of publications have reported data from patch clamp recordings from SF1+ cells. The studies by Dhillon et al 2006 and Sohn et al., 2016 investigated the effects of leptin on SF1+ cells. Dhillon et al 2006 reported the Vm (-47.7 ± 1.4 mV, SEM) and cell attached firing rate (0.52 ± 0.09 Hz, SEM), while Sohn et al., 2016 reported the Vm (-53.2 ± 1.1 mV, SEM), as well as the Ri (1.1 ± 0.6 GΩ, SEM).

Dhillon et al 2006 made another insightful finding, namely that that the SF1+ neuron responses to leptin are homogenous, i.e. almost all SF1+ cells are depolarised by leptin and none hyperpolarised. This is in line with my own findings of homogeneity within the SF1+ cells. However, Sohn et al. 2016 claimed that the responses are not homogenous, but dependent on the medial-lateral position within the VMH, with the cells positioned more laterally being more hyperpol-

arized by leptin. However, it is possible that these cells in fact belong to the VMHvl population of cells instead of the VMHdm.

Findings in relation to recordings from other hypothalamic areas

The electrophysiological properties of SF1+ neurons are largely similar to those found in other hypothalamic regions. For example, the Ri of AGRP neurons in the arcuate nucleus is equal to 1.5 GΩ (Branco et al, 2016). It is interesting to consider these properties from an evolutionary perspective. Survival of an animal depends on its ability to make fast decisions to choose the most appropriate behaviours. The properties of SF1+ neurons render them sensitive to activation by a small number of inputs, unlike for example neurons in cortical areas, which need to receive a large number of inputs in order to increase their firing rate. It is possible that these properties make the hypothalamic neurons in effect more sensitive to detecting cues related to danger and other innate cues, such as food and reproduction. While high sensitivity is beneficial to the animal, overreacting to stimuli is not because of the unnecessary energy expenditure. It is therefore possible that the VMHdm has more of a "motivational" role in setting the driving force for avoidance of danger, rather than triggering the escape behaviour directly. It is interesting to consider these roles in the context of other functions of the VMH, such as metabolism or reproduction. This is discussed further in Chapter 6.

4.3.2 *MEA input integration*

The connectivity rate between MEA and VMHdm is high and the inputs are largely homogenous. The connection is reliable with strongly depolarizing currents, which in combination with high Ri of SF1+ neurons results in large membrane depolarizations. At the same time, the depression at the synapses limits how much the VMHdm can be activated by inputs from this one single source.

Behavioural implications

The high connectivity rate and large current inflow at the synapses suggest a high efficiency of information transfer between MEA and VMHdm. Considering low baseline levels of activity in MEA, any increase in the MEA firing rate is likely to convey significant information about the changes in the environment. Therefore none of this information should be ignored or missed out.

However, I have also shown that repeated stimulation of the MEA projections produces synaptic depression. As a result, high frequency of activity in MEA is not translated to high frequency of activity in the VMHdm, with these synapses acting effectively as low pass filters. One possible explanation is that the synaptic depression is specific to olfactory inputs, limiting what kind of behaviour can be elicited by olfactory cues. Olfaction does not convey a very direct information about the threat, as the predator does not have to be present in the same direction as the origin of the smell. Often the predator might have left alltogether, leaving only the scent behind. Ultimately, one of the most elements for survival is the energy preservation, so overreacting to stimuli which are not directly threatening should be limited.

In some of my experiments the viral injection has spread beyond the MEA, into the basolateral nuclei. Interestingly, in these experiments I have not observed any synaptic facilitation, although it could have been overriden by the activity of inputs evoked from the MEA. It would be therefore insightful to record inputs from other brain areas to investigate whether the synaptic depression is also present on other synapses. My preliminary recordings of inputs to SF1+ cells from the midbrain region of the parabrachial nucleus (data not shown) have also shown presence of synaptic depression. However, extracellular electrical stimulation recordings have indicated presence of both depression and facilitation at SF1+ neurons (data not shown). I hypothesize that facilitating synapses might be present on the projections

from other medial hypothalamic nuclei, such as the AH or the dPMN, which are heavily interconnected.

Limitations of slice electrophysiology and optogenetics

Optogenetics has been an incredibly useful tool for describing neural circuits, however the results have to be interpreted with caution. Firstly, one has to consider whether the light induced activation of presynaptic neurons is physiological, in slices as well as in vivo.

To begin with, one cannot be sure that the synaptic depression observed is not due to the properties of ChR2 itself, which has been shown to produce artificial depression in some cell types (Jackman et al., 2014). Although my extracellular electrical stimulation recordings have shown that depressing synapses are indeed present on the SF1+ cells, it would be necessary to perform dual cell recordings in order to confirm that these synapses are present on the inputs from the MEA. Since MEA cell bodies are separated from their projections during slice preparation, it would be necessary to patch the axons of MEA neurons, which is achievable but technically challenging.

Secondly, since ChR2 was injected relatively unspecifically in MEA, all MEA inputs in the VMHdm were activated through light stimulation, not just those synapsing onto SF1+ neurons. Jo, 2012 reported presence of local inhibitory inputs onto SF1+ neurons and it cannot be excluded that MEA neurons also synapse onto these inhibitory interneurons. It is possible that these local inhibitory inputs might also be acting on SF1+ cells, for instance through the means of shunting inhibition. To investigate this further, one could record MEA inputs onto SF1- cells, in combination with recording the SF1- inputs onto SF1+ cells.

Finally, ChR2 stimulation results in a very artificial, synchronous activation of inputs, not allowing for temporal integration which might be occurring physiologically.

Limitations of in vivo optogenetic stimulation experiments

Govic and Paolini, 2015 showed that in the presence of cat odour, rat MEA activity increases only to 2.5 Hz. This raises questions of relevance of looking at the effects of high frequency stimulation of the MEA projections, which might never be present in vivo. It is however the only study published and it cannot be excluded that some MEA neurons might be active at higher frequencies.

Moreover, there are strong reciprocal connections between the VMHdm and other hypothalamic areas. It cannot be excluded that during such an artificial, synchronous activation of the projections through ChR2, the network enters some kind of an oscillatory state. A possibility of back propagation of action potentials should also be considered. It is possible that MEA cell bodies are also activated while stimulating MEA projections, which might have effects on other parts of the brain through their collateral projections.

Finally, since it is impossible to infect selectively the MEA region, due to absence of MEA specific cell markers, it is likely that the viral infection has spread over to the neighbouring amygdala nuclei, such as the central or basolateral amygdala. Since inputs from the AOB localise to a small part of MEA (Mohedano-Moriano et al., 2007), it is not possible to claim that the inputs I have stimulated and measured are purely olfactory in origin. However, it is interesting that while other areas of amygdala might have been coinfected, synaptic depression was present across all recordings.

There are a few ways which could be used to circumvent this problem. One would be to inject anterogradely transported viruses in the AOB to allow expression selectively in the olfaction related neurons in MEA (Zingg et al., 2017). Another possible solution would involve injecting retrogradely transported viruses in a CRE-dependent manner in SF1+ cells (Ciabatti et al., 2017), thereby solving the problem of activating projections synapsing onto local interneurons (assuming lack of collateral projections to both of these populations). Finally,

one could look at the predator specific connections by using fos-creER system and expressing CRE selectively in the cells which were active during predator presentation (Vooijs et al., 2001). While I have tried this latter approach, the cell labelling efficiency was really low, which could be explained by the low firing rate even in the presence of predator cues (Govic, Paolini 2015).

4.3.3 *Conclusion*

Through my electrophysiological recordings from SF1+ neurons I have concluded that this population of cells is homogenous with respect to its electrophysiological properties. There was also no observed heterogeneity in the pattern of inputs from the MEA or the way that SF1+ cells integrate these inputs. How can activity in one population of cells trigger a variety of behaviours and what is the role of these cells in the control of defensive behaviours?

Activation of SF1+ neurons triggers behaviours through the downstream effects, so the differences in the behaviour elicited could be due to the downstream regions being activated to different degrees. It remains unclear how the level of activity in SF1+ neurons is determined.

It cannot be excluded that the inputs SF1+ cells receive are homogenous in their properties, but heterogenous in terms of their connectivity pattern. It is possible that the behaviour specific information is encoded already in the amygdala and preserved through a specific pattern of input onto SF1+ cells.

In order to investigate this, I next performed Ca^{2+} imaging in the VMHdm in freely moving animals. The results of these experiments are described in the following chapter.

5

VMHDM ACTIVITY IN RESPONSE TO PREDATOR CUES

5.1 INTRODUCTION

Electrophysiological recordings from SF1+ neurons in the VMHdm (Chapter 4) suggest that the population of SF1+ cells is largely biophysically homogenous. There were no observed differences in the way these cells integrate inputs, leaving the question of heterogeneity of the evoked behaviours unanswered. If there are no differences in the way the inputs are processed, I next questioned whether the choice of behaviour elicited could be determined by the pattern of the input.

I speculated that different aspects of information about predators could be fed into different groups of cells in the VMHdm, similar in their biophysical properties but differing in their input pattern. Thus, the information signalling a more immediate threat, such as an ultrasound, might activate a different population of SF1+ cells than an olfactory cue, which is less direct. While Ishii et al., 2017 have recently shown the presence of such labeled-line organisation in the VMHdm, their study compared the cellular responses to predators with responses to sex pheromones from the same species.

The second question I wanted to address concerned the levels of in vivo activity in the VMHdm. Using optogenetics to elicit behaviour in vivo results in a synchronous activation of a large population of cells, often at an arbitrary frequency. Does the VMHdm ever experience such high levels of activation in vivo and are any of these optogenetic experiments physiologically relevant?

Moreover, as my previous experiments have shown (Chapter 3), there is a relatively long delay between onset of stimulation of SF1+ neurons and the onset of escape, lasting between 1 and 3 seconds, depending on the frequency of stimulation. This is significantly longer than the behavioural responses to naturally evoked stimuli, where the reaction time can be a fraction of a second. This raises a question whether activity in the VMHdm is actually controlling escape behaviour, and brings us back to the question of the role of VMHdm in triggering defensive behaviour.

Kunwar et al. 2015 and Silva et al. 2016 have suggested that the VMHdm might be important for setting the emotional state of the animal, rather than simply triggering the motor outputs. On top of that, SF1+ neurons in the VMHdm are involved in a variety of other behaviours, such as metabolism and social behaviour (Cheung et al., 2015). As such, the VMHdm could act as a centre coordinating expression of a range of behaviours, including a defensive behaviour.

I decided to address these two questions by measuring the activity of individual VMHdm neurons in vivo in freely moving animals. To investigate the hypothesis of a labeled-line organisation in the VMHdm, I presented animals with olfactory and auditory predator cues. To ensure I could reliably compare responses to different stimuli in the same cell, I used single cell calcium imaging. This also allowed me to target specifically the glutamatergic output cells in the VMHdm. These experiments also allowed me to investigate the question of the physiological levels of activity in the VMHdm in response to predator stimuli. Moreover, by performing these experiments in freely moving animals, I was also able to correlate neuronal activity with the behavioural output.

This is the first study to report the levels of VMHdm activity in response to predator stimuli, thereby contributing to our understanding of the role of the VMHdm in control of innate defensive behaviours.

Two photon vs single photon excitation microscopy

Calcium imaging can be performed using either single photon or two photon microscopy. While currently available methods technically allow for either to be performed in freely moving animals (Resendez et al., 2016, Helmchen et al., 2001), two photon imaging is less established in freely moving animals and is usually performed in head-fixed animals. As a result I had a choice of performing my experiments using either two photon microscopy in head-fixed animals or single photon microscopy in freely moving animals, both of which have their own advantages. The methods are explained in Chapter 2.

There are multiple advantages of using two photon excitation microscopy. Thanks to reducing the excitation volume with two photon excitation, there is no out of focus light collected. The amount of scattered light is also reduced, as longer excitation wavelengths are used. As a result, spatial resolution of images obtained from two photon imaging is higher than from single photon imaging.

Reduced excitation volume also reduces bleaching, which not only further improves the signal to noise ratio, but also and enables longer experiments. Moreover, longer excitation wavelengths enable dual colour imaging, since two photon excitation spectra of the red and green fluophores are further apart from each other than the single photon excitation spectra (Drobizhev et al., 2011). This gives the advantage of simultaneously performing structural imaging, which enables post acquisition correction of movement artefacts, such as cells moving in and out of focus.

Most importantly, I was hoping to establish a technique of collecting data during acute implantation of GRIN lenses, rather than from chronically implanted lenses, as is commonly done. This would allow me to record from different areas of the VMHdm in the dorso-ventral axis in a single animal, thereby greatly increasing the data output and allowing a cross section study of the VMHdm in a single animal.

The biggest limitation of two photon excitation imaging is the need to perform the experiments in a head-fixed animal. First and foremost, the animal cannot freely respond to the stimulus and therefore it is difficult to correlate neuronal activity with the behavioural output. This is especially true when investigating behavioural responses such as risk assessment, which are difficult to reproduce in a head-fixed setting. Moreover, head-fixing itself is anxiogenic, even in trained animals, which is likely to introduce artefacts. It has been shown that physical restraint in rats is an emotional stressor and increases c-Fos expression in medial amygdala (Dayas et al., 1999).

The main advantage of single photon imaging is the possibility to conduct the experiments in freely moving animals. They can be tested in a much more natural environment, either in a behavioural arena (as described in Chapter 3) or even in their home cage, which reduces anxiety. They also can respond to stimuli behaviorally and therefore the recorded neuronal activity can be correlated not only with the stimulus, but also with the behavioural output.

Since both techniques have their advantages and disadvantages, I decided to attempt both of them. I first tried to perform calcium imaging experiments using two photon excitation microscopy in a head-fixed, awake animal. I have spent some time optimising the two photon microscopy set up to allow imaging during acute implantation. However, results showed that over the course of the lens implantation in the brain, the image quality drastically decreased. I speculated that this was most likely due to bleeding and accumulation of tissue in front of the lens, which becomes more problematic the deeper the brain area of interest is located.

Since it was not possible to obtain data during acute lens implantation, I decided to perform single photon imaging in freely moving animals. As mentioned, not only the animals are in a more natural, less anxiety-inducing environment, but the cell activity can also be correlated with the behaviour. Since the experiments could be con-

ducted in any behavioural arena, I could then compare the results to those described in Chapter 3.

As it turned out, spatial resolution of the acquired images from single photon imaging was high enough to easily distinguish individual ROIs in the field of view. There were also fewer motion artefacts than expected, probably due to the depth of GRIN lens implantation, with surrounding tissue holding the lens firmly in place. I therefore decided that the benefits of the animal being freely moving were greater the advantages of improving the resolution using two photon excitation. Consequently, all the data from the VMHdm has been collected using a single photon imaging set up. I first present the data illustrating my attempts at two photon imaging during acute implantation of GRIN lenses.

5.2 RESULTS

5.2.1 *Two-photon excitation microscopy imaging*

The first aim of this project was to test the possibility of performing calcium imaging of deep brain regions during acute implantation of GRIN lenses. There are no studies reporting the use this technique and all published data have been collected using chronically implanted lenses.

I started the project by performing a set of preparatory experiments to optimise the technique of two photon imaging in an awake head-fixed animal. To begin with, I imaged the cerebral cortex through an acute cranial window in a head-fixed animal, first anaesthetised and then awake. I used a transgenic VGAT:tdTomato mouse, which expresses a tdTomato fluophore in the GABA-ergic neurons across all layers in the cortex. I chose a tdTomato fluophore rather than GCaMP for these preparatory experiments, as it is brighter and more photostable compared to EGFP (Drobizhev et al. 2011).

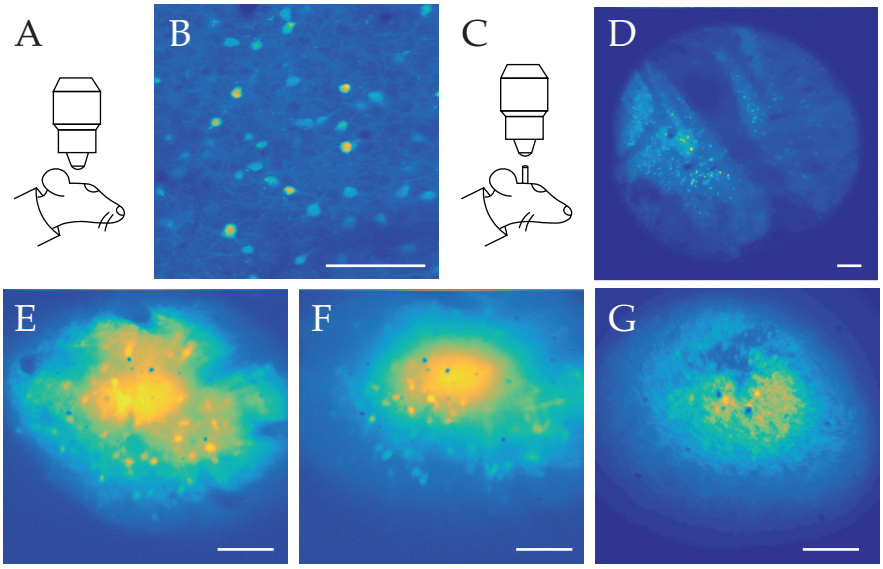

Figure 5.1: Two photon excitation imaging of cytoplasmic tdTomato through a GRIN lens. A. Illustration of a head-fixed mouse under a two photon microscope B. tdTomato in the VGAT+ cells of the somatosensory cortex, imaged through a cranial window C. Illustration of a head-fixed mouse under a two photon microscope through a GRIN lens D. tdTomato in the VGAT+ cells of the somatosensory cortex, imaged through a GRIN lens (d=1 mm) E. and F. tdTomato in the VGAT+ cells of the somatosensory cortex, acute implantation, imaged through a GRIN lens (d=0.5 mm) G. tdTomato in the VGLUT2+ cells of the thalamus, acute implantation, imaged through a GRIN lens (d=0.5mm). scale bar, 100 µm

On the day of the imaging session, a craniotomy was performed to create a small cranial window over the somatosensory cortex and covered with a 3 mm diameter coverslip. The methods are described in detail in Chapter 2. An example of the image of the cortex obtained through the two photon microscope can be seen in Figure 5.1B.

Since two photon microscopy allows imaging of only up to a few hundred µm of tissue (Oheim et al. 2001) and the VMHdm is located at the depth of 5.5 mm, it is currently necessary to use GRIN lenses to image cells in the VMHdm. I first repeated the experiment of imaging the somatosensory cortex in a VGAT:tdTomato mouse, this time using a GRIN lens (d=1mm) on top of the cranial window. The GRIN lens was mounted on a holder and the focus adjusted manually to achieve the right distance between the objective and the focal plane of the GRIN lens. The lens was then lowered onto the brain while at the same time readjusting the focus with the objective. The image

of the cortex through the GRIN lens was very promising, as seen in Figure 5.1D.

I was then ready to begin the main phase of this experiment, namely two photon imaging during simultaneous insertion of the lens into the brain tissue. I again used a VGAT:tdTomato mouse and first attempted to image different layers of the somatosensory cortex through the GRIN lens (d=0.5mm). As seen in Figure 5.1E and F, the image quality deteriorated as the lens was inserted deeper into the brain across the cortical layers. This image deterioration was likely due to bleeding and tissue drag during lens insertion, which then occluded the field of view. Even though the image quality was less than I hoped for, at this stage individual cells were still distinguishable.

I therefore proceeded to image a deeper brain area. I chose the thalamus, a brain region larger and more superficial than the VMHdm, and attempted acute implantation in a VGLUT2:tdTomato mouse. Unfortunately, the image quality was markedly worse than during cortex implantation, as seen in Figure 5.1G. This was probably due to further accumulation of tissue in front of the lens, which was somewhat proportional to the distance traveled by the lens. While there was still visible fluorescence present, it is was impossible to distinguish individual cells.

Since acute implantation did not produce expected results, I decided to conduct my experiments in freely moving animals using single photon imaging. This meant that the study could be extended to correlate the VMHdm activity not only with the stimulus, but also the subsequent behavioural response.

5.2.2 *Baseline levels of activity in the VMHdm*

The experimental set up for single photon imaging in freely moving mice has been well established in the lab; the methods are explained in Chapter 2. I first aimed to image SF1+ cells in the VMHdm in the

Nr5a1:CRE mouse line. However, despite optimising the injection and implantation conditions, the intensity of GCaMP6s expression was very low. In most animals there was no fluorescence visible, while in those few animals where cells were visible, high LED intensities had to be used to visualise the cells, which bleached the fluorescence quickly and made long recording sessions impossible. Since studies have reported that all VGLUT2+ cells in the VMHdm are also SF1+ (Tong et al. 2007), I decided to try using a VGLUT2:CRE mouse line instead. In this mouse line the GCaMP6s expression was much higher, which could be due to differences in expression levels of cre recombinase between these two mouse lines. Therefore all of the data presented in this chapter has been collected from VGLUT2:CRE mice rather than Nr5a1:CRE mice. Figure 5.2C shows a histological image of a coronal section of the brain containing the VMHdm, with the site of GCaMP6s injection and a visible track from the lens implant.

The image quality from the single photon imaging set up was stable during the recording session, with little movements artefacts. A sample field of view can be seen in Figure 5.2E. There were small differences in the field of view between recording sessions on different days, so the cells (also referred to as ROIs, regions of interest) recorded on different days were analysed as different cells. The animals had several habituation sessions each, which reduced their anxiety and improved mobility with the head mounted camera. The data presented in this chapter has been analysed from five animals across a total of 12 experiments (2 or 3 experiments per animal).

The first thing I observed was a variable baseline level of activity across the cells. To quantify the baseline activity rate I calculated the number of events per ROI over 1 minute long recording during the habituation period, the histogram of which can be found in Figure 5.2F. This is just an approximation of the activity levels within the VMHdm. While technically it is possible to use the size of each calcium transient to estimate the number of action potentials, more

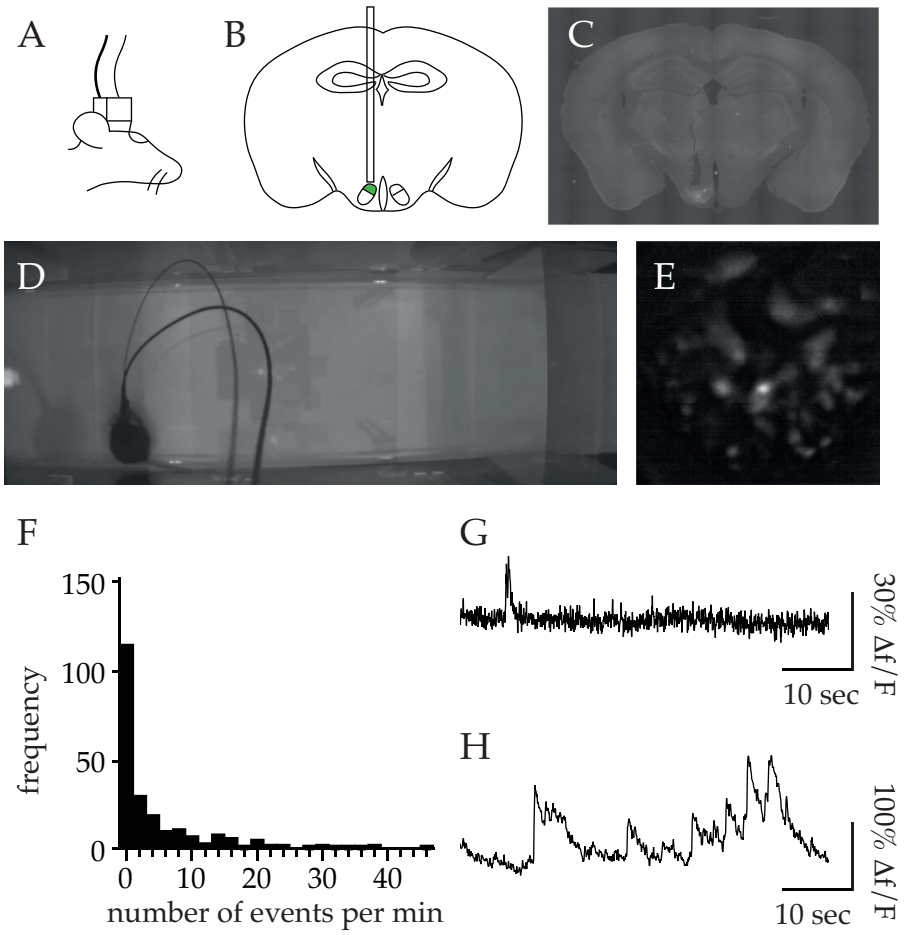

Figure 5.2: Single cell calcium imaging in the VMH. A. Illustration of a mouse with a head mounted microscope B. Illustration of a coronal brain section containing the VMHdm (green) and an implanted GRIN lens. C. Histology of a coronal coronal brain section containing the VMHdm injected with GCaMP6s and a visible track from the lens implant D. Image of the behavioural arena with a mouse connected to the imaging set up. E. Example of the GCaMP6s fluorescence as seen through the GRIN lens, average projection of 711 frames. F. Histogram of the number of spontaneous events recorded in 1 minute in each ROI during the habituation period. G., H. Spontaneous activity during habituation period, two different ROIs.

accurate ways to quantify the baseline activity levels in the VMHdm are discussed in section 5.3.

The majority of cells were only sparsely active. Half of cells were completely silent and over 75% of cells had only 6 events per minute (0.01 Hz) or fewer. However, there was a small number of cells with a high level of baseline activity of up to 46 events per minute (0.78 Hz). Figure 5.2 shows calcium transients from two representative ROIs, recorded when mouse was exploring the arena during the habituation period; one is an example of a particularly active ROI (H) and the other a largely silent one (G). The mean number of events per minute was 4.6 (0.08 Hz).

The finding that some VMHdm cells are spontaneously active and others largely silent is in line with my electrophysiological recordings described in the previous chapter; Dhillon et al., 2006 reported that SF1+ neurons have a cell attached firing rate of 0.52 ± 0.09 Hz (SEM). The variability in the baseline activity levels between different cells suggests a possibility that some cells might be receiving more tonic excitatory inputs than others. Moreover, the cells with the highest baseline activity levels were mostly present in 2 out of the 5 tested animals, which suggests that the baseline activity levels might also be related to the location of the cells within the VMH. It would be necessary to test a larger number animals to investigate this further.

Having recorded the baseline activity levels in the VMHdm, I next investigated changes in the VMHdm activity during exposure to predator cues.

5.2.3 *VMHdm responses to sensory stimuli*

I recorded activity of the glutamatergic VMHdm neurons in the presence of ultrasound, snake skin and petri dish, as well as during different behavioural responses of the animal, such as sniffing or escape to the shelter. To classify whether ROI was responsive or not, z-score

was calculated using a 5 second baseline before the stimulus onset. If the peak z-score was greater than 2 for a period of at least 500 ms within 5 seconds following the stimulus presentation, the ROI was classified as responsive.

The responses were quantified in relation to all active ROIs, i.e. ROIs which had at least one calcium transient at any point during the whole recording session. As a control, three random time points were chosen during the habituation period and using the same criteria as above each ROI was classified as a responsive or not. The probability of each ROI being active during this control period was then calculated using these three time points. The probability of ROIs being active during presentation of the stimulus was then compared to the control using a paired t test. While this comparison should ideally be done individually for each ROI, this was not possible due to a low number of trials for each ROI.

53% of all active ROIs in the VMHdm increased their activity in response to at least one of the stimuli (olfactory or auditory). Out of all ROIs active at least once across all recording sessions, 32% responded to snake skin and 29% responded to ultrasound. 8% of all active ROIs responded to both snake skin and ultrasound. 11% of snake skin responsive ROIs also responded to petri dish. None of the ultrasound responsive ROIs responded to petri dish. The responses were not correlated with the behavioural output, as discussed below.

Responses to auditory stimuli

After a period of habituation, the animal was given three presentations of 3-second-long ultrasound stimuli, separated by at least 20 s each. 29% of all active ROIs (76 out of 266 ROIs) responded to ultrasound at least once. Figure 5.4A shows the raster plot of the average responses from all ROIs classified as active, aligned to the stimulus onset at 5 s. The reliability of the response was high, with a mean response probability of 0.68 ± 0.28. This was significantly higher than the response probability of the same set of ROIs during the control

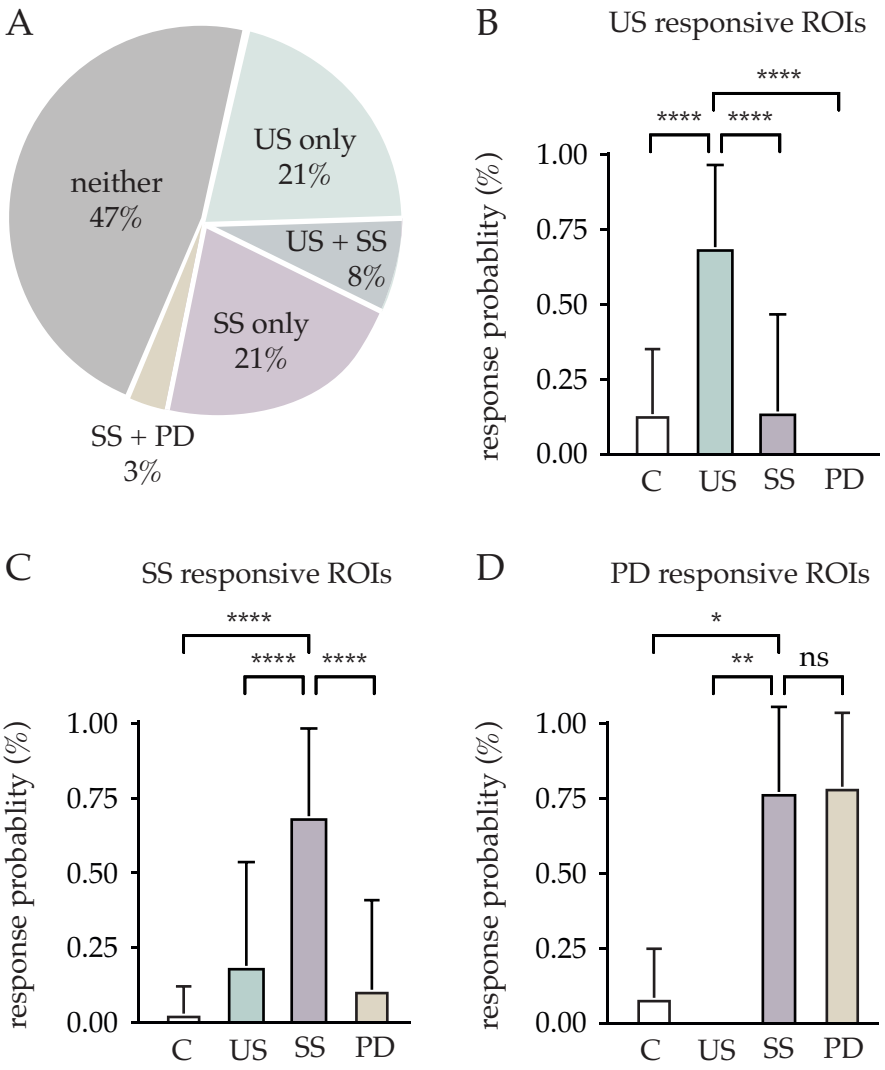

Figure 5.3: Overview of responses to different stimuli. A. Pie chart illustrating proportion of responses to different stimuli. n = 266 B. Probability of US-responsive ROIs responding to other stimuli. C. Probability of SS-responsive ROIs responding to other stimuli. D. Probability of PD-responsive ROIs responding to other stimuli. SS – snake skin, US – ultrasound, PD – petri dish, C – control (habituation period)

period (0.13 ± 0.22, p<0.0001). 37% of ROIs responded to all three presentations. Figure 5.4B shows the calcium transients from a cell which responded to all three presentations, and Figure 5.4C a cell which responded only twice.

The latency between the onset of the ultrasound and the onset of calcium transient was variable, with mean latency equal 571 ± 538 ms. Figure 5.5A shows the histogram of all latencies from all responsive ROIs. It is a large range of latencies, with some equal 200 ms and others as long as 2 s. The extremely short latency below 100 ms was present mostly in the cells with high baseline activity levels and might be due to some events being coincidental rather than induced by the stimulus. The variability in latencies was largely due to differences between ROIs, with latencies for a given ROIs across subsequent ultrasound presentations being largely consistent. Figure 5.4BC shows calcium transients from two ROIs, one with a small and one with a large response latency.

Figure 5.5B shows calcium traces of all active ROIs in a given field of view in one experiment. The distribution of latencies from that trial is presented in Figure 5.5C, with a mean latency across all ROIs from this particular trial equal 527 ± 168 ms.

In terms of behaviour, the first behavioural response shown following the onset of the ultrasound was a signal detection response, usually seen as a rapid head turn movement. It is the first behavioural indicator that the animal has detected the stimulus. The delay between the ultrasound onset and the signal detection response was 247 ± 77 ms (Figure 5.5D). The variability in the onset of this behaviour could be partly attributed to the variability in the tagging of the behaviour, which was performed manually based on the camera recording. However, this response happened significantly earlier than the onset of the calcium transient in the VMHdm neurons (p<0.0001).

Following the signal detection response, animals showed a variety of behaviours, including a body turn, forward walking, escape to the shelter and no movement. An example of the calcium activity of one

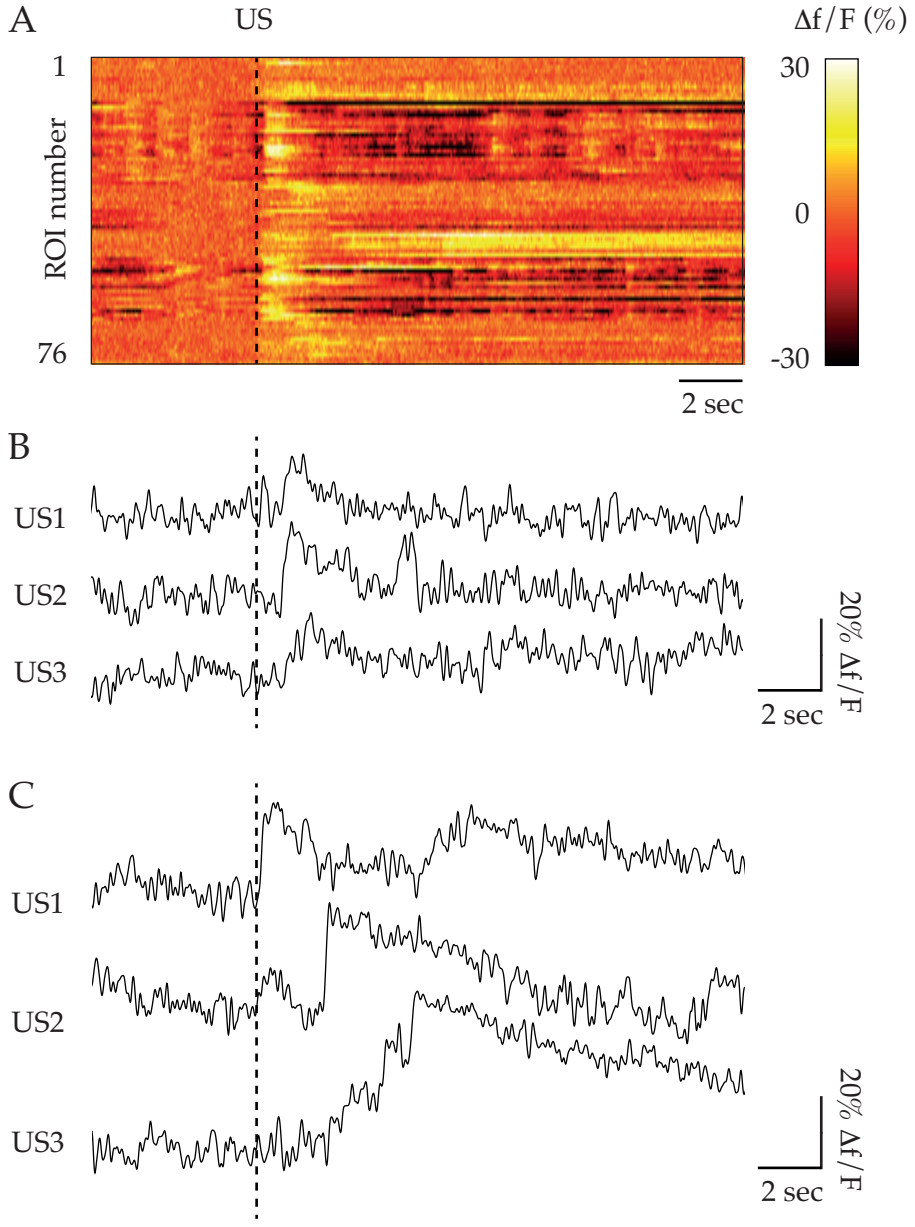

Figure 5.4: Calcium transients in the VMHdm in response to a 3-second 17-20 kHz ultrasound stimulus (US) A. Raster plot showing average responses of US-responsive ROIs, average of 3 trials per ROI B., C. Individual calcium transients in response to US presentation. US onset marked with a dashed line.

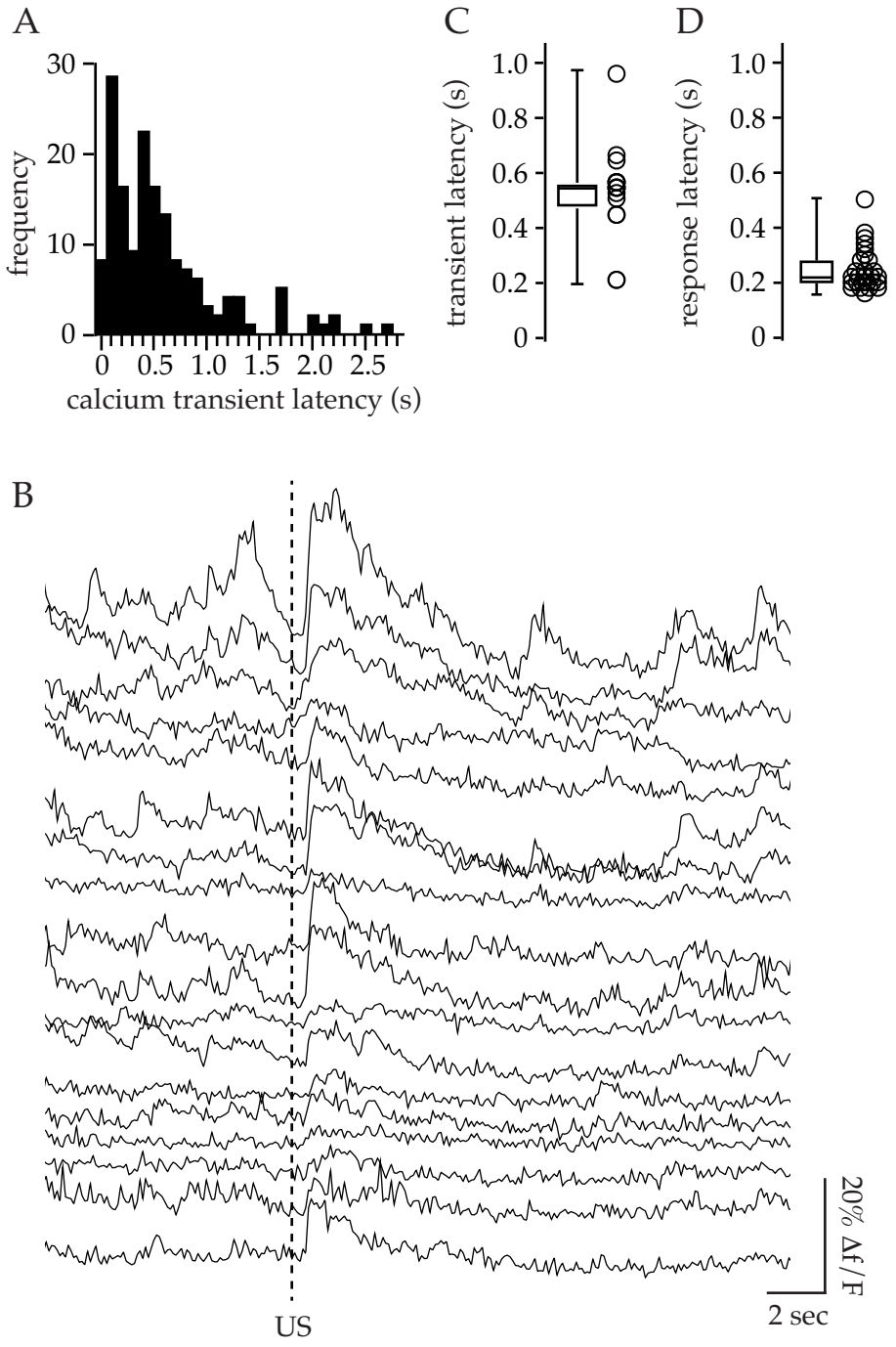

Figure 5.5: Latency between ultrasound (US) stimulation and onset of activity. A. Histogram of all latencies to calcium transient onset, n=159 B. Examples traces showing change in fluorescence across all US-responsive ROIs in a given trial, US onset marked with a dashed line C. Distribution of latencies to calcium transient onset from ROIs presented in B. D. Latency between US stimulation and signal detection response, n=27.

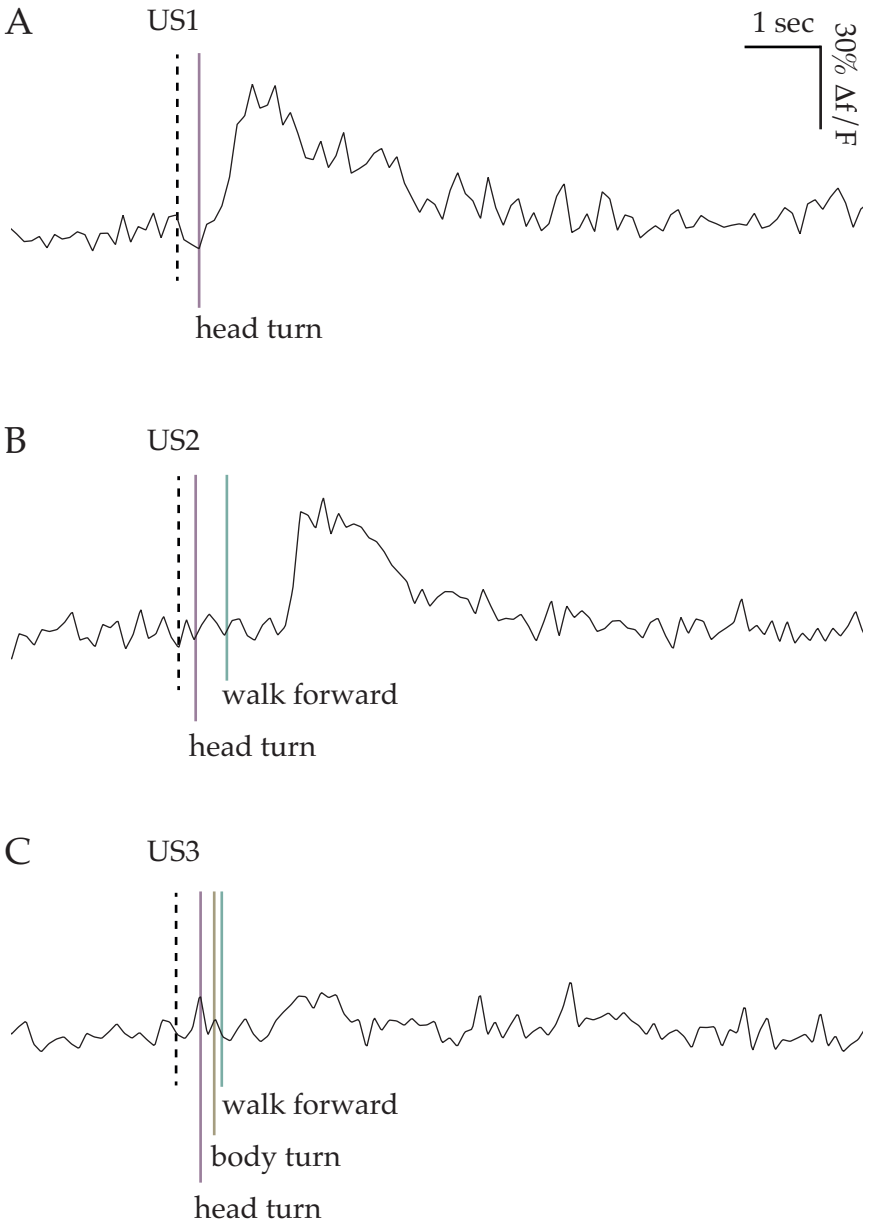

Figure 5.6: Calcium transients and behavioural outputs in response to ultrasound (US). Three US presentations, traces from a single ROI.

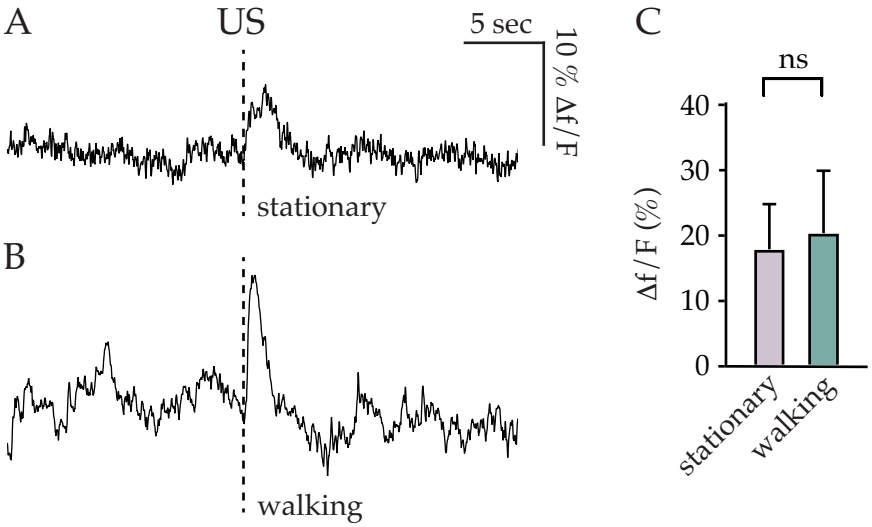

Figure 5.7: Calcium transients during different behavioural outcomes following ultrasound stimulation. A. Trace of the average change in fluorescence when the animal remained stationary. B. Trace of the average change in fluorescence when the animal initiated forward walking movement. C. Peak Δf/F following ultrasound stimulation when the animal remained stationary and when it responded with walking.

ROI across 3 trials where the animals showed different behaviours can be seen in Figure 5.6.

The peak Δf/F was not statistically different (p=0.0683) when comparing the trials in which the animals remained stationary and in those where the animal responded by walking forward (Figure 5.7), although the p value was relatively small and it is possible that given a higher number of trials it might become significant. Based on this measure, as well as the long latency to onset of the calcium transients, I concluded that the transients were not correlated with the subsequent behaviour.

This raises two interesting points regarding the role of the VMHdm in control of defensive behaviours. Firstly, the majority of cells in the VMHdm responded later than the behavioural response to stimulus. Secondly, the response in the VMHdm was correlated with the stimulus and not with the behavioural output. These findings are discussed further in section 5.3.

5.2.3.1 *Responses to snake skin*

After a period of habituation, snake skin was inserted in the arena and placed at the end of the arena opposite to the shelter. In the majority of cases the animal approached the snake skin to investigate it. The approach and each sniff of the snake skin were manually tagged offline and ROI activity was assessed in relation to the tagged events.

32% of all active ROIs (85 out of 266 cells) responded to snake skin within the time window of 1 second before the tagged sniffing until 4 seconds afterwards. Figure 5.8A shows the raster plot of the average activity of all ROIs classified as active, aligned to sniffing as tagged at 5s.

The reliability of responses to snake skin sniffing was harder to calculate than in case of responses to ultrasound. Often multiple sniffing events happened within seconds of each other, and subsequent calcium peaks were difficult to distinguish in the ongoing fluorescence due to the long decay half time of the GCaMP6s fluorescence (decay half time over 1s, Chen et al., 2013). The reliability of responses was therefore calculated by considering only the activity during the first sniff in each series of sniffs. The response probability to snake skin sniffing in the snake skin responsive ROIs was 0.69 ± 0.29. This was significantly higher than the response probability of the same set of ROIs during the control period (0.03 ± 0.09, $p<0.0001$).

The measurements of latency between the sniffing and onset of the calcium transient were not very accurate due to variability in the tagging of sniffing, which was done manually. Distribution of the latencies can be found in Figure 5.9. The mean latency was -10.8 ± 51.0 ms, and the negative value suggests that stimulus detection through sniffing happened before the time it was tagged. It is also worth remembering that the acquisition rate of the camera was 50 fps, equivalent to 20 ms.

The majority of active ROIs showed very distinct responses to each sniff, very similar to the responses showed during ultrasound present-

ation (Figure 5.8B). A small subset of cells showed a more prolonged activity, when the snake skin was in the arena, as well as during sniffing of snake skin (Figure 5.8C).

To control for the stimulus of manually inserting snake skin into the arena, as well as for the presence of a new object in the environment, neuronal responses were also tested in the presence of a petri dish.

5.2.3.2 *Responses to petri dish*

After a period of habituation, a clean petri dish was inserted in the arena and placed within the ROI, at the end of the arena opposite to the shelter. In the majority of cases the animal approached the petri dish to investigate it. Unlike in case of snake skin presentation, the animals quickly lost interest in the petri dish and often did not investigate it more than once.

Only a small number of all active ROIs (4 out of 266 cells) increased their activity during inspection of the petri dish, with a response probability of 0.79 ± 0.25 (baseline response probability 0.08 ± 0.17, p=0.0252). Interestingly, these cells were also active during inspection of snake skin with a probability of 0.78 ± 0.29 (not significantly different, p=0.9026).

In addition, a small number of all active ROIs (5 out of 266 cells) increased their activity during insertion of the petri dish into the arena. Unfortunately it was not possible to calculate the response probability for these cells, as there was only one insertion per experiment. The response probability of these cells during the baseline period was 0. Interestingly, the same cells increased their activity during insertion of snake skin, with examples shows in Figure 5.10. It is possible that these cells might have been responding to the overhead movement during the insertion.

In total, 11% of snake skin responsive ROIs also responded to the petri dish. There were no cells active in response to the petri dish which have not responded to snake skin. In addition, none of the petri dish responsive cells responded to ultrasound. I therefore speculate

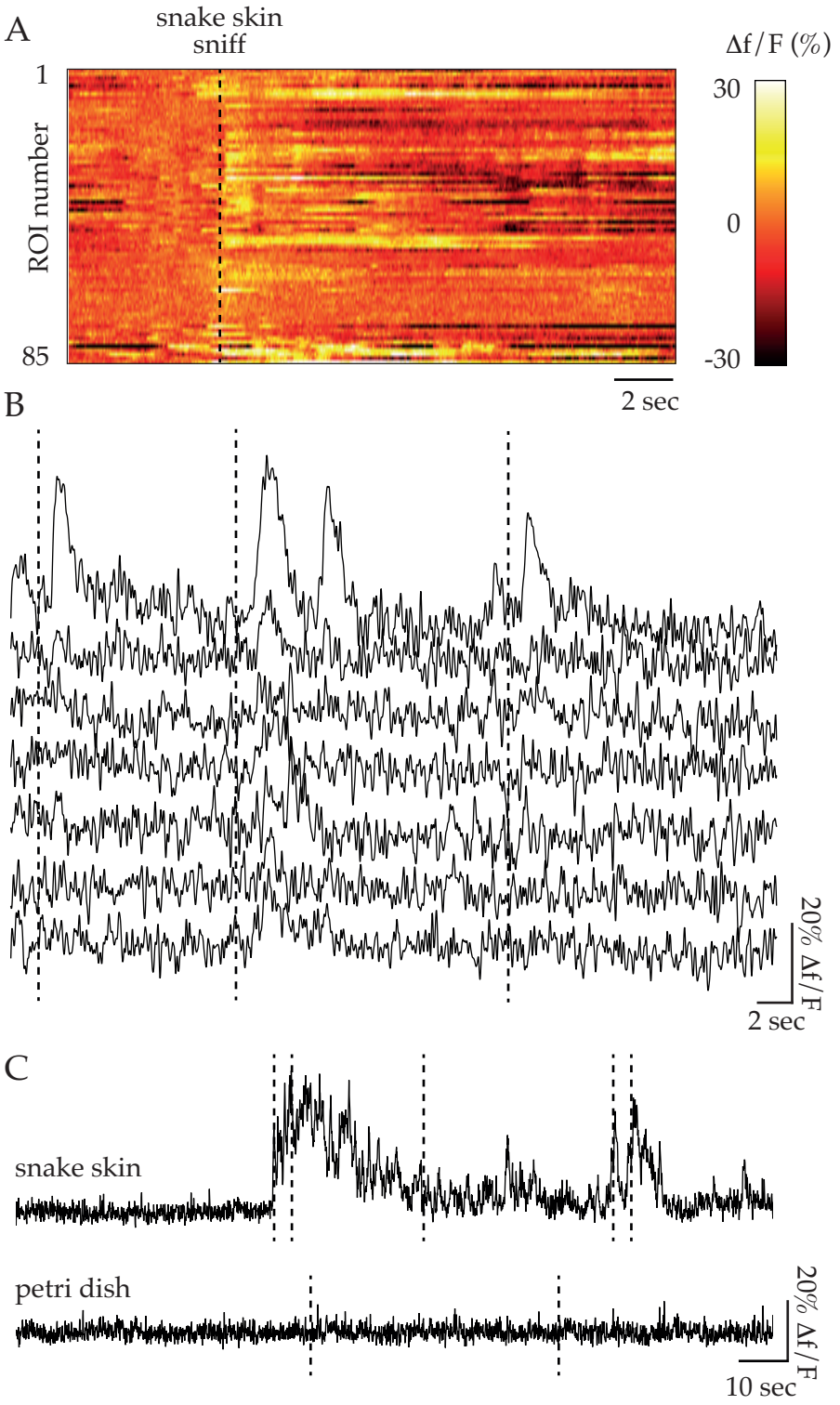

Figure 5.8: Calcium transients in the VMHdm in response to snake skin. A. Raster plot showing average responses of snake skin-responsive ROIs. B. An example of increase in fluorescence in response to individual sniffs of snake skin from all ROIs classified as active in this session. C. An example of a change in fluorescence in one ROI in response to snake skin and petri dish sniffing. Sniffing marked with a dashed line.

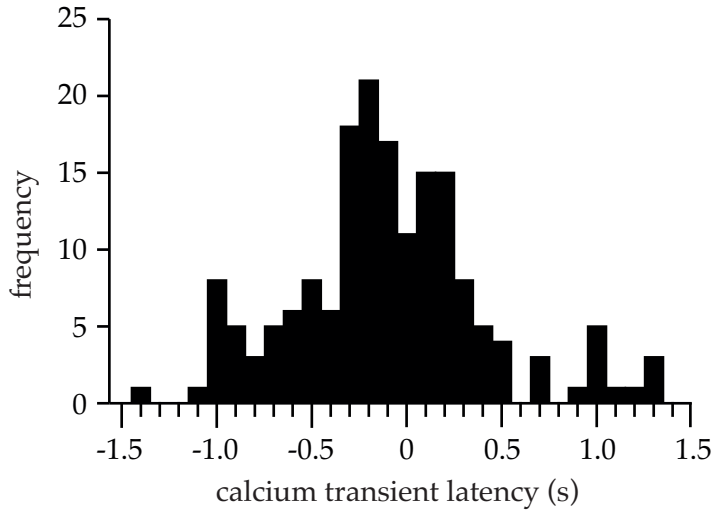

Figure 5.9: Latency between the snake skin sniff and onset of calcium transient. Sniff tagged at t = 0. n = 171

that these cells might be signalling either a change in the environment or presence of a potentially dangerous object inside the arena.

Overlap of responses to auditory and olfactory stimuli

There was heterogeneity with regards to whether a cell responded to snake skin or ultrasound, with the majority of cells responding selectively to only one or the other, and a small proportion of cells responding to both. Around 8% of all active ROIs responded to both ultrasound and snake skin, although most of these cells had a relatively low response probability to each. Example of one ROI which had 100% reliability of response to both is shown in Figure 5.11. None of these cells responded to petri dish. The overlap of responses is likely to be underestimated because of the response probability being <1 and a relatively low number of trials.

The reliability of responses to ultrasound and snake skin was not significantly different (p=0.9679). The peak $\Delta f/F$ of each individual transient was significantly higher in case of the snake skin evoked transients (p=0.0006), although the stimuli cannot be easily compared as it is not possible to be sure how many sniffs a mouse took at a time and how strong each sniff was, while the ultrasound stimulus was

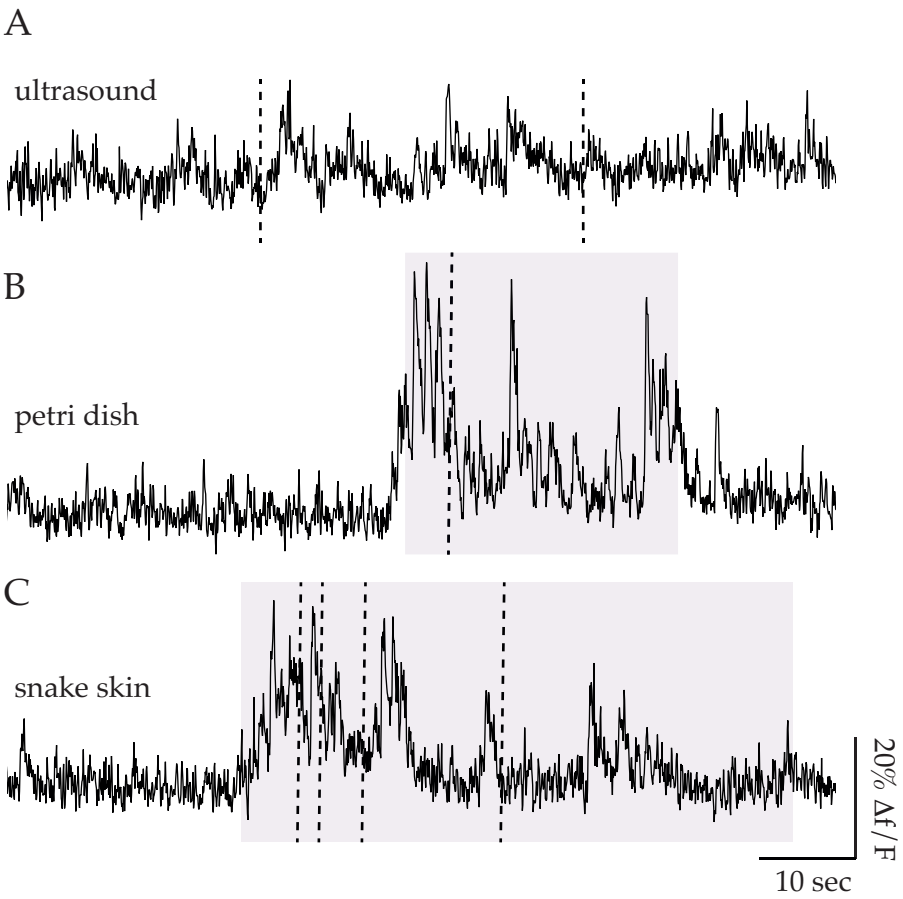

Figure 5.10: Calcium transients in the VMHdm in response to petri dish and snake skin. The period when snake skin/petri dish was in the arena is shaded in grey. Ultrasound onset and snake skin/petri dish sniffs are marked with a dashed line.

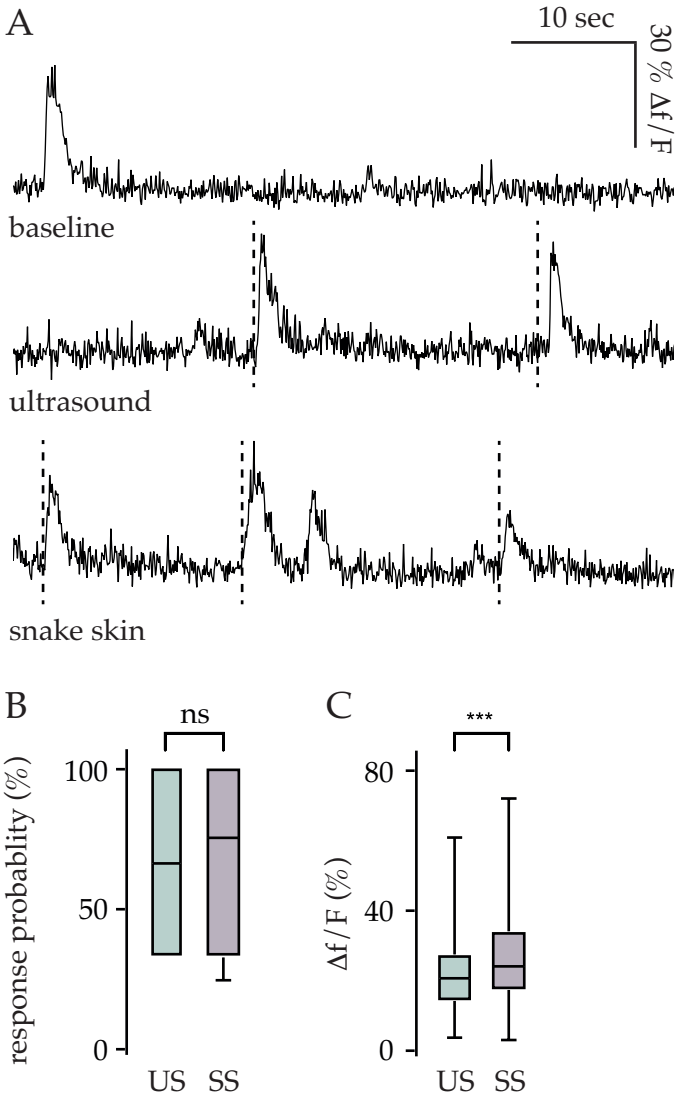

Figure 5.11: Comparison of the VMHdm responses to snake skin and ultrasound. A. An example of a cell responding to both ultrasound (US) and snake skin, US onset and snake skin sniff marked with a dashed line. B. Response reliability in snake skin and ultrasound responsive ROIs to the respective stimuli. C. Peak Δf/F of individual transient responses to snake skin and ultrasound.

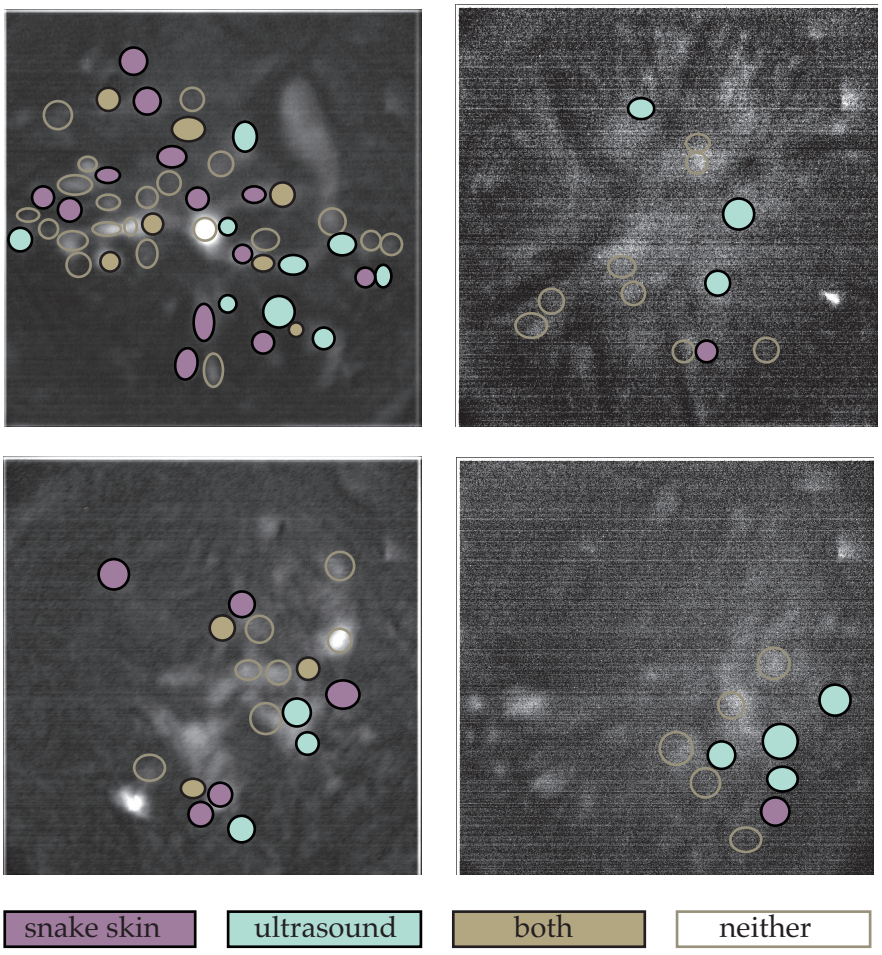

Figure 5.12: Position of cells responsive to ultrasound and snake skin in the VMH, 4 animals.

constant across all experiments. Higher $\Delta f/F$ in case of snake skin presentation could therefore be explained by the olfactory stimulus being relatively stronger and than the auditory stimulus. Figure 5.12 shows the spatial distribution of cells responsive to snake skin, ultrasound or both from 4 different sessions.

All together, these results suggest some heterogeneity in the pattern of the olfactory and auditory inputs, although both types of inputs result in similar responses in the VMHdm, with a similar number of cells being activated by each stimulus, resulting in a comparable increase in neuronal activity.

5.3 DISCUSSION

This is the first study to report the in vivo neuronal activity in the VMHdm in the presence of predator stimuli. By performing calcium imaging in awake, freely moving animals I was able to describe the responses to auditory and olfactory predator stimuli in the glutamatergic population of VMHdm neurons and correlate them with the behavioural output.

5.3.1 *In vivo activity in the VMHdm*

The first interesting finding from these results points to the diversity in the baseline levels of activity of the VMHdm cells, with the majority of cells being largely silent and a small number of cells firing spontaneously at a higher rate. The overall low baseline level of activity is in line with my predictions based on the electrophysiological recordings presented in Chapter 4. Since SF1+ cells have a resting membrane potential of -50 mV (15 mV below the action potential threshold) and a relatively low frequency of spontaneous excitatory events, I expected the majority of VMHdm neurons to be largely silent. However, the study by Dhillon et al., 2006 reported the mean

cell attached firing rate in slices to be 0.52 ± 0.09 Hz (SEM). Similarly, single unit recordings from the VMHvl performed by Nomoto and Lima, 2015 show that activity in the VMHvl is 2.65 ± 0.30 Hz. However, extracellular recordings do not take into account the cells which are silent and therefore only represent the average activity of the active units, unlike the data collected from calcium imaging experiments.

It is possible that the animals were anxious during the experiment, even in the absence of predator stimuli, and this might have been signalled through the activity of these spontaneously active cells. While the levels of activity were largely similar for a given ROI throughout the recording session, it would be necessary to perform an experiment of a longer duration to determine whether these more active cells reduce their activity over time, which would suggest that they might indeed be signalling anxiety, for instance from being in a different environment.

It is interesting to consider why it might be beneficial for an animal to have a small sub-population of cells in the VMHdm which have a higher baseline activity. Since I have not observed any differences in the electrophysiological properties within the population of SF1+ cells which could explain this variability in the baseline activity levels, it is possible that these might be receiving different amounts of excitatory input in vivo. A degree of baseline activity might help the animal maintain a level of alertness. Moreover, a tonic level of activity allows for downstream control through downregulation of this activity. It might be interesting to investigate whether cells with the high baseline level of activity are more likely to project to a specific brain area. This could be tested by injecting a retrogradely transported GCaMP6 in the AH and the PAG (shown by Wang et al., 2016 to be the two main targets of SF1+ neurons) and imaging only these subpopulations of cells in the VMHdm.

One must remember that the VMHdm has also been implied in regulation of other functions, such as metabolism and feeding beha-

viour. The activity of these cells might be conveying other types of information, not necessarily directly related to immediate threat.

5.3.2 *VMHdm responds to a variety of sensory stimuli*

Responses to snake skin

Presented data confirms that the VMHdm activity increases in response to snake skin. While Ishii et al., 2017 showed an upregulation of c-Fos in the VMHdm in response to snake skin, Crisanto et al. 2015 did not observe any changes in c-Fos expression levels. Differences in the published literature can perhaps be explained by the variability in the stimulus used, as the snake skin will inadvertly differ between the research groups, even when using the same species.

The most prevalent response to snake skin consisted of short calcium transients, which were linked to the sniffing of snake skin, although some cells responded with larger, longer lasting transients. Since the olfactory stimulus was not constant (the animals decided themselves how much to sniff and how long for), it is not possible to determine whether these were different types of responses, as they could simply reflect different stimulus strength. It cannot be excluded though that some of these cells were indeed signalling a more general presence of danger, rather than responding specifically to an olfactory stimulus.

It may come as a surprise that such a relatively high proportion of cells is active in response to what seems a very specific stimulus. In order to determine whether these responses are specific to snake skin or in general to the smell of a predator, it would be necessary to present the animals with olfactory stimuli from other types of predators, such as cats and rats.

Responses to ultrasound

While the VMHdm is thought not to be necessary for expression of behavioural responses to ultrasound (Xiong et al., 2015), it does have elevated c-Fos expression levels following exposure to ultrasound (Mongeau et al., 2013). The data presented in this chapter confirms an increase in activity in the VMHdm in response to ultrasound stimulation.

Responses to ultrasound were easier to analyse than responses to snake skin, as both the onset and strength of the stimulus could be very precisely defined. The size of the calcium transient in each responsive ROI was consistent across the trials. As opposed to the responses seen in the presence of snake skin, there was no prolonged activity in response to auditory stimulation. This could be either because the stimulus strength was constant, unlike in case of snake skin presentation, or because the animal did not perceive danger to be continuously present in the arena in between the ultrasound presentations. The latency between the ultrasound stimulus and the onset of the calcium transient was variable, which could suggest heterogeneity in the population of the VMHdm cells. The data suggests that the activity in the VMHdm is linked to the stimulus.

Comparison of responses to different stimuli

Interestingly, there was heterogeneity with regards to which cells responded to olfactory versus auditory stimuli. There were groups of cells which responded only to ultrasound or snake skin, but there was also a small subpopulation of cells which responded to both. It can be concluded then that there exists at least a small subpopulation of cells in the VMHdm which receives inputs of different modalities, although the exact nature of the inputs is unknown. It would be interesting to investigate a possibility of multimodal integration in the VMHdm on a behavioural level, and I discuss this further in Chapter 6.

There were no major differences when comparing the responses to olfactory and auditory stimuli. There were no differences in the number of cells activated by snake skin as compared to the ultrasound. The mean increase in $\Delta f/F$ was higher for snake skin, although this difference could be explained by the variability in the perceived strength of the stimuli. While the auditory stimulus was constant across all sessions, the intensity and duration of direct exposure to the olfactory stimulus was variable. The lack of differences in responses to the stimuli align with the electrophysiological results presented in Chapter 4, which indicate lack of heterogeneity in electrophysiological properties of SF1+ neurons. However, these results do suggest a heterogeneity of the input pattern.

The projection pattern of the VMHdm output neurons has been described by Wang et al., 2015. They established that the main projection targets of the VMHdm include AH and the PAG, and activating VMHdm fibres in the AH results in avoidance while activating projections in the PAG triggers immobility. It would be interesting to investigate whether the cells responding only to one of the stimuli (either auditory or olfactory) are more likely to project to either AH or the PAG, thereby preferentially promoting one behaviour over the other. This could be tested by imaging a retrogradely transported GCaMP6, injected either in the AH or the PAG.

5.3.3 *Activity in the VMHdm is liked to the stimulus*

The peak $\Delta f/F$ of the calcium transient was not correlated with the behavioural output, i.e. it was not significantly different when the animal remained stationary as compared to when it responded to the stimulus with walking. However, there were only three ultrasound presentations per experiment and the behavioural response consisted of multiple components. Performing more trials per animal would allow comparison of responses from the same set of ROIs during

different behavioural outputs, instead of a comparison on the population level. Interestingly though, in cases when the animal responded differently to all three ultrasound presentations, individual ROIs showed similar levels of activity irrespective of the behavioural outcome.

Moreover, the mean latency between the ultrasound stimulus and the onset of the calcium transient was around 500 ms; on average 250 ms after the first behavioural response of the stimulus detection. It is interesting to consider these results together with the optogenetic experiments described in Chapter 3. While direct stimulation of SF1+ cells in the VMHdm does trigger defensive behaviour, the latency between the onset of the stimulation and the escape is around 1s at 40 Hz stimulation and increases to 4s with 5 Hz stimulation. This is in contrast to the naturally evoked escape behaviour, where the latency to escape is on average around 500 ms, and can reach values as low as 100 ms (Vale et al., 2017). Similarly, optogenetic activation of the downstream PAG results in escape with a latency of around 300 ms (Dom Evans, unpublished data), which is comparable to the reaction time in response to a natural stimulus.

The above results suggest that the natural behavioural response to a predator stimulus is not directly controlled by the VMHdm. What is the role of the VMHdm then? It is possible that the VMHdm might instead act as a centre which encodes the internal state of the animal, which can be described as "alertness", modulating the immediate behavioural response according to the internal state of the animal. This hypothesis and suggested follow up experiments are further discussed in Chapter 6.

5.3.4 *Limitations*

There are a few disadvantages to using the technique of single photon calcium imaging. Most importantly for this project, it was only pos-

sible to conduct a few trials of each experimental condition per ROI, since the number of experiments that can be performed in one session is limited due to bleaching of the GCaMP6s fluorescence. Since the field of view changes slightly from one session to another, it is often hard to identify a given ROI to be the same as in the previous session. Because of the variability of the behaviour, it is necessary to have a higher number of trials in order to correlate the behavioural output with the activity of individual ROIs rather than the whole population.

Another downside is the inability to determine the firing rate of the neurons from the GCaMP6s signal. It is possible that there exist differences in the neuronal responses to auditory and olfactory stimuli, which are lost in the slowly decaying calcium signal. While using GCaMP6f would improve the temporal resolution, it also would result in a decrease of the signal to noise ratio. Ultimately, the most suitable experiment to assess the in vivo firing rates in the VMHdm would involve extracellular probe recordings. However, extracellular probe recordings would have to be combined with optogenetics in order to enable identification of the glutamatergic cells from the population of local interneurons.

Finally, movement artefacts can never be completely excluded. While the risk of misclassifying a ROI as active has been minimised by carefully examining each calcium transient trace after the script based analysis, it is always possible the cell might have moved in or out of focus, creating a waveform of the fluorescence signal very similar to what is expected. Ideally, one would perform dual imaging of GCaMP6 together with a structural marker, such as a red cytoplasmic fluophore.

5.3.5 *Conclusion*

These results for the first time report in vivo activity in the VMHdm in response to predator stimuli. By comparing responses to auditory and olfactory stimuli in the glutamatergic output neurons in the VMHdm, I have concluded that while the neuronal responses are similar for both types of stimuli, there exist differences regarding which cells are activated by which stimuli. The results also suggest that the activity in the VMHdm might not be directly responsible for controlling the immediate behavioural response to a threatening stimulus. The possible explanations of the function of the VMHdm in the light of these results are discussed in the following chapter.

Part IV

DISCUSSION

6

GENERAL DISCUSSION

The aim of this thesis was to investigate the role of the VMHdm in control of innate defensive behaviours in response to predatory threat. I begun the project by quantifying mouse defensive behaviours in response to olfactory and auditory predator cues, as well as to optogenetic activation of SF1+ neurons. Having observed that different behaviours could be elicited by these different stimuli, I set to investigate how SF1+ neurons contribute towards this behavioural decision making.

By performing patch clamp recordings from acute brain slices, I first quantified the electrophysiological properties of SF1+ neurons. I then used slice electrophysiology in combination with optogenetics to describe how SF1+ neurons integrate excitatory inputs from the medial amygdala, and quantified the behavioural effects of optogenetically activating this projection in vivo. Finally, by performing calcium imaging in the VMHdm in freely moving mice, I described in vivo activity in the VMHdm in response to ultrasound and snake skin.

6.1 SUMMARY OF FINDINGS

6.1.1 *Behavioural responses to different stimuli*

Auditory and olfactory stimulation

Stimulation with either ultrasound or snake skin produced avoidance of the area of stimulation and increased the proportion of time spent in the shelter, indicating a fearful state. They both elicited escape from

the stimulus towards the shelter, although fleeing from ultrasound was faster than from snake skin. Moreover, snake skin triggered risk assessment behaviour, which was absent in case of ultrasound stimulation.

Responses to ultrasound were similar across all tested animals, with all animals quickly fleeing to the shelter. Responses to snake skin were on the other hand very variable, with a third of tested animals actively investigating the snake skin, rather than fleeing away from it and avoiding it.

These differences in behaviour are likely to be advantageous for the animal. Ultrasound is a directional stimulus, often produced by the predator itself. The most suitable response should therefore be a fast escape away from the source of the stimulus, towards a safe hiding space. Avoidance of the area where animal detected the stimulus reduces the risk of further exposure to threat.

Snake skin, on the other hand, is primarily an olfactory stimulus. Since kairomones are not very volatile, in most cases the odour is encountered after the predator has already left, as it requires close proximity to be detected. It is often not clear at first in which direction the predator has gone, therefore escape might not be the most suitable first response. In this case reduced mobility might be more suitable to reduce the risk of being captured. If hiding space is available nearby, a careful escape back to that safe space might be the safest behavioural response. After initial escape, mice need to carefully assess the danger in order to estimate the risk of predation and decide whether they can continue other activities such as foraging. The strength and type of the olfactory stimulus might help the animal decide what type of predator it was and how long ago they have left.

It is not clear whether it is the strength of the stimulus that determines the behavioural response, or whether the behaviour is specific to the type of the stimulus.

Optogenetic stimulation

Optogenetic stimulation of SF1+ neurons showed that activation of these cells can elicit immobility and avoidance, and at high frequencies of stimulation also jumping escape. However, I noticed that the latency to jumping or escape from the area of stimulation was in the order of seconds. This is significantly longer than the latency to escape as evoked by natural stimuli, such as ultrasound, which has a timescale of a few hundred milliseconds. This observation has not been highlighted in the published literature, which has largely focused on the general behavioural trends during a period of stimulation, rather than the immediate response.

Because of this long latency to escape it becomes questionable whether activity in SF1+ neurons is what triggers escape behaviours under physiological conditions, which require fast reaction times. Moreover, such an intense and long lasting optogenetic stimulation of SF1+ neurons might not be reflective of the physiological level of activity in these neurons during predator encounter.

It is therefore possible that under physiological conditions of exposure to a natural threatening stimulus, the VMHdm might primarily promote avoidance and immobility, rather than jumping escape. Perhaps at a point when fear levels reach a certain threshold, encoded through a prolonged high level activity in the VMHdm, the downstream brain areas become primed to trigger escape instead of immobility in response to the stimulus.

6.1.2 *Electrophysiological properties of SF1+ cells*

By performing patch clamp recordings from SF1+ neurons in slices I described the electrophysiological properties of these cells. Firstly, SF1+ neurons have a very high input resistance, which means that they are highly sensitive and small current inputs are sufficient to depolarise the cells and trigger action potential firing.

This efficiency in input integration is also observed in the relatively long membrane time constant, which allows for inputs to be accumulated over a longer period of time. In combination with the high input resistance, these properties may help to ensure that none of the incoming inputs are lost. Long membrane time constant also means that the timing of the stimulus can be less precise, which suggests that the exact stimulus timing might be of a lesser importance.

While high sensitivity to threat is beneficial to the animal, overreacting to indirectly threatening stimuli is not. Not only it unnecessarily increases the energy expenditure, but also interferes with other behaviours, such as foraging and mating. In the wild animals are constantly exposed to danger and they need to maintain an internal representation of this danger without reacting to all of it. For instance, predator odour should alert the animal and increase its sensitivity to other threatening signals, without necessarily triggering immediate escape.

The data from my electrophysiological recordings suggests that the properties of SF1+ neurons make them well suited to encode information about the threat levels. Optogenetic activation of SF1+ further supports this hypothesis, as the long latency between SF1+ activation and onset of escape suggests that activity in the VMHdm might not directly trigger escape in response to a natural stimulus. Instead, it is more likely that the VMHdm is involved in integrating information about the threat to allow modulation of the behavioural response on a longer time scale.

6.1.3 *MEA inputs in the VMHdm*

I characterized excitatory inputs from MEA to SF1+ cells by performing patch clamp recordings from SF1+ neurons while optogenetically activating glutamatergic projections from MEA. I found that 80% of SF1+ neurons received inputs from MEA or neighbouring amyg-

dalar nuclei. Optogenetic stimulation elicited strong inward currents, which in combination with high input resistance of SF1+ neurons often triggered action potential firing even in response to a single 1 ms light stimulation. The connectivity rate was high, and so was the probability of eliciting a response in the connected cells. These results suggest a high efficiency of information transfer between MEA and VMHdm. These findings are in line with the data discussed earlier, which suggest that SF1+ neurons are highly sensitive to their inputs, efficiently integrating incoming activity.

Interestingly, stimulation with a fast train of light pulses showed that repeated stimulation of MEA projections produces synaptic depression. As a result, high frequency of activity in MEA was not directly translated into a high level of activity in the SF1+ neurons. In line with this observation, high frequency in vivo activation of MEA inputs in the VMHdm was not capable of producing jumping behaviour, which was observed with direct SF1+ stimulation. Naturally, it cannot be excluded that this synaptic depression is a channelrhodopsin induced artefact, and paired recordings should be performed to confirm this finding. However, it is possible that this synaptic depression has a physiological function of limiting MEA induced activity in the VMHdm. This would again support the hypothesis that the VMHdm accumulates information about the general state of danger in the environment, increasing the overall sensitivity of the circuit and priming it to respond to threat, rather than directly triggering the behavioural response.

6.1.4 *VMHdm activity during exposure to predator stimuli*

In vivo calcium imaging recordings showed that excitatory cells in the VMHdm have a low baseline level of activity, which increases in response to a threatening stimulus, such as ultrasound and snake skin. At least half of cells responded to either stimulus, with 32% of

cells responding to snake skin and 29% responding to ultrasound. A small proportion of cells (8%) responded to both stimuli. Due to a small number of trials per cell, these proportions are likely to be underestimated.

The responses to snake skin and ultrasound did not differ regarding the increase in activity or the response probability, which was around 66% for either stimulus. These findings confirm the data from electrophysiological recordings from SF1+ neurons, suggesting homogeneity within this population of cells. Moreover, cell activity was correlated with the stimulus, and the latency between the stimulus and onset of calcium transient was longer than the latency to the behavioural response of stimulus detection. Change in fluorescence was not correlated with the behavioural output, although small number of trials and variability in behavioural response mean that the data set was small. Given a larger number of trials, the difference in fluorescence might become significant.

The long latency to onset of activity in the VMHdm is in line with the earlier observations that the VMHdm is unlikely to directly trigger escape in response to threat. It is possible though that higher levels of activity in the VMHdm correlate with a more robust expression of behaviour, for instance larger avoidance or faster escape.

6.2 PROPOSED FUNCTION OF THE VMHDM IN CONTROL OF DEFENSIVE BEHAVIOURS

The electrophysiological and calcium imaging data I collected suggest that the VMHdm is efficient at gathering information about the predator threat. They also suggest that SF1+ neurons in the VMHdm are physiologically homogenous and receive similar inputs. Considering the high connectivity rate with the medial amygdala and a large proportion of cells responding to ultrasound and snake skin, I conclude that majority of these cells are responsive to threat.

At the same time, activity in the VMHdm was correlated with the stimulus rather than the behavioural output. Moreover, the latency between the stimulus and activity in the VMHdm was longer than the latency to behaviour. Similarly, optogenetic activation of SF1+ neurons triggered behaviour with a latency longer than when evoked through natural stimuli.

Based on my results, in combination with data published in other studies, I conclude that rather than directly producing behavioural outcomes, the function of the VMHdm might be to encode the internal state of the animal and facilitate the choice of the most appropriate behavioural response by modulating downstream regions. The internal state, which can be described as "alertness", can be increased through exposure to predator stimuli, but also factors such as the internal energetic state of the animal.

Based on the published literature, the majority of SF1+ cells are also leptin and insulin responsive, as well as receive inputs from glucose sensitive neurons. There is a large body of evidence suggesting that SF1+ cells are involved in control of feeding and metabolism, helping to inhibit food intake and increase glucose uptake into skeletal muscle. It is therefore possible that SF1+ neurons might in fact be integrating these two types of information, that is information about the presence of danger in the environment, and the internal availability of energy. Integration of these different types of information is necessary to allow the most optimal choice of behaviour, which is determined not only by the threat itself, but also the internal energy resources of the animal.

Upon integration of this information the VMHdm may have the following functions:

1. Modulate the downstream control of threat response (e.g. increase the sensitivity of the circuit, promote immobility instead of flight)

2. Increase the energy utilisation to prepare the animal for a possibility of escape (e.g. increase glucose uptake to skeletal muscle)

3. Downregulate other conflicting behaviours to reduce the risk of predation (e.g. feeding)

Increased activity in the VMHdm in response to predator stimuli in the environment indicates risk of predation. The VMHdm might then activate downstream brain areas, such as the PAG, to increase their sensitivity to upcoming stimuli which might pose a direct threat to the animal. Therefore the subsequent stimulus might result in a more robust behavioural response. In addition, increased activity in the VMHdm might upregulate glucose uptake in skeletal muscle to mobilise energy resources and enable the animal to respond more robustly, while downregulating feeding might reduce the risk of exposure to predators.

Projection from SF1+ neurons to the PAG has been shown to promote immobility (Wang et al., 2015). It has also been shown that higher anxiety is correlated with increased probability of freezing over fleeing (Mongeau et al., 2003). Low blood glucose, sensed by SF1+ neurons, indicates low availability of energy. It is possible that increased activity in the VMHdm, which can indicate both danger of predation as well as low energy supplies, might prime the animal to respond with freezing rather than fleeing. Reducing mobility reduces the risk of detection, while at the same time preserving energy which might be sparse.

Finally, since SF1+ neurons are inhibited during eating (Viskaitis et al., 2017), downregulating the VMHdm activity during feeding might act to reduce the avoidance of the area where the food has been found, despite the threats which might be present in the environment. It is important to remember that the interaction between different innate behaviours is likely to be bidirectional.

VMHdm is unlikely to be the only modulatory center of threat response. It is possible that the VMHdm might coordinate defensive

behaviours with metabolism and feeding, while other MHDC components might regulate other behaviours. For instance, PMD lies close to the ventral premammillary nucleus (PMV), which is important for reproductive behaviour (Canteras, 2002; Yokosuka et al., 1999) and it has been suggested that the interplay between the two of these may help regulate the two behaviours (Apfelbach et al., 2015).

6.3 FUTURE DIRECTIONS

Modulation of the behavioural response

In order to investigate whether activity in the VMHdm modulates defensive behaviours, I would begun by testing the effects of increased SF1+ activity on expression of naturally evoked defensive behaviours. Firstly, I would increase the levels of activity in SF1+ neurons by using DREADDs (Roth, 2016) and test whether this activity affects the latency to escape from auditory stimuli. If the latency was shorter than in the absence of this activation, this would provide some evidence that the downstream areas, such as the PAG, might become "primed" through the input from SF1+ neurons. The next step would then be to repeat the above experiment while stimulating SF1+ projections specifically in one brain area, such as the PAG, from which the local circuitry could be further investigated.

Secondly, I would like to test whether low levels of activity in the SF1+ neurons promote immobility over escape behaviour. To test this I would activate the SF1+ projections in the PAG with a short train of optogenetic stimulation shortly before exposing the animal to an auditory stimulus. By using conditions in which the animal has a certain probability of responding with freezing (for instance by using a larger arena), I could measure whether the probability of freezing versus fleeing is increased in the presence of SF1+ stimulation. If these two experiments showed a significant difference, I would then iden-

tify the population of cells onto which the SF1+ neurons are projecting in the PAG and investigate how they feed into the local circuitry.

Multimodal integration

To test whether VMHdm is necessary for multimodal integration, I would investigate the importance of VMHdm for control of behaviour during simultaneous presentation of two different stimuli. I would start by comparing the responses to auditory stimuli in the presence of an olfactory stimulus, and test whether the latency to escape from ultrasound and the speed of escape are different in the presence of the olfactory stimulus. If these experiments showed a significant difference in behaviour, I would then repeat the experiment by inactivating the VMHdm, for instance by using DREADDs, and assess whether the effect of modulating the response to ultrasound by the olfactory stimulus is reduced.

Secondly, I would like to test the effect of the internal metabolic state on the expression of defensive behaviour and investigate the contribution of the VMHdm in coordination of the two. I would start by comparing behavioural responses to ultrasound in fed and food deprived mice. Then I would repeat the experiment after having inactivated the VMHdm and assess whether the effect of food deprivation on the expression of behaviour is reduced.

Coordination of non-defensive behaviours

To test the role of VMHdm in coordination of non-defensive behaviours, I would like to assess whether feeding in the presence of predator odour stimulus is still suppressed when the VMHdm is inactivated, for example by impregnating food with predator odour (Coulston et al., 1993) and using DREADDs to pharmacologically inactivate SF1+ neurons.

Labelled lines

Despite having shown that VMHdm contains cells which respond to both auditory and olfactory stimuli, it cannot be excluded that there are populations of cells which are specific to one particular type of input and which project to a specific downstream area. For instance, snake skin responsive cells might be more likely than ultrasound responsive cells to project to the AH to promote avoidance.

To address this question, I would like to investigate whether SF1+ neurons responding to one stimulus (e.g. snake skin) are more likely to project to a different brain area than those responding to a different stimulus (e.g. ultrasound). To test this, I would retrogradely inject GCaMP6 in either PAG or AH and perform in vivo calcium imaging in the VMHdm. By stimulating the animal with ultrasound and snake skin I could quantify whether cells projecting to PAG or AH are more likely to be activated by one stimulus than the other. Naturally, absence of a difference would not exclude the possibility of SF1+ neurons feeding into separate neuronal populations within the PAG or AH itself.

6.4 FINAL REMARKS

The aim of the thesis was to investigate the role of the VMHdm in control of innate defensive behaviours. The data presented in this dissertation, in combination with other published studies, suggests that the VMHdm acts as a centre encoding the internal state of the animal, modulating the behavioural response to danger according to that state. Behaviours can never be expressed independently of each other and perhaps the role of the VMHdm is to coordinate the behavioural and physiological response to predator threat.

BIBLIOGRAPHY

Albert, D J and G L Chew (1980). "REVIEW The Septal Forebrain and the Inhibitory Modulation of Attack and Defense in the Rat. A Review I." In: *Behavioral and neural biology* 30, pp. 357–388.

Anderson, David J. and Ralph Adolphs (2014). "A Framework for Studying Emotions across Species." In: *Cell* 157.1, pp. 187–200.

Apfelbach, Raimund, Caroline D Blanchard, Robert J Blanchard, R Andrew Hayes, and Iain S McGregor (2005). "The effects of predator odors in mammalian prey species: a review of field and laboratory studies." In: *Neuroscience and biobehavioral reviews* 29.8, pp. 1123–44.

Atasoy, D., Y. Aponte, H. H. Su, and S. M. Sternson (2008). "A FLEX Switch Targets Channelrhodopsin-2 to Multiple Cell Types for Imaging and Long-Range Circuit Mapping." In: *Journal of Neuroscience* 28.28, pp. 7025–7030.

Berton, F, E Vogel, and C Belzung (1998). "Modulation of mice anxiety in response to cat odor as a consequence of predators diet." In: *Physiology & Behavior* 65.2, pp. 247–254.

Bester, H, J M Besson, and J F Bernard (1997). "Organization of efferent projections from the parabrachial area to the hypothalamus: a Phaseolus vulgaris-leucoagglutinin study in the rat." In: *The Journal of comparative neurology* 383.3, pp. 245–81.

Bian, Xiling, Yuchio Yanagawa, Wei R Chen, and Minmin Luo (2008). "Cortical-like functional organization of the pheromone-processing circuits in the medial amygdala." In: *Journal of neurophysiology* 99.1, pp. 77–86.

Bindman, L.J., T. Meyer, and C.A. Prince (1988). "Comparison of the electrical properties of neocortical neurones in slices in vitro and in

the anaesthetized rat." In: *Experimental Brain Research* 69.3, pp. 489–496.

Blanchard, D C and R J Blanchard (1988). "Ethoexperimental Approaches to the Biology of Emotion." In: *Annual Review of Psychology* 39.1, pp. 43–68.

Blanchard, D C, R L Spencer, S M Weiss, R J Blanchard, B McEwen, and R R Sakai (1995). "Visible burrow system as a model of chronic social stress: behavioral and neuroendocrine correlates." In: *Psychoneuroendocrinology* 20.2, pp. 117–34.

Blanchard, D. Caroline and Robert J. Blanchard (1972). "Innate and conditioned reactions to threat in rats with amygdaloid lesions." In: *Journal of Comparative and Physiological Psychology* 81.2, pp. 281–290.

Blanchard, D. Caroline, Chris Markham, Mu Yang, David Hubbard, Eric Madarang, and Robert J. Blanchard (2003). "Failure to produce conditioning with low-dose trimethylthiazoline or cat feces as unconditioned stimuli." In: *Behavioral Neuroscience* 117.2, pp. 360–368.

Blanchard, D. Caroline and Jeffrey Rosen (2008). "Olfaction and defense." In: *Neuroscience & Biobehavioral Reviews* 32.7, pp. 1207–1208.

Blanchard, R J, R Agullana, L McGee, S Weiss, and D C Blanchard (1992). "Sex differences in the incidence and sonographic characteristics of antipredator ultrasonic cries in the laboratory rat (Rattus norvegicus)." In: *Journal of comparative psychology (Washington, D.C. : 1983)* 106.3, pp. 270–7.

Blanchard, R J and D C Blanchard (1989a). "Antipredator defensive behaviors in a visible burrow system." In: *Journal of comparative psychology (Washington, D.C. : 1983)* 103.1, pp. 70–82.

– (1989b). "Attack and defense in rodents as ethoexperimental models for the study of emotion." In: *Progress in neuro-psychopharmacology & biological psychiatry* 13 Suppl, S3–14.

Blanchard, R J, D C Blanchard, R Agullana, and S M Weiss (1991). "Twenty-two kHz alarm cries to presentation of a predator, by laboratory rats living in visible burrow systems." In: *Physiology & behavior* 50.5, pp. 967–72.

Blanchard, Robert J, Julia N Nikulina, Randall R Sakai, Christina McKittrick, Bruce McEwen, and D.Caroline Blanchard (1998). "Behavioral and Endocrine Change Following Chronic Predatory Stress." In: *Physiology & Behavior* 63.4, pp. 561–569.

Borowski, Zbigniew (1998). "Influence of weasel (Mustela nivalis Linnaeus, 1766) odour on spatial behaviour of root voles (Microtus oeconomus Pallas, 1776)." In: *Canadian Journal of Zoology* 76.10, pp. 1799–1804.

Borowski, Zbigniew and Edyta Owadowska (2010a). "Field vole (Microtus agrestis) seasonal spacing behavior: the effect of predation risk by mustelids." In: *Naturwissenschaften* 97.5, pp. 487–493.

– (2010b). "Field vole (Microtus agrestis) seasonal spacing behavior: the effect of predation risk by mustelids." In: *Naturwissenschaften* 97.5, pp. 487–493.

Bosch, Oliver J (2013). "Maternal aggression in rodents: brain oxytocin and vasopressin mediate pup defence." In: *Philosophical transactions of the Royal Society of London. Series B, Biological sciences* 368.1631, p. 20130085.

Branco, Tiago, Kevin Staras, Kevin J. Darcy, and Yukiko Goda (2008). "Local Dendritic Activity Sets Release Probability at Hippocampal Synapses." In: *Neuron* 59.3, pp. 475–485.

Branco, Tiago, Adam Tozer, Christopher J. Magnus, Ken Sugino, Shinsuke Tanaka, Albert K. Lee, John N. Wood, and Scott M. Sternson (2016). "Near-Perfect Synaptic Integration by Na v 1.7 in Hypothalamic Neurons Regulates Body Weight." In: *Cell* 165.7, pp. 1749–1761.

Brechbuhl, J., M. Klaey, and M.-C. Broillet (2008). "Grueneberg Ganglion Cells Mediate Alarm Pheromone Detection in Mice." In: *Science* 321.5892, pp. 1092–1095.

Cádiz-Moretti, Bernardita, Marcos Otero-García, Fernando Martínez-García, and Enrique Lanuza (2016). "Afferent projections to the different medial amygdala subdivisions: a retrograde tracing study in the mouse." In: *Brain Structure and Function* 221.2, pp. 1033–1065.

Canteras, N S, S Chiavegatto, L E Ribeiro do Valle, and L W Swanson (1997). "Severe reduction of rat defensive behavior to a predator by discrete hypothalamic chemical lesions." In: *Brain research bulletin* 44.3, pp. 297–305.

Canteras, N. S., R. B. Simerly, and L. W. Swanson (1994). "Organization of projections from the ventromedial nucleus of the hypothalamus: APhaseolus vulgaris-Leucoagglutinin study in the rat." In: *The Journal of Comparative Neurology* 348.1, pp. 41–79.

– (1995). "Organization of projections from the medial nucleus of the amygdala: A PHAL study in the rat." In: *The Journal of Comparative Neurology* 360.2, pp. 213–245.

Canteras, Newton S (2002). "The medial hypothalamic defensive system: hodological organization and functional implications." In: *Pharmacology, biochemistry, and behavior* 71.3, pp. 481–91.

Canteras, Newton Sabino and Marina Goto (1999). "Fos-like immunoreactivity in the periaqueductal gray of rats exposed to a natural predator." In: *NeuroReport* 10.2, pp. 413–418.

Canteras, N.S, S Chiavegatto, L.E Ribeiro do Valle, and L.W Swanson (1997). "Severe Reduction of Rat Defensive Behavior to a Predator by Discrete Hypothalamic Chemical Lesions." In: *Brain Research Bulletin* 44.3, pp. 297–305.

Cardinal, Pierre et al. (2014). "CB1 cannabinoid receptor in SF1-expressing neurons of the ventromedial hypothalamus determines metabolic responses to diet and leptin." In: *Molecular Metabolism* 3.7, pp. 705–716.

Cezario, A F, E R Ribeiro-Barbosa, M V C Baldo, and N S Canteras (2008). "Hypothalamic sites responding to predator threats–the role of the dorsal premammillary nucleus in unconditioned and conditioned antipredatory defensive behavior." In: *The European journal of neuroscience* 28.5, pp. 1003–15.

Chen, Tsai-Wen et al. (2013). "Ultrasensitive fluorescent proteins for imaging neuronal activity." In: *Nature* 499.7458, pp. 295–300.

Cheung, Clement C., William C. Krause, Robert H. Edwards, Cindy F. Yang, Nirao M. Shah, Thomas S. Hnasko, and Holly A. Ingraham (2015). "Sex-dependent changes in metabolism and behavior, as well as reduced anxiety after eliminating ventromedial hypothalamus excitatory output." In: *Molecular Metabolism* 4.11, pp. 857–866.

Choi, Gloria B., Hong-wei Dong, Andrew J. Murphy, David M. Valenzuela, George D. Yancopoulos, Larry W. Swanson, and David J. Anderson (2005). "Lhx6 Delineates a Pathway Mediating Innate Reproductive Behaviors from the Amygdala to the Hypothalamus." In: *Neuron* 46.4, pp. 647–660.

Ciabatti, Ernesto, Ana González-Rueda, Letizia Mariotti, Fabio Morgese, and Marco Tripodi (2017). "Life-Long Genetic and Functional Access to Neural Circuits Using Self-Inactivating Rabies Virus." In: *Cell* 170.2, 382–392.e14.

Cloues, Robin K and William A Sather (2003). "Afterhyperpolarization regulates firing rate in neurons of the suprachiasmatic nucleus." In: *The Journal of neuroscience : the official journal of the Society for Neuroscience* 23.5, pp. 1593–604.

Comoli, E, E R Ribeiro-Barbosa, and N S Canteras (2000). "Afferent connections of the dorsal premammillary nucleus." In: *The Journal of comparative neurology* 423.1, pp. 83–98.

Cook, C B, I Kakucska, R M Lechan, and R J Koenig (1992). "Expression of thyroid hormone receptor beta 2 in rat hypothalamus." In: *Endocrinology* 130.2, pp. 1077–1079.

Coulston, S., D. M. Stoddart, and D. R. Crump (1993). "Use of predator odors to protect chick-peas from predation by laboratory and wild mice." In: *Journal of Chemical Ecology* 19.4, pp. 607–612.

Courtney, Robert J., Larry D. Reid, and Ronald E. Wasden (1968). "Suppression of running times by olfactory stimuli." In: *Psychonomic Science* 12.7, pp. 315–316.

Coutinho, Eulalia A. et al. (2017). "Activation of SF1 Neurons in the Ventromedial Hypothalamus by DREADD Technology Increases In-

sulin Sensitivity in Peripheral Tissues." In: *Diabetes* 66.9, pp. 2372–2386.

Cucchiaro, Josephine B. and Daniel J. Uhlrich (1990). "Phaseolus vulgaris leucoagglutinin (PHA-L): A neuroanatomical tracer for electron microscopic analysis of synaptic circuitry in the cat's dorsal lateral geniculate nucleus." In: *Journal of Electron Microscopy Technique* 15.4, pp. 352–368.

Cuomo, V, R Cagiano, M A De Salvia, M Mazzoccoli, M Persichella, and G Renna (1992). "Ultrasonic vocalization as an indicator of emotional state during active avoidance learning in rats." In: *Life sciences* 50.14, pp. 1049–55.

Day, Heidi E.W., Cher V. Masini, and Serge Campeau (2004). "The pattern of brain c-fos mRNA induced by a component of fox odor, 2,5-dihydro-2,4,5-Trimethylthiazoline (TMT), in rats, suggests both systemic and processive stress characteristics." In: *Brain Research* 1025.1-2, pp. 139–151.

Dayas, C V, K M Buller, and T A Day (1999). "Neuroendocrine responses to an emotional stressor: evidence for involvement of the medial but not the central amygdala." In: *The European journal of neuroscience* 11.7, pp. 2312–22.

de Oliveira Crisanto, Karen, Wylqui Mikael Gomes de Andrade, Kayo Diogenes de Azevedo Silva, Ramón Hypolito Lima, Miriam Stela Maris de Oliveira Costa, Jeferson de Souza Cavalcante, Ruthnaldo Rodrigues Melo de Lima, Expedito Silva do Nascimento, and Judney Cley Cavalcante (2015). "The differential mice response to cat and snake odor." In: *Physiology & Behavior* 152, pp. 272–279.

Dhillon, Harveen et al. (2006). "Leptin Directly Activates SF1 Neurons in the VMH, and This Action by Leptin Is Required for Normal Body-Weight Homeostasis." In: *Neuron* 49.2, pp. 191–203.

Dicke, Marcel and Paul Grostal (2001). "Chemical Detection of Natural Enemies by Arthropods: An Ecological Perspective." In: *Annual Review of Ecology and Systematics* 32.1, pp. 1–23.

Dickman, C. R. (1992). "Predation and Habitat Shift in the House Mouse, Mus Domesticus." In: *Ecology* 73.1, pp. 313–322.

Dielenberg, R A and I S McGregor (1999). "Habituation of the hiding response to cat odor in rats (Rattus norvegicus)." In: *Journal of comparative psychology (Washington, D.C. : 1983)* 113.4, pp. 376–87.

Dielenberg, R.A, P Carrive, and I.S McGregor (2001). "The cardiovascular and behavioral response to cat odor in rats: unconditioned and conditioned effects." In: *Brain Research* 897.1-2, pp. 228–237.

Dielenberg, Robert A. and Iain S. McGregor (2001). "Defensive behavior in rats towards predatory odors: a review." In: *Neuroscience & Biobehavioral Reviews* 25.7-8, pp. 597–609.

DiMicco, J A and V M Abshire (1987). "Evidence for GABAergic inhibition of a hypothalamic sympathoexcitatory mechanism in anesthetized rats." In: *Brain research* 402.1, pp. 1–10.

Drobizhev, Mikhail, Nikolay S Makarov, Shane E Tillo, Thomas E Hughes, and Aleksander Rebane (2011). "Two-photon absorption properties of fluorescent proteins." In: *Nature Methods* 8.5, pp. 393–399.

Dulac, Catherine and A. Thomas Torello (2003). "Sensory systems: Molecular detection of pheromone signals in mammals: from genes to behaviour." In: *Nature Reviews Neuroscience* 4.7, pp. 551–562.

Fahrbach, S E, J I Morrell, and D W Pfaff (1989). "Studies of ventromedial hypothalamic afferents in the rat using three methods of HRP application." In: *Experimental brain research* 77.2, pp. 221–33.

Fendt, Markus and Thomas Endres (2008). "2,3,5-Trimethyl-3-thiazoline (TMT), a component of fox odor – Just repugnant or really fear-inducing?" In: *Neuroscience & Biobehavioral Reviews* 32.7, pp. 1259–1266.

Fendt, Markus, Thomas Endres, Catherine A. Lowry, Raimund Apfelbach, and Iain S. McGregor (2005). "TMT-induced autonomic and behavioral changes and the neural basis of its processing." In: *Neuroscience & Biobehavioral Reviews* 29.8, pp. 1145–1156.

Fenn, M. G. P. and D. W. Macdonald (1995). "Use of Middens by Red Foxes: Risk Reverses Rhythms of Rats." In: *Journal of Mammalogy* 76.1, pp. 130–136.

Ferrero, D. M., J. K. Lemon, D. Fluegge, S. L. Pashkovski, W. J. Korzan, S. R. Datta, M. Spehr, M. Fendt, and S. D. Liberles (2011). "Detection and avoidance of a carnivore odor by prey." In: *Proceedings of the National Academy of Sciences* 108.27, pp. 11235–11240.

File, Sandra E., Helio Zangrossi, Fiona L. Sanders, and P.S. Mabbutt (1993). "Dissociation between behavioral and corticosterone responses on repeated exposures to cat odor." In: *Physiology & Behavior* 54.6, pp. 1109–1111.

Firestein, Stuart (2001). "How the olfactory system makes sense of scents." In: *Nature* 413.6852, pp. 211–218.

Fox, Andrew S., Jonathan A. Oler, Do P.M. Tromp, Julie L. Fudge, and Ned H. Kalin (2015). "Extending the amygdala in theories of threat processing." In: *Trends in Neurosciences* 38.5, pp. 319–329.

Franklin, Tamara B et al. (2017). "Prefrontal cortical control of a brainstem social behavior circuit." In: *Nature neuroscience* 20.2, pp. 260–270.

Fuchs, S A, H M Edinger, and A Siegel (1985). "The role of the anterior hypothalamus in affective defense behavior elicited from the ventromedial hypothalamus of the cat." In: *Brain research* 330.1, pp. 93–107.

Gabbott, Paul L.A., Tracy A. Warner, Paul R.L. Jays, Phillip Salway, and Sarah J. Busby (2005). "Prefrontal cortex in the rat: Projections to subcortical autonomic, motor, and limbic centers." In: *The Journal of Comparative Neurology* 492.2, pp. 145–177.

Garfield, Alastair S et al. (2014). "A parabrachial-hypothalamic cholecystokinin neurocircuit controls counterregulatory responses to hypoglycemia." In: *Cell metabolism* 20.6, pp. 1030–7.

Govic, Antonina and Antonio G Paolini (2014). "In vivo electrophysiological recordings in amygdala subnuclei reveal selective and dis-

tinct responses to a behaviorally identified predator odor." In: *Journal of neurophysiology*, jn.00373.2014.

Gross, Cornelius T and Newton Sabino Canteras (2012). "The many paths to fear." In: *Nature reviews. Neuroscience* 13.9, pp. 651–8.

Hameed, Saira et al. (2017). "Thyroid Hormone Receptor Beta in the Ventromedial Hypothalamus Is Essential for the Physiological Regulation of Food Intake and Body Weight." In: *Cell reports* 19.11, pp. 2202–2209.

Heikkila, J, K Kaarsalo, O Mustonen, and P Pekkarinen (1993). *Influence of predation risk on early development and maturation in three species of Clethrionomys voles*.

Hogg, Sandy and Sandra E. File (1994). "Responders and nonresponders to cat odor do not differ in other tests of anxiety." In: *Pharmacology Biochemistry and Behavior* 49.1, pp. 219–222.

Hubbard, D T, D C Blanchard, M Yang, C M Markham, A Gervacio, L Chun-I, and R J Blanchard (2004). "Development of defensive behavior and conditioning to cat odor in the rat." In: *Physiology & behavior* 80.4, pp. 525–30.

Hunsperger, RW (1956). "Affektreaktionen auf elektrische Reizung im Hirnstamm der Katze." In: *Helv. physiol. pharmacol. Acta* 14.1, pp. 70–92.

Ikeda, Y, X Luo, R Abbud, J H Nilson, and K L Parker (1995). "The nuclear receptor steroidogenic factor 1 is essential for the formation of the ventromedial hypothalamic nucleus." In: *Molecular Endocrinology* 9.4, pp. 478–486.

Ishii, Kentaro K., Takuya Osakada, Hiromi Mori, Nobuhiko Miyasaka, Yoshihiro Yoshihara, Kazunari Miyamichi, and Kazushige Touhara (2017). "A Labeled-Line Neural Circuit for Pheromone-Mediated Sexual Behaviors in Mice." In: *Neuron* 95.1, 123–137.e8.

Jackman, Skyler L, Brandon M Beneduce, Iain R Drew, and Wade G Regehr (2014). "Achieving high-frequency optical control of synaptic transmission." In: *The Journal of neuroscience : the official journal of the Society for Neuroscience* 34.22, pp. 7704–14.

Jo, Young-Hwan (2012). "Endogenous BDNF regulates inhibitory synaptic transmission in the ventromedial nucleus of the hypothalamus." In: *Journal of neurophysiology* 107.1, pp. 42–9.

Jochym, M. and S. Halle (2013). "Influence of predation risk on recruitment and litter intervals in common voles (Microtus arvalis)." In: *Canadian Journal of Zoology* 91.5, pp. 281–286.

Johansen, Joshua P., Christopher K. Cain, Linnaea E. Ostroff, and Joseph E. LeDoux (2011). "Molecular Mechanisms of Fear Learning and Memory." In: *Cell* 147.3, pp. 509–524.

Kang, N., M. J. Baum, and J. A. Cherry (2011). "Different Profiles of Main and Accessory Olfactory Bulb Mitral/Tufted Cell Projections Revealed in Mice Using an Anterograde Tracer and a Whole-Mount, Flattened Cortex Preparation." In: *Chemical Senses* 36.3, pp. 251–260.

Kang, Ningdong, Michael J Baum, and James A Cherry (2011). "Different profiles of main and accessory olfactory bulb mitral/tufted cell projections revealed in mice using an anterograde tracer and a whole-mount, flattened cortex preparation." In: *Chemical senses* 36.3, pp. 251–60.

Kavaliers, Martin, John P. Wiebe, and Liisa A.M. Galea (1994). "Reduction of predator odor-induced anxiety in mice by the neurosteroid 3α-hydroxy-4-pregnen-20-one (3αHP)." In: *Brain Research* 645.1-2, pp. 325–329.

Keshavarzi, Sepideh, Robert K P Sullivan, Damian J Ianno, and Pankaj Sah (2014). "Functional Properties and Projections of Neurons in the Medial Amygdala." In: *Journal of Neuroscience* 34.26, pp. 8699–8715.

Kim, D W, T Uetsuki, Y Kaziro, N Yamaguchi, and S Sugano (1990). "Use of the human elongation factor 1 alpha promoter as a versatile and efficient expression system." In: *Gene* 91.2, pp. 217–23.

Kim, Ki Woo, Shen Li, Hongyu Zhao, Boya Peng, Stuart A. Tobet, Joel K. Elmquist, Keith L. Parker, and Liping Zhao (2010). "CNS-Specific Ablation of Steroidogenic Factor 1 Results in Impaired Fe-

male Reproductive Function." In: *Molecular Endocrinology* 24.6, pp. 1240–1250.

King, Bruce M. (2006). "The rise, fall, and resurrection of the ventromedial hypothalamus in the regulation of feeding behavior and body weight." In: *Physiology & Behavior* 87.2, pp. 221–244.

King, Jean A., Washington L. De Oliveira, and Nihal Patel (2005). "Deficits in testosterone facilitate enhanced fear response." In: *Psychoneuroendocrinology* 30.4, pp. 333–340.

Klöckener, Tim et al. (2011). "High-fat feeding promotes obesity via insulin receptor/PI3K-dependent inhibition of SF-1 VMH neurons." In: *Nature Neuroscience* 14.7, pp. 911–918.

Koivisto, Elina and Jyrki Pusenius (2003). "Effects of temporal variation in the risk of predation by least weasel (Mustela nivalis) on feeding behavior of field vole (Microtus agrestis)." In: *Evolutionary Ecology* 17.5-6, pp. 477–489.

Kubo, Takao, Tomohiro Kanaya, Hiroyuki Numakura, Hideaki Okajima, Yukihiko Hagiwara, and Ryuji Fukumori (2002). "The lateral septal area is involved in mediation of immobilization stress-induced blood pressure increase in rats." In: *Neuroscience Letters* 318.1, pp. 25–28.

Kunwar, Prabhat S, Moriel Zelikowsky, Ryan Remedios, Haijiang Cai, Melis Yilmaz, Markus Meister, and David J Anderson (2015). "Ventromedial hypothalamic neurons control a defensive emotion state." In: *eLife* 4, e06633.

Kurrasch, D. M., C. C. Cheung, F. Y. Lee, P. V. Tran, K. Hata, and H. A. Ingraham (2007). "The Neonatal Ventromedial Hypothalamus Transcriptome Reveals Novel Markers with Spatially Distinct Patterning." In: *Journal of Neuroscience* 27.50, pp. 13624–13634.

Lala, D S, D A Rice, and K L Parker (1992). "Steroidogenic factor I, a key regulator of steroidogenic enzyme expression, is the mouse homolog of fushi tarazu-factor I." In: *Molecular Endocrinology* 6.8, pp. 1249–1258.

Lammers, J.H.C.M., M.R. Kruk, W. Meelis, and A.M. van der Poel (1988). "Hypothalamic substrates for brain stimulation-induced patterns of locomotion and escape jumps in the rat." In: *Brain Research* 449.1-2, pp. 294–310.

Leak, Rehana K and Robert Y Moore (1997). "Identification of retinal ganglion cells projecting to the lateral hypothalamic area of the rat." In: *Brain Research* 770.1-2, pp. 105–114.

Li, Chun-I, Thomas L. Maglinao, and Lorey K. Takahashi (2004). "Medial Amygdala Modulation of Predator Odor-Induced Unconditioned Fear in the Rat." In: *Behavioral Neuroscience* 118.2, pp. 324–332.

Lima, Steven L. and Peter A. Bednekoff (1999). "Temporal Variation in Danger Drives Antipredator Behavior: The Predation Risk Allocation Hypothesis." In: *The American Naturalist* 153.6, pp. 649–659.

Lima, Steven L. and Lawrence M. Dill (1990). "Behavioral decisions made under the risk of predation: a review and prospectus." In: *Canadian Journal of Zoology* 68.4, pp. 619–640.

Liu, Yu-Xiang, Ya-Nan Cheng, Yi-Long Miao, De-Li Wei, Li-Hua Zhao, Ming-Jiu Luo, and Jing-He Tan (2012). "Psychological Stress on Female Mice Diminishes the Developmental Potential of Oocytes: A Study Using the Predatory Stress Model." In: *PLoS ONE* 7.10, e48083.

Masini, C. V., S. Sauer, and S. Campeau (2005). "Ferret Odor as a Processive Stress Model in Rats: Neurochemical, Behavioral, and Endocrine Evidence." In: *Behavioral Neuroscience* 119.1, pp. 280–292.

McGregor, Iain S, Laurens Schrama, Polly Ambermoon, and Robert A Dielenberg (2002). "Not all 'predator odours' are equal: cat odour but not 2,4,5 trimethylthiazoline (TMT; fox odour) elicits specific defensive behaviours in rats." In: *Behavioural brain research* 129.1-2, pp. 1–16.

Meredith, M. and Jenne M Westberry (2004). "Distinctive Responses in the Medial Amygdala to Same-Species and Different-Species Pheromones." In: *Journal of Neuroscience* 24.25, pp. 5719–5725.

Miyazaki, J, S Takaki, K Araki, F Tashiro, A Tominaga, K Takatsu, and K Yamamura (1989). "Expression vector system based on the chicken beta-actin promoter directs efficient production of interleukin-5." In: *Gene* 79.2, pp. 269–77.

Mohedano-Moriano, Alicia, Palma Pro-Sistiaga, Isabel Úbeda-Bañón, Carlos Crespo, Ricardo Insausti, and Alino Martinez-Marcos (2007). "Segregated pathways to the vomeronasal amygdala: differential projections from the anterior and posterior divisions of the accessory olfactory bulb." In: *European Journal of Neuroscience* 25.7, pp. 2065–2080.

Mongeau, Raymond, Gabriel A Miller, Elizabeth Chiang, and David J Anderson (2003). "Neural correlates of competing fear behaviors evoked by an innately aversive stimulus." In: *The Journal of neuroscience : the official journal of the Society for Neuroscience* 23.9, pp. 3855–68.

Motta, S. C., M. Goto, F. V. Gouveia, M. V. C. Baldo, N. S. Canteras, and L. W. Swanson (2009). "Dissecting the brain's fear system reveals the hypothalamus is critical for responding in subordinate conspecific intruders." In: *Proceedings of the National Academy of Sciences* 106.12, pp. 4870–4875.

Muñoz-Abellán, Cristina, Cristina Rabasa, Nuria Daviu, Roser Nadal, and Antonio Armario (2011). "Behavioral and Endocrine Consequences of Simultaneous Exposure to Two Different Stressors in Rats: Interaction or Independence?" In: *PLoS ONE* 6.6, e21426.

Nader, K., P Majidishad, P Amorapanth, and J E LeDoux (2001). "Damage to the Lateral and Central, but Not Other, Amygdaloid Nuclei Prevents the Acquisition of Auditory Fear Conditioning." In: *Learning & Memory* 8.3, pp. 156–163.

Nomoto, Kensaku and Susana Q. Lima (2015). "Enhanced Male-Evoked Responses in the Ventromedial Hypothalamus of Sexually Receptive Female Mice." In: *Current Biology* 25.5, pp. 589–594.

Norrdahl, Kai and Erkki Korpimäki (1998). "Does mobility or sex of voles affect risk of predation by mammalian predators?" In: *Ecology* 79.1, pp. 226–232.

Oheim, M, E Beaurepaire, E Chaigneau, J Mertz, and S Charpak (2001). "Two-photon microscopy in brain tissue: parameters influencing the imaging depth." In: *Journal of neuroscience methods* 111.1, pp. 29–37.

Pagani, Jerome H. and Jeffrey B. Rosen (2009). "The medial hypothalamic defensive circuit and 2,5-dihydro-2,4,5-trimethylthiazoline (TMT) induced fear: Comparison of electrolytic and neurotoxic lesions." In: *Brain Research* 1286, pp. 133–146.

Papes, Fabio, Darren W Logan, and Lisa Stowers (2010). "The vomeronasal organ mediates interspecies defensive behaviors through detection of protein pheromone homologs." In: *Cell* 141.4, pp. 692–703.

Pardo-Bellver, Cecília, Bernardita Cádiz-Moretti, Amparo Novejarque, Fernando Martínez-García, and Enrique Lanuza (2012). "Differential efferent projections of the anterior, posteroventral, and posterodorsal subdivisions of the medial amygdala in mice." In: *Frontiers in Neuroanatomy* 6, p. 33.

Parker, Keith L et al. (2002). "Steroidogenic factor 1: an essential mediator of endocrine development." In: *Recent progress in hormone research* 57, pp. 19–36.

Perrot-Sinal, T S, K P Ossenkopp, and M Kavaliers (1999). "Brief predator odour exposure activates the HPA axis independent of locomotor changes." In: *Neuroreport* 10.4, pp. 775–80.

Pro-Sistiaga, Palma, Alicia Mohedano-Moriano, Isabel Ubeda-Bañon, Maria del mar Arroyo-Jimenez, Pilar Marcos, Emilio Artacho-Pérula, Carlos Crespo, Ricardo Insausti, and Alino Martinez-Marcos (2007). "Convergence of olfactory and vomeronasal projections in the rat basal telencephalon." In: *The Journal of Comparative Neurology* 504.4, pp. 346–362.

Ranaldi, Robert (2014). "Dopamine and reward seeking: the role of ventral tegmental area." In: *Reviews in the Neurosciences*, pp. 621–30.

Redgrave, Peter and Paul Dean (1991). "Does the PAG Learn about Emergencies from the Superior Colliculus?" In: *The Midbrain Periaqueductal Gray Matter*. Boston, MA: Springer US, pp. 199–209.

Resendez, Shanna L, Josh H Jennings, Randall L Ung, Vijay Mohan K Namboodiri, Zhe Charles Zhou, James M Otis, Hiroshi Nomura, Jenna A McHenry, Oksana Kosyk, and Garret D Stuber (2016). "Visualization of cortical, subcortical and deep brain neural circuit dynamics during naturalistic mammalian behavior with head-mounted microscopes and chronically implanted lenses." In: *Nature Protocols* 11.3, pp. 566–597.

Rickenbacher, Elizabeth, Rosemarie E Perry, Regina M Sullivan, and Marta A Moita (2017). "Freezing suppression by oxytocin in central amygdala allows alternate defensive behaviours and mother-pup interactions." In: *eLife* 6.

Risold, P. Y., N. S. Canteras, and L. W. Swanson (1994). "Organization of projections from the anterior hypothalamic nucleus: APhaseolus vulgaris-leucoagglutinin study in the rat." In: *The Journal of Comparative Neurology* 348.1, pp. 1–40.

Risold, P. Y. and L. W. Swanson (1995). "Evidence for a hypothalamothalamocortical circuit mediating pheromonal influences on eye and head movements." In: *Proceedings of the National Academy of Sciences* 92.9, pp. 3898–3902.

Root, Cory M., Christine A. Denny, René Hen, and Richard Axel (2014). "The participation of cortical amygdala in innate, odour-driven behaviour." In: *Nature* 515.7526, pp. 269–273.

Rosen, Jeffrey B., Arun Asok, and Trisha Chakraborty (2015). "The smell of fear: innate threat of 2,5-dihydro-2,4,5-trimethylthiazoline, a single molecule component of a predator odor." In: *Frontiers in Neuroscience* 9, p. 292.

Roth, Bryan L (2016). "DREADDs for Neuroscientists." In: *Neuron* 89.4, pp. 683–94.

Ruxton, G.D. GD D. and S.L. L. SL S.L. Lima (1997). "Predator-induced breeding suppression and its consequences for predator–prey pop-

ulation dynamics." In: *Royal Society Proceedings: Biological Sciences* 264.1380, pp. 409–415.

Sah, P., E. S. L. Faber, M. Lopez de Armentia, and J. Power (2003). "The Amygdaloid Complex: Anatomy and Physiology." In: *Physiological Reviews* 83.3, pp. 803–834.

Schwartz, Michael W., Stephen C. Woods, Daniel Porte, Randy J. Seeley, and Denis G. Baskin (2000). "Central nervous system control of food intake." In: *Nature* 404.6778, pp. 661–671.

Shang, C., Z. Liu, Z. Chen, Y. Shi, Q. Wang, S. Liu, D. Li, and P. Cao (2015). "A parvalbumin-positive excitatory visual pathway to trigger fear responses in mice." In: *Science* 348.6242, pp. 1472–1477.

Shima, Yuichi, Mohamad Zubair, Satoru Ishihara, Yuko Shinohara, Sanae Oka, Shioko Kimura, Shiki Okamoto, Yasuhiko Minokoshi, Sachiyo Suita, and Ken-ichirou Morohashi (2005). "Ventromedial Hypothalamic Nucleus-Specific Enhancer of Ad4BP/SF-1 Gene." In: *Molecular Endocrinology* 19.11, pp. 2812–2823.

Silva, Bianca A, Cornelius T Gross, and Johannes Gräff (2016). "The neural circuits of innate fear: detection, integration, action, and memorization." In: *Learning & memory (Cold Spring Harbor, N.Y.)* 23.10, pp. 544–55.

Silva, Bianca A, Camilla Mattucci, Piotr Krzywkowski, Emanuele Murana, Anna Illarionova, Valery Grinevich, Newton S Canteras, Davide Ragozzino, and Cornelius T Gross (2013). "Independent hypothalamic circuits for social and predator fear." In: *Nature neuroscience* 16.12, pp. 1731–3.

Sohn, Jong-Woo, Youjin Oh, Ki Woo Kim, Syann Lee, Kevin W. Williams, and Joel K. Elmquist (2016). "Leptin and insulin engage specific PI3K subunits in hypothalamic SF1 neurons." In: *Molecular Metabolism* 5.8, pp. 669–679.

Srivastava, A, E W Lusby, and K I Berns (1983). "Nucleotide sequence and organization of the adeno-associated virus 2 genome." In: *Journal of virology* 45.2, pp. 555–64.

Stallings, N. R., Neil A. Hanley, Gregor Majdic, Liping Zhao, Marit Bakke, and Keith L. Parker (2002). "Development of a Transgenic Green Fluorescent Protein Lineage Marker for Steroidogenic Factor 1." In: *Molecular Endocrinology* 16.10, pp. 2360–2370.

Staples, L.G., I.S. McGregor, R. Apfelbach, and G.E. Hunt (2008). "Cat odor, but not trimethylthiazoline (fox odor), activates accessory olfactory and defense-related brain regions in rats." In: *Neuroscience* 151.4, pp. 937–947.

Sternson, Scott M, Gordon M.G. Shepherd, and Jeffrey M Friedman (2005). "Topographic mapping of VMH → arcuate nucleus microcircuits and their reorganization by fasting." In: *Nature Neuroscience* 8.10, pp. 1356–1363.

Stoddard-Apter, S L and M F MacDonnell (1980). "Septal and amygdalar efferents to the hypothalamus which facilitate hypothalamically elicited intraspecific aggression and associated hissing in the cat. An autoradiographic study." In: *Brain research* 193.1, pp. 19–32.

Stowers, Lisa, Peter Cameron, and Jason A Keller (2013). "Ominous odors: olfactory control of instinctive fear and aggression in mice." In: *Current opinion in neurobiology* 23.3, pp. 339–45.

Stuber, Garret D and Roy A Wise (2016). "Lateral hypothalamic circuits for feeding and reward." In: *Nature neuroscience* 19.2, pp. 198–205.

Suzuki, N. and J. M. Bekkers (2011). "Two Layers of Synaptic Processing by Principal Neurons in Piriform Cortex." In: *Journal of Neuroscience* 31.6, pp. 2156–2166.

Swanson, L W and G D Petrovich (1998). "What is the amygdala?" In: *Trends in neurosciences* 21.8, pp. 323–31.

Sziklas, V and Michael Petrides (1998). "Memory and the region of the mammillary bodies." In: *Progress in Neurobiology* 54.1, pp. 55–70.

Takahashi, Hiroo and Akio Tsuboi (2016). "Olfactory Avoidance Test (Mouse)." In: *The Journal of Neuroscience* 7.5.

Takahashi, Lorey K., David T. Hubbard, Iris Lee, Yasmin Dar, and Sara M. Sipes (2007). "Predator odor-induced conditioned fear in-

volves the basolateral and medial amygdala." In: *Behavioral Neuroscience* 121.1, pp. 100–110.

Thompson, R. H. and L. W. Swanson (1998). *Organization of inputs to the dorsomedial nucleus of the hypothalamus: A reexamination with Fluorogold and PHAL in the rat*.

Tong, Qingchun et al. (2007). "Synaptic glutamate release by ventromedial hypothalamic neurons is part of the neurocircuitry that prevents hypoglycemia." In: *Cell metabolism* 5.5, pp. 383–93.

Tripathy, Shreejoy J., Judith Savitskaya, Shawn D. Burton, Nathaniel N. Urban, and Richard C. Gerkin (2014). "NeuroElectro: a window to the world's neuron electrophysiology data." In: *Frontiers in Neuroinformatics* 8, p. 40.

Vale, Ruben, Dominic A. Evans, and Tiago Branco (2017). "Rapid Spatial Learning Controls Instinctive Defensive Behavior in Mice." In: *Current Biology* 27.9, pp. 1342–1349.

Vertes, Robert P., Alison M. Crane, Luis V. Colom, and Brian H. Bland (1995). "Ascending projections of the posterior nucleus of the hypothalamus: PHA-L analysis in the rat." In: *The Journal of Comparative Neurology* 359.1, pp. 90–116.

Viskaitis, Paulius et al. (2017). "Modulation of SF1 Neuron Activity Coordinately Regulates Both Feeding Behavior and Associated Emotional States." In: *Cell Reports* 21.12, pp. 3559–3572.

Vooijs, M, J Jonkers, and A Berns (2001). "A highly efficient ligand-regulated Cre recombinase mouse line shows that LoxP recombination is position dependent." In: *EMBO reports* 2.4, pp. 292–7.

Wang, Li, Irene Z. Chen, and Dayu Lin (2015). "Collateral Pathways from the Ventromedial Hypothalamus Mediate Defensive Behaviors." In: *Neuron* 85.6, pp. 1344–1358.

Wang, Xinjun, Chunzhao Zhang, Gábor Szábo, and Qian Quan Sun (2013). "Distribution of CaMKIIα expression in the brain in vivo, studied by CaMKIIα-GFP mice." In: *Brain Research* 1518, pp. 9–25.

Wang, Yong and Paul B. Manis (2005). "Synaptic Transmission at the Cochlear Nucleus Endbulb Synapse During Age-Related Hearing Loss in Mice." In: *Journal of Neurophysiology* 94.3, pp. 1814–1824.

Wei, Pengfei et al. (2015). "Processing of visually evoked innate fear by a non-canonical thalamic pathway." In: *Nature Communications* 6, p. 6756.

Wiedenmayer, Christoph P (2009). "Plasticity of defensive behavior and fear in early development." In: *Neuroscience and biobehavioral reviews* 33.3, pp. 432–41.

Wilent, W Bryan, Michael Y Oh, Cathrin M Buetefisch, Julian E Bailes, Diane Cantella, Cindy Angle, and Donald M Whiting (2010). "Induction of panic attack by stimulation of the ventromedial hypothalamus." In: *Journal of neurosurgery* 112.6, pp. 1295–8.

Williams, Jon L. and David K. Scott (1989). "Influence of conspecific and predatory Stressors and their associated odors on defensive burying and freezing responses." In: *Animal Learning & Behavior* 17.4, pp. 383–393.

Xiong, Xiaorui R, Feixue Liang, Brian Zingg, Xu-ying Ji, Leena A Ibrahim, Huizhong W Tao, and Li I Zhang (2015). "Auditory cortex controls sound-driven innate defense behaviour through corticofugal projections to inferior colliculus." In: *Nature communications* 6, p. 7224.

Xu, H.-Y., Y.-J. Liu, M.-Y. Xu, Y.-H. Zhang, J.-X. Zhang, and Y.-J. Wu (2012). "Inactivation of the bed nucleus of the stria terminalis suppresses the innate fear responses of rats induced by the odor of cat urine." In: *Neuroscience* 221, pp. 21–27.

Xu, Yong, Latrice D Faulkner, and Jennifer W Hill (2011). "Cross-Talk between Metabolism and Reproduction: The Role of POMC and SF1 Neurons." In: *Frontiers in endocrinology* 2, p. 98.

Yardley, C.P. and S.M. Hilton (1986). "The hypothalamic and brainstem areas from which the cardiovascular and behavioural components of the defence reaction are elicited in the rat." In: *Journal of the Autonomic Nervous System* 15.3, pp. 227–244.

Yilmaz, Melis and Markus Meister (2013). "Rapid innate defensive responses of mice to looming visual stimuli." In: *Current biology : CB* 23.20, pp. 2011–5.

Ylönen, Hannu (1994). "Vole cycles and antipredatory behaviour." In: *Trends in ecology & evolution* 9.11, pp. 426–430.

Yokosuka, M, M Matsuoka, R Ohtani-Kaneko, M Iigo, M Hara, K Hirata, and M Ichikawa. "Female-soiled bedding induced fos immunoreactivity in the ventral part of the premammillary nucleus (PMv) of the male mouse." In: *Physiology & behavior* 68.1-2, pp. 257–61.

Zangrossi, H and S E File (1994). "Habituation and generalization of phobic responses to cat odor." In: *Brain research bulletin* 33.2, pp. 189–94.

Zhao, Liping, Ki Woo Kim, Yayoi Ikeda, Kimberly K Anderson, Laurel Beck, Stephanie Chase, Stuart A Tobet, and Keith L Parker (2008). "Central nervous system-specific knockout of steroidogenic factor 1 results in increased anxiety-like behavior." In: *Molecular endocrinology (Baltimore, Md.)* 22.6, pp. 1403–15.

Zhao, Xinyu, Mingna Liu, and Jianhua Cang (2014). "Visual Cortex Modulates the Magnitude but Not the Selectivity of Looming-Evoked Responses in the Superior Colliculus of Awake Mice." In: *Neuron* 84.1, pp. 202–213.

Zingg, Brian, Xiao-Lin Chou, Zheng-Gang Zhang, Lukas Mesik, Feixue Liang, Huizhong Whit Tao, and Li I Zhang (2017). "AAV-Mediated Anterograde Transsynaptic Tagging: Mapping Corticocollicular Input-Defined Neural Pathways for Defense Behaviors." In: *Neuron* 93.1, pp. 33–47.

Zufferey, R, J E Donello, D Trono, and T J Hope (1999). "Woodchuck hepatitis virus posttranscriptional regulatory element enhances expression of transgenes delivered by retroviral vectors." In: *Journal of virology* 73.4, pp. 2886–92.

This document was typeset using the typographical look-and-feel `classicthesis` developed by André Miede. The style was inspired by Robert Bringhurst's seminal book on typography *"The Elements of Typographic Style"*.